

# Variational Bayes Inference for Spatial Error Models with Missing Data

Anjana Wijayawardhana\*, David Gunawan, and Thomas Suesse

School of Mathematics and Applied Statistics, University of Wollongong,  
Wollongong, NSW, Australia

## Abstract

The spatial error model (SEM) is a type of simultaneous autoregressive (SAR) model for analysing spatially correlated data. Markov chain Monte Carlo (MCMC) is one of the most widely used Bayesian methods for estimating SEM, but it has significant limitations when it comes to handling missing data in the response variable due to its high computational cost. Variational Bayes (VB) approximation offers an alternative solution to this problem. Two VB-based algorithms employing Gaussian variational approximation with factor covariance structure are presented, joint VB (JVB) and hybrid VB (HVB), suitable for both missing at random and not at random inference. When dealing with many missing values, the JVB is inaccurate, and the standard HVB algorithm struggles to achieve accurate inferences. Our modified versions of HVB enable accurate inference within a reasonable computational time, thus improving its performance. The performance of the VB methods is evaluated using simulated and real datasets.

Keywords: Missing at random; Missing not at random; Selection model; Factor covariance structure; Stochastic gradient ascent

---

\*Corresponding author: [anjanaw@uow.edu.au](mailto:anjanaw@uow.edu.au)

# 1 Introduction

The simultaneous autoregressive (SAR) models are ideal for analysing spatially correlated data, since they extend a linear regression model to take into account spatial correlations. There are three commonly used types of SAR models: spatial error models (SEMs), spatial autoregressive models (SAMs), and spatial Durbin models (SDMs). SAR models are applied in diverse applied research, including ecology (Cassemiro et al., 2007; Ver Hoef et al., 2018), political science (Di Salvatore and Ruggeri, 2021), social network analysis (Leenders, 2002; Zhu et al., 2020), and epidemiology (Mollalo et al., 2020; Wong and Li, 2020).

An extensive literature explores sampling-based Bayesian Markov chain Monte Carlo (MCMC) methods for estimating SAR models (Gelfand et al., 1990; LeSage, 1997; De Oliveira and Song, 2008). However, it is computationally expensive to estimate SAR models with many observations and missing data. Variational Bayes (VB) has recently emerged as a faster alternative to MCMC for estimating complex statistical models (Chappell et al., 2008; Han et al., 2016; Ong et al., 2018; Gunawan et al., 2021, 2023); see Section 3 for further details on VB methods. There are several commonly used VB methods, including mean-field variational Bayes (MFVB) (Ormerod and Wand, 2010), integrated non-factorised variational inference (INFVB) (Han et al., 2013), and Gaussian variational approximation (Ong et al., 2018; Tan and Nott, 2018).

Although VB methods are a promising alternative to MCMC methods, their use in estimating SAR models has been limited even where there are no missing values in the response variable. Wu (2018) employed two variational Bayes methods, hybrid mean-field variational Bayes (MFVB) and integrated non-factorised variational Bayes (INFVB), to estimate the spatial autoregressive confused (SAC) and matrix exponential spatial specification (MESS) models, both belonging to the SAR family. In Bansal et al. (2021), spatial count data models were estimated using MFVB and INFVB, incorporating a MESS model to capture spatial dependence in error terms.

Having missing values in the response variable is common in practice. When estimating SAR models, ignoring missing response values can lead to inconsistency and bias

(Wang and Lee, 2013; Benedetti et al., 2020). Extensive literature has explored the estimation of SAR models under missing at random (MAR) mechanism (LeSage and Pace, 2004; Wang and Lee, 2013; Suesse and Zammit-Mangion, 2017; Suesse, 2018; Wijayawardhana et al., 2024). There has been a limited exploration of estimating SEM under the missing not at random (MNAR) mechanism. Flores-Lagunes and Schnier (2012) introduced a Generalized Method of Moments (GMM) estimator that performs poorly with small sample sizes. Seya et al. (2021) and Doğan and Taşpınar (2018) used Metropolis-Hastings (MH) algorithms, which are computationally expensive when the number of observations is large. A more recent study by Rabovič and Čížek (2023) examined the estimation of the SEM using a partial maximum likelihood (ML) method.

Current VB methods have only been applied to estimate SAR models with full data (Wu, 2018; Bansal et al., 2021). The MFVB method is not suitable for estimating SAR models with missing data because it assumes posterior independence over the model parameters and missing values, resulting in underestimating posterior variance (Blei and Jordan, 2006). To address this issue, we employ the Gaussian variational approximation with a factor covariance structure proposed by Ong et al. (2018) in Section 3.

Our paper proposes two efficient VB algorithms, called joint VB (JVB) and hybrid VB (HVB), that are less computationally demanding than MCMC for estimating SEM under MAR and MNAR. The JVB method uses a Gaussian variational approximation with a factor covariance structure to approximate the joint posterior of the model parameters and the missing values. The HVB method significantly modifies the VB methods proposed by Loaiza-Maya et al. (2022) and Dao et al. (2024), which combine VB optimisation with MCMC steps. A Gaussian variational approximation with a factor covariance structure is used for approximating the posterior distribution of the model parameters, and MCMC steps are used to sample the missing response values from their conditional posterior distribution. The conditional posterior distribution of missing response values is available in closed form under MAR. Under MNAR, however, the conditional posterior distribution is not available in closed form, making Bayesian inference more challenging. We propose several MCMC schemes for the HVB method under MNAR to address low acceptance

percentages, especially for cases with many missing values.

The performance of the VB methods is investigated using simulated and real datasets with different numbers of observations and missing data percentages. We compare the performance of the VB methods with Hamiltonian Monte Carlo (HMC) (Duane et al., 1987; Neal et al., 2011), implemented using RStan, an interface to the Stan programming language (Stan Development Team, 2023). In particular, we use the HMC algorithm of Hoffman et al. (2014), called the No U-Turn Sampler (NUTS), which adaptively selects the number of leapfrogs and the step size. Section S3 of the online supplement provides detailed information on the HMC algorithm used.

The rest of this paper is organised as follows. Section 2 presents the spatial error models and discusses different missing data mechanisms. In Section 3, we present the variational Bayes methods to estimate the SEM with missing data. In Section 4, Simulation studies are conducted to evaluate the performance of the VB methods. Section 5 applies the VB methods to a real-world dataset. Section 6 discusses our major results and findings. The paper also has an online supplement with additional technical details.

## 2 Spatial Error Models and Missing Data Mechanisms

### 2.1 Spatial Error Model

Let  $\mathbf{y} = (y_1, y_2, \dots, y_n)^\top$  be the vector of response variable observed at  $n$  spatial locations  $s_1, \dots, s_n$ ,  $\mathbf{X}$  be the  $n \times (r + 1)$  design matrix containing the covariates, and  $\mathbf{W}$  be the  $n \times n$  spatial weight matrix. The SEM is given by

$$\begin{aligned} \mathbf{y} &= \mathbf{X}\boldsymbol{\beta} + \mathbf{v}, \\ \mathbf{v} &= \rho\mathbf{W}\mathbf{v} + \mathbf{e}, \end{aligned} \tag{1}$$

where  $\mathbf{e} \sim N(0, \sigma_y^2 \mathbf{I}_n)$ ,  $\mathbf{I}_n$  denotes the  $n \times n$  identity matrix, and  $\sigma_y^2$  is a variance parameter. The vector  $\boldsymbol{\beta} = (\beta_0, \beta_1, \dots, \beta_r)^\top$  contains the fixed effects parameters, and  $\rho$  is the

Table 1: Expressions for mean vector ( $\boldsymbol{\mu}_y$ ), covariance matrix ( $\boldsymbol{\Sigma}_y$ ),  $\mathbf{V}_y$ , and precision matrix ( $\mathbf{M}_y$ ) of SEM with  $\mathbf{A} = \mathbf{I}_n - \rho\mathbf{W}$

Term	Expression
$\boldsymbol{\mu}_y$	$\mathbf{X}\boldsymbol{\beta}$
$\boldsymbol{\Sigma}_y$	$\sigma_y^2(\mathbf{A}^\top\mathbf{A})^{-1}$
$\mathbf{V}_y$	$(\mathbf{A}^\top\mathbf{A})^{-1}$
$\mathbf{M}_y = \mathbf{V}_y^{-1}$	$\mathbf{A}^\top\mathbf{A}$

spatial autocorrelation parameter which measures the strength and the direction of spatial dependence (Anselin, 1988; Allison, 2001; LeSage and Pace, 2009).

Let  $W_{ij}$  be the  $i^{\text{th}}$  row and  $j^{\text{th}}$  column entry of the spatial weight matrix  $\mathbf{W}$ . The entry  $W_{ij}$  is non-zero if the unit  $i$  is a neighbour of the unit  $j$ . The diagonal of the spatial weight matrix  $\mathbf{W}$  is zero. There have been several strategies proposed for constructing  $\mathbf{W}$  in the literature (see Ord (1975); Anselin (1988); Kelley pace and Barry (1997) for further details). The  $\mathbf{W}$  is commonly constructed to be sparse and symmetric.

For the SEM, when the error vector  $\mathbf{e}$  is normally distributed, the response variable  $\mathbf{y}$  is multivariate Gaussian with the mean vector  $\boldsymbol{\mu}_y = \mathbf{X}\boldsymbol{\beta}$  and covariance matrix  $\boldsymbol{\Sigma}_y = \sigma_y^2(\mathbf{A}^\top\mathbf{A})^{-1}$ . To ensure the validity of  $\boldsymbol{\Sigma}_y$  as a proper covariance matrix, the parameter  $\rho$  does not take on any of the values  $\frac{1}{\lambda_{(1)}}, \frac{1}{\lambda_{(2)}}, \dots, \frac{1}{\lambda_{(n)}}$ , where  $\lambda_{(1)}, \lambda_{(2)}, \dots, \lambda_{(n)}$  represent the eigenvalues of the matrix  $\mathbf{W}$  sorted in ascending order (Li et al., 2012). It is common practice to perform row or column normalisation (ensuring that the sum of the rows or columns is 1) on  $\mathbf{W}$ , thus restricting  $\rho$  to the range  $\frac{1}{\lambda_{(1)}} < \rho < 1$  (LeSage and Pace, 2009).

Table 1 provides expressions for the mean vector, covariance matrix, and precision matrix for the distribution of  $\mathbf{y}$ . Let  $\boldsymbol{\phi} = (\boldsymbol{\beta}^\top, \rho, \sigma_y^2)^\top$  be the vector of model parameters of the SEM. The log-likelihood of  $\mathbf{y}$  is given by

$$\log p(\mathbf{y} | \boldsymbol{\phi}) = -\frac{n}{2}\log(2\pi) - \frac{n}{2}\log(\sigma_y^2) + \frac{1}{2}\log|\mathbf{M}_y| - \frac{1}{2\sigma_y^2}\mathbf{r}^\top\mathbf{M}_y\mathbf{r}, \quad (2)$$

where  $\mathbf{r} = \mathbf{y} - \boldsymbol{\mu}_y$ .

## 2.2 Missing Data Mechanisms

Consider that the response vector  $\mathbf{y}$  of an SEM in Equation (1) contains missing values. Let  $\mathbf{y}_o$  be the subset of  $\mathbf{y}$  with  $n_o$  observed units, and  $\mathbf{y}_u$  be the subset of  $\mathbf{y}$  with  $n_u$  unobserved units. The complete response vector is  $\mathbf{y} = (\mathbf{y}_o^\top, \mathbf{y}_u^\top)^\top$ . A missing data indicator vector  $\mathbf{m}$  of length  $n$  containing 1's and 0's is defined. If an element in  $\mathbf{y}$  is missing, then the corresponding element in  $\mathbf{m}$  is 1 and 0, otherwise. The missing data mechanism is characterised by the conditional distribution of  $\mathbf{m}$  given  $\mathbf{y}$ , say  $p(\mathbf{m}|\mathbf{y}, \boldsymbol{\psi}, \mathbf{X}^*)$ , where  $\boldsymbol{\psi}$  is a vector of unknown parameters, and  $\mathbf{X}^*$  is an  $n \times (q + 1)$  design matrix containing the covariates of the missing data model. The covariates of the missing data model can be a subset of the covariates of the SEM. The main process of interest ( $\mathbf{y}$ ) and the missing data mechanism ( $\mathbf{m}$ ) should be jointly modeled in statistical modeling Rubin (1976). There are three missing data mechanisms (Rubin, 1976). The first mechanism is missing completely at random (MCAR). In MCAR, there is no relationship between the values of the vector  $\mathbf{y}$  (both observed and missing values) and the probability that they are missing,  $p(\mathbf{m}|\mathbf{y}, \boldsymbol{\psi}, \mathbf{X}^*) = p(\mathbf{m} | \boldsymbol{\psi}, \mathbf{X}^*)$ , for all  $\mathbf{y}$  and  $\boldsymbol{\psi}$ .

The second mechanism is missing at random (MAR). In this case, the probability of missing an element depends only on the observed data  $\mathbf{y}_o$  and does not depend on the missing data themselves,  $p(\mathbf{m}|\mathbf{y}, \boldsymbol{\psi}, \mathbf{X}^*) = p(\mathbf{m} | \mathbf{y}_o, \boldsymbol{\psi}, \mathbf{X}^*)$ , for all  $\mathbf{y}_o$  and  $\boldsymbol{\psi}$ . As demonstrated in Section 3, under assumptions of the MAR missing data mechanism and distinct parameters of the missing data model and the SEM, Bayesian inference on the SEM parameters can be performed without explicitly considering the missing data model and its parameters.

The third mechanism is missing not at random (MNAR). The probability that an element is missing depends on both the observed data and the unobserved data,  $p(\mathbf{m}|\mathbf{y}, \boldsymbol{\psi}, \mathbf{X}^*)$ . Under MNAR mechanism, we assume that the distribution of  $\mathbf{m}$  is independent given  $\mathbf{y}$ ,  $\mathbf{X}^*$ , and  $\boldsymbol{\psi}$ . With this assumption, the density  $p(\mathbf{m} | \mathbf{y}, \mathbf{X}^*, \boldsymbol{\psi})$  is a product of  $p(m_i | y_i, \mathbf{x}_i^*, \boldsymbol{\psi})$  for  $i = 1, \dots, n$ , where  $m_i$  and  $y_i$  denote the  $i^{th}$  elements of  $\mathbf{m}$  and  $\mathbf{y}$ , respectively, and  $\mathbf{x}_i^*$  is the  $i$ th row vector of  $\mathbf{X}^*$ . The parameter vector  $\boldsymbol{\psi} = (\boldsymbol{\psi}_x^\top, \boldsymbol{\psi}_y^\top)^\top$  consists of the fixed effects vector associated with covariates  $\mathbf{X}^*$ ;

$\boldsymbol{\psi}_{\mathbf{x}} = (\psi_0, \psi_1, \psi_2, \dots, \psi_q)^\top$ , and the fixed effect corresponding to  $\mathbf{y}$ , denoted as  $\psi_{\mathbf{y}}$ . A logistic regression model is used to model  $p(m_i | y_i, \mathbf{x}_i^*, \boldsymbol{\psi})$ , leading to:

$$p(\mathbf{m} | \mathbf{y}, \mathbf{X}^*, \boldsymbol{\psi}) = \prod_{i=1}^n \frac{e^{\mathbf{x}_i^* \boldsymbol{\psi}_{\mathbf{x}} + y_i \psi_{\mathbf{y}}}}{1 + e^{\mathbf{x}_i^* \boldsymbol{\psi}_{\mathbf{x}} + y_i \psi_{\mathbf{y}}}}. \quad (3)$$

In the presence of missing responses, the matrices  $\mathbf{X}$ ,  $\mathbf{W}$ , and  $\mathbf{M}_{\mathbf{y}}$  are divided into distinct parts as follows:

$$\mathbf{X} = \begin{pmatrix} \mathbf{X}_o \\ \mathbf{X}_u \end{pmatrix}, \quad \mathbf{W} = \begin{pmatrix} \mathbf{W}_{oo} & \mathbf{W}_{ou} \\ \mathbf{W}_{uo} & \mathbf{W}_{uu} \end{pmatrix}, \quad \mathbf{M}_{\mathbf{y}} = \begin{pmatrix} \mathbf{M}_{y,oo} & \mathbf{M}_{y,ou} \\ \mathbf{M}_{y,uo} & \mathbf{M}_{y,uu} \end{pmatrix}, \quad (4)$$

where  $\mathbf{X}_o$  and  $\mathbf{X}_u$  are the corresponding design matrices for the observed and unobserved responses, respectively, and  $\mathbf{W}_{oo}$ ,  $\mathbf{W}_{ou}$ ,  $\mathbf{W}_{uo}$ , and  $\mathbf{W}_{uu}$  represent the sub-matrices of  $\mathbf{W}$ , and  $\mathbf{M}_{y,oo}$ ,  $\mathbf{M}_{y,ou}$ ,  $\mathbf{M}_{y,uo}$ , and  $\mathbf{M}_{y,uu}$  are sub-matrices of  $\mathbf{M}_{\mathbf{y}}$ .

### 3 Bayesian Inference

Let  $\boldsymbol{\phi} = (\boldsymbol{\beta}^\top, \sigma_y^2, \rho)^\top$  and  $\boldsymbol{\psi} = (\boldsymbol{\psi}_{\mathbf{x}}^\top, \psi_{\mathbf{y}})^\top$  be the vectors of parameters of the SEM in Equation (1) and missing data model described in Section 2.2, respectively. Consider Bayesian inference for the parameters  $\boldsymbol{\phi}$ ,  $\boldsymbol{\psi}$ , and the missing values  $\mathbf{y}_u$ , with a prior distribution  $p(\mathbf{y}_u | \boldsymbol{\phi})p(\boldsymbol{\phi}, \boldsymbol{\psi})$ . The term  $p(\mathbf{y}_o, \mathbf{m} | \boldsymbol{\phi}, \boldsymbol{\psi}, \mathbf{y}_u)$  denotes the joint density of  $\mathbf{y}_o$  and  $\mathbf{m}$  conditional on  $\boldsymbol{\phi}$ ,  $\boldsymbol{\psi}$ , and  $\mathbf{y}_u$ , and the term  $p(\boldsymbol{\phi}, \boldsymbol{\psi}, \mathbf{y}_u | \mathbf{y}_o, \mathbf{m})$  is the joint posterior distribution of  $\boldsymbol{\phi}$ ,  $\boldsymbol{\psi}$  and  $\mathbf{y}_u$  and is given by

$$\begin{aligned} p(\boldsymbol{\phi}, \boldsymbol{\psi}, \mathbf{y}_u | \mathbf{y}_o, \mathbf{m}) &\propto p(\mathbf{y}_o, \mathbf{m} | \boldsymbol{\phi}, \boldsymbol{\psi}, \mathbf{y}_u) p(\mathbf{y}_u | \boldsymbol{\phi}) p(\boldsymbol{\phi}, \boldsymbol{\psi}) \\ &\propto p(\mathbf{y}, \mathbf{m} | \boldsymbol{\phi}, \boldsymbol{\psi}) p(\boldsymbol{\phi}, \boldsymbol{\psi}). \end{aligned} \quad (5)$$

The first term in RHS of Equation (5) is the joint distribution of  $\mathbf{y}$  and  $\mathbf{m}$ . The selection model (Little and Rubin, 2019) decomposes  $p(\mathbf{y}, \mathbf{m} | \boldsymbol{\phi}, \boldsymbol{\psi})$  into two factors as follows,

$$p(\mathbf{y}, \mathbf{m} | \boldsymbol{\phi}, \boldsymbol{\psi}) = p(\mathbf{y} | \boldsymbol{\phi}) p(\mathbf{m} | \mathbf{y}, \boldsymbol{\psi}), \quad (6)$$

where  $p(\mathbf{y} \mid \boldsymbol{\phi})$  denotes the density function of the SEM, which follows a multivariate Gaussian distribution with the mean vector  $\boldsymbol{\mu}_{\mathbf{y}}$  and covariance matrix  $\boldsymbol{\Sigma}_{\mathbf{y}}$  given in Table 1. Additionally,  $p(\mathbf{m} \mid \mathbf{y}, \boldsymbol{\psi})$  is the conditional distribution of  $\mathbf{m}$  given  $\mathbf{y}$  and the parameter  $\boldsymbol{\psi}$ . By substituting the selection model factorisation in Equation (6) into the joint distribution of  $\mathbf{y}$  and  $\mathbf{m}$  in Equation (5), we obtain

$$p(\boldsymbol{\phi}, \boldsymbol{\psi}, \mathbf{y}_u \mid \mathbf{y}_o, \mathbf{m}) \propto p(\mathbf{y} \mid \boldsymbol{\phi}) p(\mathbf{m} \mid \mathbf{y}, \boldsymbol{\psi}) p(\boldsymbol{\phi}, \boldsymbol{\psi}) \quad (7)$$

We now consider Bayesian inference under the MAR mechanism. Assume that  $\boldsymbol{\phi}$  and  $\boldsymbol{\psi}$  are distinct and a priori independent,  $p(\boldsymbol{\phi}, \boldsymbol{\psi}) = p(\boldsymbol{\phi})p(\boldsymbol{\psi})$ . Section 2.2 shows that under MAR  $p(\mathbf{m} \mid \mathbf{y}, \boldsymbol{\psi}) = p(\mathbf{m} \mid \mathbf{y}_o, \boldsymbol{\psi})$ . Substituting these terms to Equation (7), we obtain

$$\begin{aligned} p(\boldsymbol{\phi}, \boldsymbol{\psi}, \mathbf{y}_u \mid \mathbf{y}_o, \mathbf{m}) &\propto p(\mathbf{y} \mid \boldsymbol{\phi}) p(\mathbf{m} \mid \mathbf{y}_o, \boldsymbol{\psi}) p(\boldsymbol{\phi}) p(\boldsymbol{\psi}) \\ &\propto p(\mathbf{y}_o \mid \mathbf{y}_u, \boldsymbol{\phi}) p(\mathbf{y}_u \mid \boldsymbol{\phi}) p(\boldsymbol{\phi}) p(\mathbf{m} \mid \mathbf{y}_o, \boldsymbol{\psi}) p(\boldsymbol{\psi}) \\ &\propto p(\boldsymbol{\phi}, \mathbf{y}_u \mid \mathbf{y}_o) p(\boldsymbol{\psi} \mid \mathbf{m}, \mathbf{y}_o). \end{aligned} \quad (8)$$

The first term in Equation (8) is the posterior distribution of  $\boldsymbol{\phi}$  and  $\mathbf{y}_u$ , which does not contain  $\boldsymbol{\psi}$ . The second term is the posterior distribution of  $\boldsymbol{\psi}$ , which does not contain  $\boldsymbol{\phi}$  and  $\mathbf{y}_u$ . This suggests that Bayesian inference for  $\boldsymbol{\phi}$  and  $\mathbf{y}_u$  is based only on the posterior distribution  $p(\boldsymbol{\phi}, \mathbf{y}_u \mid \mathbf{y}_o)$ , ignoring the missing data model and its parameters,  $\boldsymbol{\psi}$ . Therefore, the joint posterior distribution of SEM parameters and missing data is

$$\begin{aligned} p(\boldsymbol{\phi}, \mathbf{y}_u \mid \mathbf{y}_o) &\propto p(\mathbf{y}_o \mid \boldsymbol{\phi}, \mathbf{y}_u) p(\mathbf{y}_u \mid \boldsymbol{\phi}) p(\boldsymbol{\phi}) \\ &\propto p(\mathbf{y} \mid \boldsymbol{\phi}) p(\boldsymbol{\phi}). \end{aligned} \quad (9)$$

We now consider Bayesian inference under the MNAR mechanism. When making Bayesian inference on parameters  $\boldsymbol{\phi}$  and missing values  $\mathbf{y}_u$ , even if we assume that  $\boldsymbol{\phi}$  and  $\boldsymbol{\psi}$  are distinct and a priori independent, we cannot ignore the missing data model.

The following notations are used in the subsequent sections. Let  $\boldsymbol{\theta}$  represent the vector of model parameters. The parameters are  $\boldsymbol{\theta} = \boldsymbol{\phi}$  under MAR and  $\boldsymbol{\theta} = (\boldsymbol{\phi}^\top, \boldsymbol{\psi}^\top)^\top$



Table 2: The vector of parameters ( $\boldsymbol{\theta}$ ), the set of observed data ( $\mathbf{O}$ ),  $h(\boldsymbol{\theta}, \mathbf{y}_u)$ , and the number of parameters to be estimated ( $S$ ) under MAR and MNAR

Missing mechanism	MAR	MNAR
$\boldsymbol{\theta}$	$\boldsymbol{\phi}$	$(\boldsymbol{\phi}^\top, \boldsymbol{\psi}^\top)^\top$
$\mathbf{O}$	$\mathbf{y}_o$	$(\mathbf{y}_o, \mathbf{m})$
$h(\boldsymbol{\theta}, \mathbf{y}_u)$	$p(\mathbf{y}   \boldsymbol{\phi})p(\boldsymbol{\phi})$	$p(\mathbf{y}   \boldsymbol{\phi}) p(\mathbf{m}   \mathbf{y}, \boldsymbol{\psi})p(\boldsymbol{\phi}, \boldsymbol{\psi})$
$S$	$r + 3$	$r + q + 5$

under MNAR. Let  $\mathbf{O}$  be the observed data. The observed data  $\mathbf{O} = \mathbf{y}_o$  under MAR and  $\mathbf{O} = (\mathbf{y}_o, \mathbf{m})$  under MNAR. Given the prior  $p(\mathbf{y}_u | \boldsymbol{\theta})p(\boldsymbol{\theta})$ , the joint posterior distribution of  $\boldsymbol{\theta}$  and  $\mathbf{y}_u$  given  $\mathbf{O}$ , denoted as  $p(\boldsymbol{\theta}, \mathbf{y}_u | \mathbf{O})$ , is

$$p(\boldsymbol{\theta}, \mathbf{y}_u | \mathbf{O}) \propto p(\mathbf{O} | \boldsymbol{\theta}, \mathbf{y}_u) p(\mathbf{y}_u | \boldsymbol{\theta}) p(\boldsymbol{\theta}), \quad (10)$$

where  $p(\mathbf{O} | \boldsymbol{\theta}, \mathbf{y}_u)$  denotes the density of  $\mathbf{O}$  conditional on  $\boldsymbol{\phi}$ ,  $\boldsymbol{\psi}$ , and  $\mathbf{y}_u$ . We also let  $h(\boldsymbol{\theta}, \mathbf{y}_u) = p(\mathbf{O} | \boldsymbol{\theta}, \mathbf{y}_u) p(\mathbf{y}_u | \boldsymbol{\theta}) p(\boldsymbol{\theta})$ . Table 2 summarises  $\boldsymbol{\theta}$ ,  $\mathbf{O}$ , the number of parameters  $S$ , and expressions for  $h(\boldsymbol{\theta}, \mathbf{y}_u)$  under different missing data mechanisms.

### 3.1 Variational Bayes Inference

Consider Bayesian inference for the parameters  $\boldsymbol{\theta}$  and the missing values  $\mathbf{y}_u$  given the observed values  $\mathbf{O}$ . Table 2 gives the parameters  $\boldsymbol{\theta}$  and the observed data  $\mathbf{O}$  for different missing data mechanisms. We consider the variational approximation  $q_\lambda(\boldsymbol{\theta}, \mathbf{y}_u)$ , indexed by the variational parameter  $\boldsymbol{\lambda}$  to approximate the joint posterior  $p(\boldsymbol{\theta}, \mathbf{y}_u | \mathbf{O})$ . The VB approach approximates this posterior distribution by minimising the Kullback-Leibler (KL) divergence between  $q_\lambda(\boldsymbol{\theta}, \mathbf{y}_u)$  and  $p(\boldsymbol{\theta}, \mathbf{y}_u | \mathbf{O})$ . The KL divergence between these two distributions is

$$\begin{aligned} \text{KL}(\boldsymbol{\lambda}) &= \text{KL}(q_\lambda(\boldsymbol{\theta}, \mathbf{y}_u) || p(\boldsymbol{\theta}, \mathbf{y}_u | \mathbf{O})) \\ &= \int \log \left( \frac{q_\lambda(\boldsymbol{\theta}, \mathbf{y}_u)}{p(\boldsymbol{\theta}, \mathbf{y}_u | \mathbf{O})} \right) q_\lambda(\boldsymbol{\theta}, \mathbf{y}_u) d\boldsymbol{\theta} d\mathbf{y}_u. \end{aligned} \quad (11)$$

Minimising KL divergence between  $q_{\lambda}(\boldsymbol{\theta}, \mathbf{y}_u)$  and  $p(\boldsymbol{\theta}, \mathbf{y}_u \mid \mathbf{O})$  is equivalent to maximising evidence lower bound (ELBO) on the marginal likelihood,  $\log p(\mathbf{O})$ , denoted by  $\mathcal{L}(\boldsymbol{\lambda})$ , with  $p(\mathbf{O}) = \int p(\mathbf{O} \mid \boldsymbol{\theta}, \mathbf{y}_u)p(\mathbf{y}_u \mid \boldsymbol{\theta})p(\boldsymbol{\theta}) d\boldsymbol{\theta}d\mathbf{y}_u$  (Blei et al., 2017). The ELBO is

$$\mathcal{L}(\boldsymbol{\lambda}) = \int \log \left( \frac{h(\boldsymbol{\theta}, \mathbf{y}_u)}{q_{\lambda}(\boldsymbol{\theta}, \mathbf{y}_u)} \right) q_{\lambda}(\boldsymbol{\theta}, \mathbf{y}_u) d\boldsymbol{\theta}d\mathbf{y}_u, \quad (12)$$

where  $h(\boldsymbol{\theta}, \mathbf{y}_u) = p(\mathbf{O} \mid \boldsymbol{\theta}, \mathbf{y}_u)p(\mathbf{y}_u \mid \boldsymbol{\theta})p(\boldsymbol{\theta})$ . Table 2 provides expressions for  $h(\boldsymbol{\theta}, \mathbf{y}_u)$  for SEM under MAR and MNAR. The ELBO does not have a closed form solution in general. To maximise ELBO with respect to variational parameters,  $\boldsymbol{\lambda}$ , stochastic gradient ascent (SGA) methods are used (Nott et al., 2012; Rezende et al., 2014a; Titsias and Lázaro-Gredilla, 2014; Titsias and Lázaro-Gredilla, 2015). The SGA method updates the initial value for  $\boldsymbol{\lambda}$  (say  $\boldsymbol{\lambda}^0$ ) according to the iterative scheme,

$$\boldsymbol{\lambda}^{(t+1)} = \boldsymbol{\lambda}^{(t)} + \mathbf{a}_t \circ \widehat{\nabla_{\boldsymbol{\lambda}} \mathcal{L}(\boldsymbol{\lambda}^{(t)})}, \quad (13)$$

where  $\widehat{\nabla_{\boldsymbol{\lambda}} \mathcal{L}(\boldsymbol{\lambda})}$  is an unbiased estimate of the gradient  $\nabla_{\boldsymbol{\lambda}} \mathcal{L}(\boldsymbol{\lambda})$ ,  $\mathbf{a}_t$  ( $t = 0, 1, \dots$ ), is a sequence of vector-valued learning rates, and they are chosen to satisfy the Robbins-Monro conditions  $\sum_t \mathbf{a}_t = \infty$  and  $\sum_t (\mathbf{a}_t)^2 \leq \infty$  (Robbins and Monro, 1951), that ensure convergence of the sequence  $\boldsymbol{\lambda}^{(t)}$  to a local optimum as  $t \rightarrow \infty$ , under regularity conditions (Bottou, 2010). The symbol  $\circ$  is the element-wise product of two vectors. The updating of Equation (13) is done until a stopping criterion is satisfied.

Adaptive learning rates are crucial for achieving rapid convergence of the algorithm. In this paper, we implement the ADADELTA algorithm proposed by Zeiler (2012) for calculating adaptive learning rates; see Section S1.3 of the online supplement for the algorithm. It is important to minimise the variance of the unbiased estimator of the gradient  $\widehat{\nabla_{\boldsymbol{\lambda}} \mathcal{L}(\boldsymbol{\lambda})}$  in Equation (13) since it influences both stability and convergence speed of the VB algorithm. In this study, we utilise the so-called reparameterisation trick (Kingma and Welling, 2013; Rezende et al., 2014b), which is often much more efficient compared to alternative methods (Xu et al., 2019).

### 3.2 Joint Variational Bayes algorithm

In this section, we introduce the first VB algorithm, which we call the joint variational Bayes (JVB) algorithm, which approximates the joint posterior of  $\theta$  and  $\mathbf{y}_u$  with a Gaussian variational approximation with a factor covariance structure (Ong et al., 2018). The variational distribution is parameterised as  $q_\lambda(\boldsymbol{\theta}, \mathbf{y}_u) \sim N((\boldsymbol{\theta}, \mathbf{y}_u); \boldsymbol{\mu}, \mathbf{B}\mathbf{B}^\top + \mathbf{D}^2)$ , where  $\boldsymbol{\mu}$  is the  $(S + n_u) \times 1$  mean vector,  $\mathbf{B}$  is an  $(S + n_u) \times p$  full rank matrix with  $p \ll (S + n_u)$ , and  $\mathbf{D}$  is an  $(S + n_u) \times (S + n_u)$  diagonal matrix having diagonal elements  $\mathbf{d} = (d_1, \dots, d_{S+n_u})$ . We further impose the restriction that the upper triangular elements of  $\mathbf{B}$  are all zero.

The ELBO in Equation (12) is an expectation with respect to  $q_\lambda$ ,

$$\mathcal{L}(\boldsymbol{\lambda}) = E_q [\log h(\boldsymbol{\theta}, \mathbf{y}_u) - \log q_\lambda(\boldsymbol{\theta}, \mathbf{y}_u)], \quad (14)$$

where  $E_q[\cdot]$  denotes the expectation with respect to  $q_\lambda$ . To apply the reparameterisation trick, we first need to generate samples from  $q_\lambda(\boldsymbol{\theta}, \mathbf{y}_u)$ . This can be achieved by first drawing  $\boldsymbol{\zeta} = (\boldsymbol{\eta}^\top, \boldsymbol{\epsilon}^\top)^\top$  (where  $\boldsymbol{\eta}$  is  $p$ -dimensional and  $\boldsymbol{\epsilon}$  is  $(S + n_u)$ -dimensional vectors) from a fixed density  $f_\zeta(\boldsymbol{\zeta})$  that does not depend on the variational parameters, and then calculating  $(\boldsymbol{\theta}, \mathbf{y}_u) = u(\boldsymbol{\zeta}, \boldsymbol{\lambda}) = \boldsymbol{\mu} + \mathbf{B}\boldsymbol{\eta} + \mathbf{d} \circ \boldsymbol{\epsilon}$ . We let  $\boldsymbol{\zeta} = (\boldsymbol{\eta}^\top, \boldsymbol{\epsilon}^\top)^\top \sim N(\mathbf{0}, \mathbf{I}_{S+n_u+p})$ , where  $\mathbf{0}$  is the zero mean vector of length  $(S + n_u + p)$  and  $\mathbf{I}_{m+n_u+p}$  is the identity matrix of size  $S + n_u + p$ . i.e., the distribution  $f_\zeta(\cdot)$  is standard normal. Then, the expectation in Equation (14) is expressed with respect to the distribution  $f_\zeta$  as

$$\begin{aligned} \mathcal{L}(\boldsymbol{\lambda}) &= E_q [\log h(\boldsymbol{\theta}, \mathbf{y}_u) - \log q_\lambda(\boldsymbol{\theta}, \mathbf{y}_u)] \\ &= E_{f_\zeta} [\log h(u(\boldsymbol{\zeta}, \boldsymbol{\lambda})) - \log q_\lambda(u(\boldsymbol{\zeta}, \boldsymbol{\lambda}))], \end{aligned} \quad (15)$$

and differentiating  $\mathcal{L}(\boldsymbol{\lambda})$  under the integral sign, we obtain

$$\begin{aligned} \nabla_\lambda \mathcal{L}(\boldsymbol{\lambda}) &= E_{f_\zeta} [\nabla_\lambda \log h(u(\boldsymbol{\zeta}, \boldsymbol{\lambda})) - \nabla_\lambda \log q_\lambda(u(\boldsymbol{\zeta}, \boldsymbol{\lambda}))], \\ &= E_{f_\zeta} \left[ \frac{du(\boldsymbol{\zeta}, \boldsymbol{\lambda})^\top}{d\boldsymbol{\lambda}} \{ \nabla_{\boldsymbol{\theta}, \mathbf{y}_u} \log h(\boldsymbol{\theta}, \mathbf{y}_u) - \nabla_{\boldsymbol{\theta}, \mathbf{y}_u} \log q_\lambda(\boldsymbol{\theta}, \mathbf{y}_u) \} \right], \end{aligned} \quad (16)$$

where  $\frac{du(\boldsymbol{\zeta}, \boldsymbol{\lambda})}{d\boldsymbol{\lambda}}$  is the derivative of the transformation  $u(\boldsymbol{\zeta}, \boldsymbol{\lambda}) = \boldsymbol{\mu} + \mathbf{B}\boldsymbol{\eta} + \mathbf{d} \circ \boldsymbol{\epsilon}$  with respect to the variational parameters  $\boldsymbol{\lambda} = (\boldsymbol{\mu}^\top, \text{vech}(\mathbf{B})^\top, \mathbf{d}^\top)^\top$ , where "vech" operator is the vectorisation of a matrix by stacking its columns from left to right. Algorithm 1 gives the JVB algorithm. Analytical expressions for  $\frac{du(\boldsymbol{\zeta}, \boldsymbol{\lambda})}{d\boldsymbol{\lambda}}$ ,  $\nabla_{\boldsymbol{\theta}, \mathbf{y}_u} \log q_\lambda(\boldsymbol{\theta}, \mathbf{y}_u)$ ,  $\nabla_{\boldsymbol{\theta}, \mathbf{y}_u} \log h(\boldsymbol{\theta}, \mathbf{y}_u)$ , and the formulae for constructing an unbiased estimate  $\widehat{\nabla_{\boldsymbol{\lambda}} \mathcal{L}(\boldsymbol{\lambda})}$  for  $\nabla_{\boldsymbol{\lambda}} \mathcal{L}(\boldsymbol{\lambda})$  in step 4 of Algorithm 1 are given in Section S1.1 of the online supplement.

---

**Algorithm 1** JVB algorithm

---

- 1: Initialize  $\boldsymbol{\lambda}^{(0)} = (\boldsymbol{\mu}^{\top(0)}, \text{vech}(\mathbf{B})^{\top(0)}, \mathbf{d}^{\top(0)})^\top$  and set  $t = 0$
  - 2: **repeat**
  - 3:   Generate  $(\boldsymbol{\eta}^{(t)}, \boldsymbol{\epsilon}^{(t)}) \sim N(\mathbf{0}, \mathbf{I}_{S+n_u+p})$
  - 4:   Construct unbiased estimates  $\widehat{\nabla_{\boldsymbol{\mu}} \mathcal{L}(\boldsymbol{\lambda})}$ ,  $\widehat{\nabla_{\text{vech}(\mathbf{B})} \mathcal{L}(\boldsymbol{\lambda})}$ , and  $\widehat{\nabla_{\mathbf{d}} \mathcal{L}(\boldsymbol{\lambda})}$  using Equations (S3), (S4) and (S5) in Section S1.1 of the online supplement at  $\boldsymbol{\lambda}^{(t)}$ .
  - 5:   Set adaptive learning rates for the variational means,  $\mathbf{a}_{\boldsymbol{\mu}}^{(t)}$  and the variational parameters  $\text{vech}(\mathbf{B})$  and  $\mathbf{d}$ ,  $\mathbf{a}_{\text{vech}(\mathbf{B})}^{(t)}$  and  $\mathbf{a}_{\mathbf{d}}^{(t)}$ , respectively, using ADADELTA described in Section S1.3 of the online supplement.
  - 6:   Set  $\boldsymbol{\mu}^{(t+1)} = \boldsymbol{\mu}^{(t)} + \mathbf{a}_{\boldsymbol{\mu}}^{(t)} \circ \widehat{\nabla_{\boldsymbol{\mu}} \mathcal{L}(\boldsymbol{\lambda}^{(t)})}$ .
  - 7:   Set  $\text{vech}(\mathbf{B})^{(t+1)} = \text{vech}(\mathbf{B})^{(t)} + \mathbf{a}_{\text{vech}(\mathbf{B})}^{(t)} \circ \widehat{\nabla_{\text{vech}(\mathbf{B})} \mathcal{L}(\boldsymbol{\lambda}^{(t)})}$ .
  - 8:   Set  $\mathbf{d}^{(t+1)} = \mathbf{d}^{(t)} + \mathbf{a}_{\mathbf{d}}^{(t)} \circ \widehat{\nabla_{\mathbf{d}} \mathcal{L}(\boldsymbol{\lambda}^{(t)})}$ .
  - 9:   Set  $\boldsymbol{\lambda}^{(t+1)} = (\boldsymbol{\mu}^{\top(t+1)}, \text{vech}(\mathbf{B})^{\top(t+1)}, \mathbf{d}^{\top(t+1)})^\top$ , and  $t = t + 1$
  - 10: **until** some stopping rule is satisfied
- 

### 3.3 Hybrid Variational Bayes algorithm

In this section, we describe the second VB algorithm, which we call the hybrid variational Bayes (HVB) algorithm. The variational distribution  $q_\lambda(\boldsymbol{\theta}, \mathbf{y}_u)$  is given by

$$q_\lambda(\boldsymbol{\theta}, \mathbf{y}_u) = p(\mathbf{y}_u \mid \mathbf{O}, \boldsymbol{\theta}) q_\lambda^0(\boldsymbol{\theta}), \quad (17)$$

where  $p(\mathbf{y}_u \mid \mathbf{O}, \boldsymbol{\theta})$  is the conditional distribution of missing data  $\mathbf{y}_u$  given observed data  $\mathbf{O}$  and the model parameters  $\boldsymbol{\theta}$  and  $q_\lambda^0(\boldsymbol{\theta})$  is the Gaussian variational approximation with a factor covariance structure for approximating the posterior distribution of  $\boldsymbol{\theta}$ .

Given the variational approximation  $q_\lambda(\boldsymbol{\theta}, \mathbf{y}_u)$  in Equation (17), the expectation in

Equation (14) is expressed as

$$\begin{aligned}\mathcal{L}(\boldsymbol{\lambda}) &= E_q(\log h(\boldsymbol{\theta}, \mathbf{y}_u) - \log q_{\boldsymbol{\lambda}}(\boldsymbol{\theta}, \mathbf{y}_u)) \\ &= E_q(\log p(\mathbf{O} | \mathbf{y}_u, \boldsymbol{\theta}) + \log p(\mathbf{y}_u | \boldsymbol{\theta}) + \log p(\boldsymbol{\theta}) - \log q_{\boldsymbol{\lambda}}^0(\boldsymbol{\theta}) - \log p(\mathbf{y}_u | \mathbf{O}, \boldsymbol{\theta})).\end{aligned}\tag{18}$$

Using the Bayes rule, we write  $p(\mathbf{y}_u | \mathbf{O}, \boldsymbol{\theta}) = p(\mathbf{O} | \mathbf{y}_u, \boldsymbol{\theta})p(\mathbf{y}_u | \boldsymbol{\theta})/p(\mathbf{O} | \boldsymbol{\theta})$ . Substituting this into Equation (18), we obtain

$$\mathcal{L}(\boldsymbol{\lambda}) = E_q(\log p(\mathbf{O} | \boldsymbol{\theta}) + \log p(\boldsymbol{\theta}) - \log q_{\boldsymbol{\lambda}}^0(\boldsymbol{\theta})) = \mathcal{L}^0(\boldsymbol{\lambda}),\tag{19}$$

where  $\mathcal{L}^0(\boldsymbol{\lambda})$  is the ELBO resulting from approximating only the posterior distribution of model parameters;  $p(\boldsymbol{\theta} | \mathbf{O})$ , directly via the variational distribution  $q_{\boldsymbol{\lambda}}^0(\boldsymbol{\theta})$ .

We now describe the  $q_{\boldsymbol{\lambda}}^0(\boldsymbol{\theta})$  in more detail. We assume that  $q_{\boldsymbol{\lambda}}^0(\boldsymbol{\theta}) \sim N(\boldsymbol{\theta}; \boldsymbol{\mu}_{\boldsymbol{\theta}}, \mathbf{B}_{\boldsymbol{\theta}}\mathbf{B}_{\boldsymbol{\theta}}^{\top} + \mathbf{D}_{\boldsymbol{\theta}}^2)$ , where  $\boldsymbol{\mu}_{\boldsymbol{\theta}}$  is a  $S \times 1$  vector of variational means,  $\mathbf{B}_{\boldsymbol{\theta}}$  is an  $S \times p$  matrix with the upper triangular elements are set to zero, and  $\mathbf{D}_{\boldsymbol{\theta}}$  is an  $S \times S$  diagonal matrix having diagonal elements  $\mathbf{d}_{\boldsymbol{\theta}} = (d_{\boldsymbol{\theta},1}, \dots, d_{\boldsymbol{\theta},S})$ . The vector of variational parameters is  $\boldsymbol{\lambda}_{\boldsymbol{\theta}} = (\boldsymbol{\mu}_{\boldsymbol{\theta}}^{\top}, \text{vech}(\mathbf{B}_{\boldsymbol{\theta}})^{\top}, \mathbf{d}_{\boldsymbol{\theta}}^{\top})^{\top}$ .

To apply the reparameterisation trick, first we need to generate samples from  $q_{\boldsymbol{\lambda}}^0(\boldsymbol{\theta})$ . This can be achieved by first drawing  $\boldsymbol{\delta}^0 = (\boldsymbol{\eta}^{0\top}, \boldsymbol{\epsilon}^{0\top})^{\top}$  (where  $\boldsymbol{\eta}^0$  is  $p$ -dimensional and  $\boldsymbol{\epsilon}^0$  is  $S$ -dimensional vectors) from a density  $f_{\boldsymbol{\delta}^0}(\boldsymbol{\delta}^0)$  that does not depend on the variational parameters, and then calculating  $\boldsymbol{\theta} = t^0(\boldsymbol{\delta}^0, \boldsymbol{\lambda}_{\boldsymbol{\theta}}) = \boldsymbol{\mu}_{\boldsymbol{\theta}} + \mathbf{B}_{\boldsymbol{\theta}}\boldsymbol{\eta}^0 + \mathbf{d}_{\boldsymbol{\theta}} \circ \boldsymbol{\epsilon}^0$ . We let  $\boldsymbol{\delta}^0 = (\boldsymbol{\eta}^{0\top}, \boldsymbol{\epsilon}^{0\top})^{\top} \sim N(\mathbf{0}, \mathbf{I}_{S+p})$ , where  $\mathbf{I}_{S+p}$  is the identity matrix of size  $S + p$ . i.e., the distribution  $f_{\boldsymbol{\delta}^0}(\cdot)$  is standard normal.

Let  $\boldsymbol{\delta} = (\boldsymbol{\delta}^{0\top}, \mathbf{y}_u^{\top})^{\top}$  with the product density  $f_{\boldsymbol{\delta}}(\boldsymbol{\delta}) = f_{\boldsymbol{\delta}^0}(\boldsymbol{\delta}^0)p(\mathbf{y}_u | t^0(\boldsymbol{\delta}^0, \boldsymbol{\lambda}_{\boldsymbol{\theta}}), \mathbf{O})$ . There exists a vector-valued transformation  $t$  from  $\boldsymbol{\delta}$  to the parameter space and augmented missing value space given by  $(\boldsymbol{\theta}^{\top}, \mathbf{y}_u^{\top})^{\top} = t(\boldsymbol{\delta}, \boldsymbol{\lambda}_{\boldsymbol{\theta}}) = (t^0(\boldsymbol{\delta}^0, \boldsymbol{\lambda}_{\boldsymbol{\theta}})^{\top}, \mathbf{y}_u^{\top})^{\top} = ((\boldsymbol{\mu}_{\boldsymbol{\theta}} + \mathbf{B}_{\boldsymbol{\theta}}\boldsymbol{\eta}^0 + \mathbf{d}_{\boldsymbol{\theta}} \circ \boldsymbol{\epsilon}^0)^{\top}, \mathbf{y}_u^{\top})^{\top}$ . The reparameterisation gradient of the ELBO in Equa-

tion (19) is obtained by differentiating under the integral sign as follows

$$\nabla_{\boldsymbol{\lambda}} \mathcal{L}(\boldsymbol{\lambda}) = E_{f_{\boldsymbol{\delta}}} \left[ \frac{dt^0(\boldsymbol{\delta}^0, \boldsymbol{\lambda}_{\boldsymbol{\theta}})^{\top}}{d\boldsymbol{\lambda}_{\boldsymbol{\theta}}} (\nabla_{\boldsymbol{\theta}} \log h(\boldsymbol{\theta}, \mathbf{y}_u) - \nabla_{\boldsymbol{\theta}} \log q_{\boldsymbol{\lambda}}^0(\boldsymbol{\theta})) \right]; \quad (20)$$

where  $\frac{dt^0(\boldsymbol{\delta}^0, \boldsymbol{\lambda}_{\boldsymbol{\theta}})}{d\boldsymbol{\lambda}_{\boldsymbol{\theta}}}$  is the derivative of the transformation  $t^0(\boldsymbol{\delta}^0, \boldsymbol{\lambda}_{\boldsymbol{\theta}}) = \boldsymbol{\mu}_{\boldsymbol{\theta}} + \mathbf{B}_{\boldsymbol{\theta}} \boldsymbol{\eta}^0 + \mathbf{d}_{\boldsymbol{\theta}} \circ \boldsymbol{\epsilon}^0$  with respect to the variational parameters  $\boldsymbol{\lambda}_{\boldsymbol{\theta}} = (\boldsymbol{\mu}_{\boldsymbol{\theta}}^{\top}, \text{vech}(\mathbf{B}_{\boldsymbol{\theta}})^{\top}, \mathbf{d}_{\boldsymbol{\theta}}^{\top})^{\top}$ . The proof is similar to Loaiza-Maya et al. (2022) and can be found in Section S1.2 of the online supplement.

Algorithm 2 gives the HVB algorithm. Analytical expressions for  $\frac{dt^0(\boldsymbol{\delta}^0, \boldsymbol{\lambda}_{\boldsymbol{\theta}})}{d\boldsymbol{\lambda}_{\boldsymbol{\theta}}}$ ,  $\nabla_{\boldsymbol{\theta}} \log q_{\boldsymbol{\lambda}}^0(\boldsymbol{\theta})$ ,  $\nabla_{\boldsymbol{\theta}} \log h(\boldsymbol{\theta}, \mathbf{y}_u)$ , and the formulae for constructing an unbiased estimate  $\widehat{\nabla_{\boldsymbol{\lambda}} \mathcal{L}(\boldsymbol{\lambda})}$  for  $\nabla_{\boldsymbol{\lambda}} \mathcal{L}(\boldsymbol{\lambda})$  in step 6 of Algorithm 2 using a single sample  $\boldsymbol{\delta} = (\boldsymbol{\delta}^0, \mathbf{y}_u^{\top})^{\top}$  drawn from  $f_{\boldsymbol{\delta}^0}$ , and  $p(\mathbf{y}_u | \boldsymbol{\theta}, \mathbf{O})$  are detailed in Section S1.2 of the online supplement.

---

#### Algorithm 2 HVB algorithm

---

- 1: Initialize  $\boldsymbol{\lambda}_{\boldsymbol{\theta}}^{(0)} = (\boldsymbol{\mu}_{\boldsymbol{\theta}}^{\top(0)}, \text{vech}(\mathbf{B}_{\boldsymbol{\theta}})^{\top(0)}, \mathbf{d}_{\boldsymbol{\theta}}^{\top(0)})$  and set  $t = 0$
  - 2: **repeat**
  - 3:   Generate  $(\boldsymbol{\eta}^{0(t)}, \boldsymbol{\epsilon}^{0(t)}) \sim N(\mathbf{0}, \mathbf{I}_{S+p})$
  - 4:   Generate  $\boldsymbol{\theta}^{(t)} \sim q_{\boldsymbol{\lambda}^{(t)}}^0(\boldsymbol{\theta})$  using its reparameterised representation.
  - 5:   Generate  $\mathbf{y}_u^{(t)} \sim p(\mathbf{y}_u | \boldsymbol{\theta}^{(t)}, \mathbf{O})$
  - 6:   Construct unbiased estimates  $\widehat{\nabla_{\boldsymbol{\mu}_{\boldsymbol{\theta}}} \mathcal{L}(\boldsymbol{\lambda})}$ ,  $\widehat{\nabla_{\text{vech}(\mathbf{B}_{\boldsymbol{\theta}})} \mathcal{L}(\boldsymbol{\lambda})}$ , and  $\widehat{\nabla_{\mathbf{d}_{\boldsymbol{\theta}}} \mathcal{L}(\boldsymbol{\lambda})}$  using Equations (S11), (S12) and (S13) in Section S1.2 of the online supplement.
  - 7:   Set adaptive learning rates for the variational means  $\mathbf{a}_{\boldsymbol{\mu}_{\boldsymbol{\theta}}}^{(t)}$  and the variational parameters  $\text{vech}(\mathbf{B}_{\boldsymbol{\theta}})$  and  $\mathbf{d}_{\boldsymbol{\theta}}$ ,  $\mathbf{a}_{\text{vech}(\mathbf{B}_{\boldsymbol{\theta}})}^{(t)}$  and  $\mathbf{a}_{\mathbf{d}_{\boldsymbol{\theta}}}^{(t)}$ , using ADADELTA described in Section S1.3 of the online supplement.
  - 8:   Set  $\boldsymbol{\mu}_{\boldsymbol{\theta}}^{(t+1)} = \boldsymbol{\mu}_{\boldsymbol{\theta}}^{(t)} + \mathbf{a}_{\boldsymbol{\mu}_{\boldsymbol{\theta}}}^{(t)} \circ \widehat{\nabla_{\boldsymbol{\mu}_{\boldsymbol{\theta}}} \mathcal{L}(\boldsymbol{\lambda}^{(t)})}$ .
  - 9:   Set  $\text{vech}(\mathbf{B}_{\boldsymbol{\theta}})^{(t+1)} = \text{vech}(\mathbf{B}_{\boldsymbol{\theta}})^{(t)} + \mathbf{a}_{\text{vech}(\mathbf{B}_{\boldsymbol{\theta}})}^{(t)} \circ \widehat{\nabla_{\text{vech}(\mathbf{B}_{\boldsymbol{\theta}})} \mathcal{L}(\boldsymbol{\lambda}^{(t)})}$ .
  - 10:   Set  $\mathbf{d}_{\boldsymbol{\theta}}^{(t+1)} = \mathbf{d}_{\boldsymbol{\theta}}^{(t)} + \mathbf{a}_{\mathbf{d}_{\boldsymbol{\theta}}}^{(t)} \circ \widehat{\nabla_{\mathbf{d}_{\boldsymbol{\theta}}} \mathcal{L}(\boldsymbol{\lambda}^{(t)})}$ .
  - 11:   Set  $\boldsymbol{\lambda}_{\boldsymbol{\theta}}^{(t+1)} = (\boldsymbol{\mu}_{\boldsymbol{\theta}}^{\top(t+1)}, \text{vech}(\mathbf{B}_{\boldsymbol{\theta}})^{\top(t+1)}, \mathbf{d}_{\boldsymbol{\theta}}^{\top(t+1)})^{\top}$ , and  $t = t + 1$
  - 12: **until** some stopping rule is satisfied
- 

### 3.4 HVB under MAR

Implementing step 5 of Algorithm 2 involves generating the missing values  $\mathbf{y}_u$  from their conditional distribution  $p(\mathbf{y}_u | \boldsymbol{\theta}^{(t)}, \mathbf{O})$ , where  $\boldsymbol{\theta}^{(t)}$  represents the parameters generated in step 4 of  $t^{\text{th}}$  iteration of the algorithm. Under MAR, the conditional distribution  $p(\mathbf{y}_u | \boldsymbol{\theta}^{(t)}, \mathbf{O}) = p(\mathbf{y}_u | \boldsymbol{\phi}^{(t)}, \mathbf{y}_o)$  is available in closed form, which follows a multivariate

Gaussian distribution with the mean vector given by  $\mathbf{X}_u\boldsymbol{\beta} - \mathbf{M}_{y,uu}^{-1}\mathbf{M}_{y,uo}(\mathbf{y}_o - \mathbf{X}_o\boldsymbol{\beta})$  and the covariance matrix given by  $\sigma_y^2\mathbf{M}_{y,uu}^{-1}$ , see Suesse and Zammit-Mangion (2017).

As the total number of observations  $n$  and the number of missing values  $n_u$  increase, sampling directly from  $p(\mathbf{y}_u \mid \boldsymbol{\theta}^{(t)}, \mathbf{y}_o)$  becomes computationally expensive. We now discuss how to improve the efficiency of step 5 of the HVB algorithm given in Algorithm 2 under MAR. We start with partitioning the unobserved responses vector into  $k$  blocks, such that  $\mathbf{y}_u = (\mathbf{y}_{u_1}^\top, \dots, \mathbf{y}_{u_k}^\top)^\top$ . Then we implement a Gibbs step to update  $\mathbf{y}_u$  one block at a time by sampling from the full conditional distribution  $p(\mathbf{y}_{u_j} \mid \boldsymbol{\phi}^{(t)}, \mathbf{y}_o, \mathbf{y}_u^{(-j)})$ , for  $j = 1, \dots, k$ , where  $\mathbf{y}_{u_j}$  is the updated block and  $\mathbf{y}_u^{(-j)} = (\mathbf{y}_{u_1}^\top, \dots, \mathbf{y}_{u_{j-1}}^\top, \mathbf{y}_{u_{j+1}}^\top, \dots, \mathbf{y}_{u_k}^\top)^\top$  is the remaining blocks. The complete response vector  $\mathbf{y}$  can now be written as  $\mathbf{y} = (\mathbf{y}_{s_j}^\top, \mathbf{y}_{u_j}^\top)^\top$ , where  $\mathbf{y}_{s_j} = (\mathbf{y}_o^\top, \mathbf{y}_u^{(-j)\top})^\top$ . Based on this partitioning of  $\mathbf{y}$ , the following partitioned matrices are defined:

$$\mathbf{X} = \begin{pmatrix} \mathbf{X}_{s_j} \\ \mathbf{X}_{u_j} \end{pmatrix}, \quad \mathbf{W} = \begin{pmatrix} \mathbf{W}_{s_j s_j} & \mathbf{W}_{s_j u_j} \\ \mathbf{W}_{u_j s_j} & \mathbf{W}_{u_j u_j} \end{pmatrix}, \quad \mathbf{M}_y = \begin{pmatrix} \mathbf{M}_{y, s_j s_j} & \mathbf{M}_{y, s_j u_j} \\ \mathbf{M}_{y, u_j s_j} & \mathbf{M}_{y, u_j u_j} \end{pmatrix}, \quad (21)$$

where  $\mathbf{X}_{s_j}$  is the corresponding design matrix for the observed responses, and the unobserved responses that are not in the  $j^{\text{th}}$  block (i.e.  $\mathbf{X}_{s_j} = (\mathbf{X}_o^\top, \mathbf{X}_u^{(-j)\top})^\top$ ) and  $\mathbf{X}_{u_j}$  is the corresponding design matrix for  $j^{\text{th}}$  block of unobserved responses. Similarly,  $\mathbf{W}_{s_j s_j}$ ,  $\mathbf{W}_{s_j u_j}$ ,  $\mathbf{W}_{u_j s_j}$ , and  $\mathbf{W}_{u_j u_j}$  represent the sub-matrices of  $\mathbf{W}$ , and  $\mathbf{M}_{y, s_j s_j}$ ,  $\mathbf{M}_{y, s_j u_j}$ ,  $\mathbf{M}_{y, u_j s_j}$ , and  $\mathbf{M}_{y, u_j u_j}$  are sub-matrices of  $\mathbf{M}_y$ .

Algorithm 3 outlines the proposed Gibbs sampling steps. The full conditional distribution  $p(\mathbf{y}_{u_j} \mid \boldsymbol{\phi}^{(t)}, \mathbf{y}_o, \mathbf{y}_u^{(-j)}) = p(\mathbf{y}_{u_j} \mid \boldsymbol{\phi}^{(t)}, \mathbf{y}_{s_j})$ , follows a multivariate Gaussian distribution with the mean  $\mathbf{X}_{u_j}\boldsymbol{\beta} - \mathbf{M}_{y, u_j u_j}^{-1}\mathbf{M}_{y, u_j s_j}(\mathbf{y}_{s_j} - \mathbf{X}_{s_j}\boldsymbol{\beta})$  and the covariance matrix  $\sigma_y^2\mathbf{M}_{y, u_j u_j}^{-1}$ . The HVB algorithm implemented using the Gibbs steps presented in Algorithm 3, which we call HVB-G in subsequent sections, accelerates the generation of samples of missing values from their conditional distribution  $p(\mathbf{y}_u \mid \boldsymbol{\phi}, \mathbf{y}_o)$  when  $n$  and  $n_u$  are large. We replace step 5 of the HVB algorithm given in Algorithm 2 by the proposed Gibbs steps when  $n_u$  is more than 1,000 as directly sampling from  $p(\mathbf{y}_u \mid \boldsymbol{\phi}, \mathbf{y}_o)$  requires inverting a  $1000 \times 1000$  covariance matrix. In the Gibbs sampling steps, we must specify the block

size ( $k^*$ ) and the number of Gibbs iterations ( $N_1$ ). After some experimentation, we set  $N_1 = 5$  with a block size of  $k^* = 500$ , as these values consistently produce accurate inference results within a reasonable computational time.

---

**Algorithm 3** Gibbs steps within the  $t^{\text{th}}$  iteration of the HVB algorithm under MAR when  $n$  and  $n_u$  are large

---

- 1: Initialise missing values  $\mathbf{y}_{u,0} = (\mathbf{y}_{u_1,0}^\top, \dots, \mathbf{y}_{u_k,0}^\top)^\top \sim p(\mathbf{y}_u | \boldsymbol{\phi}^{(t)}, \mathbf{y}_o)$
  - 2: **for**  $i=1, \dots, N_1$  **do**
  - 3:   **for**  $j=1, \dots, k$  **do**
  - 4:     Sample  $\mathbf{y}_{u_j,i}$  from the conditional distribution  $p(\mathbf{y}_{u_j,i} | \boldsymbol{\phi}^{(t)}, \mathbf{y}_o, \mathbf{y}_{u,i-1}^{(-j)})$ , where  
 $\mathbf{y}_{u,i-1}^{(-j)} = (\mathbf{y}_{u_1,i}^\top, \mathbf{y}_{u_2,i}^\top, \dots, \mathbf{y}_{u_{j-1},i}^\top, \mathbf{y}_{u_{j+1},i-1}^\top, \dots, \mathbf{y}_{u_k,i-1}^\top)^\top$ .
  - 5:   **end for**
  - 6:    $\mathbf{y}_{u,i} = (\mathbf{y}_{u_1,i}^\top, \dots, \mathbf{y}_{u_k,i}^\top)^\top$
  - 7: **end for**
  - 8: Output  $\mathbf{y}_u^{(t)} = \mathbf{y}_{u,N_1}$
- 

### 3.5 HVB under MNAR

Under MNAR, direct sampling from the conditional distribution  $p(\mathbf{y}_u | \boldsymbol{\theta}^{(t)}, \mathbf{O}) = p(\mathbf{y}_u | \boldsymbol{\phi}^{(t)}, \boldsymbol{\psi}^{(t)}, \mathbf{y}_o, \mathbf{m})$  is not feasible, as the conditional posterior distribution is not available in closed form. To sample from  $p(\mathbf{y}_u | \boldsymbol{\phi}^{(t)}, \boldsymbol{\psi}^{(t)}, \mathbf{y}_o, \mathbf{m})$ , we employ the MCMC steps presented in Algorithm 4, which employs  $p(\mathbf{y}_u | \boldsymbol{\phi}^{(t)}, \mathbf{y}_o)$  as the proposal.

---

**Algorithm 4** MCMC steps within the  $t^{\text{th}}$  iteration of the HVB algorithm under MNAR

---

- 1: Initialize missing values  $\mathbf{y}_{u,0} \sim p(\mathbf{y}_u | \boldsymbol{\phi}^{(t)}, \mathbf{y}_o)$
  - 2: **for**  $i=1, \dots, N_1$  **do**
  - 3:   Sample  $\mathbf{y}_u^*$  from the proposal distribution  $p(\mathbf{y}_u^* | \boldsymbol{\phi}^{(t)}, \mathbf{y}_o)$ , which follows a multivariate Gaussian with the mean vector given by  $\mathbf{X}_u \boldsymbol{\beta} - \mathbf{M}_{y,uu}^{-1} \mathbf{M}_{y,uo} (\mathbf{y}_o - \mathbf{X}_o \boldsymbol{\beta})$  and the covariance matrix given by  $\sigma_y^2 \mathbf{M}_{y,uu}^{-1}$ .
  - 4:   Sample  $u$  from uniform distribution,  $u \sim \mathcal{U}(0, 1)$
  - 5:   Calculate  $a = \min \left( 1, \frac{p(\mathbf{m} | \mathbf{y}^*, \boldsymbol{\psi}^{(t)})}{p(\mathbf{m} | \mathbf{y}_{i-1}, \boldsymbol{\psi}^{(t)})} \right)$ , where  $\mathbf{y}^* = (\mathbf{y}_o^\top, \mathbf{y}_u^{*\top})$  and  $\mathbf{y}_{i-1} = (\mathbf{y}_o^\top, \mathbf{y}_{u,i-1}^\top)$
  - 6:   **if**  $a > u$  **then**
  - 7:      $\mathbf{y}_{u,i} = \mathbf{y}_u^*$
  - 8:   **else**
  - 9:      $\mathbf{y}_{u,i} = \mathbf{y}_{u,i-1}$
  - 10:   **end if**
  - 11: **end for**
  - 12: Output  $\mathbf{y}_u^{(t)} = \mathbf{y}_{u,N_1}$
- 

The MCMC steps in Algorithm 4 generates samples from the conditional distribution



$p(\mathbf{y}_u \mid \boldsymbol{\phi}^{(t)}, \boldsymbol{\psi}^{(t)}, \mathbf{y}_o, \mathbf{m})$ . However, as  $n$  and  $n_u$  increase, the HVB algorithm implemented using these MCMC steps does not estimate the parameters accurately because of the low acceptance percentage. After some experimentation, we found that achieving an acceptance percentage between 20% and 30% is necessary to balance between accurate posterior inference and computational cost. To improve the acceptance percentage, we partition  $\mathbf{y}_u$  into  $k$  blocks as discussed in Section 3.4, and update one block at a time using proposals from  $p(\mathbf{y}_{u_j} \mid \boldsymbol{\phi}^{(t)}, \mathbf{y}_o, \mathbf{y}_u^{(-j)})$ . Algorithm 5 outlines the MCMC steps for sampling the missing values one block at a time.

Updating all  $k$  blocks for each of the  $N_1$  MCMC iterations is computationally expensive, as for each block, the mean vector and covariance matrix of the conditional posterior distribution of  $p(\mathbf{y}_{u_j} \mid \boldsymbol{\phi}, \mathbf{y}_{s_j})$  must be calculated. This computational bottleneck can be overcome by updating only a randomly selected set of blocks at each iteration, so the computation of the conditional distribution is limited to the number of updated blocks, not the number of total blocks,  $k$ . We suggest that updating randomly selected 3 blocks in each MCMC iteration is sufficient to obtain reliable inference with a smaller computational cost; see simulation results in Section 4.2 for further details. The MCMC scheme for updating a randomly selected number of  $k'$  blocks can be obtained by modifying the MCMC scheme in Algorithm 5.

For the remaining sections, the HVB algorithm implemented via the MCMC scheme in Algorithm 4 without blocking  $\mathbf{y}_u$  is called the HVB-No Block abbreviated as HVB-NoB. The HVB algorithm implemented through the MCMC scheme in Algorithm 5 is called HVB-All Block abbreviated as HVB-AllB, and the HVB using the MCMC scheme that updates only randomly selected three blocks is referred to as HVB-3B. The criteria for setting tuning parameters of the proposed MCMC schemes, such as the number of MCMC steps  $N_1$  and block size  $k^*$ , are discussed in Section 4.2.

---

**Algorithm 5** MCMC steps within the  $t^{\text{th}}$  iteration of the HVB algorithm under MNAR. The missing values are updated one block at a time

---

- 1: Initialize missing values  $\mathbf{y}_{u,0} = (\mathbf{y}_{u_1,0}^\top, \dots, \mathbf{y}_{u_k,0}^\top)^\top \sim p(\mathbf{y}_u | \boldsymbol{\phi}^{(t)}, \mathbf{y}_o)$
- 2: **for**  $i=1, \dots, N_1$  **do**
- 3:   **for**  $j=1, \dots, k$  **do**
- 4:     Sample  $\mathbf{y}_{u_j}^*$  from the proposal distribution  $p(\mathbf{y}_{u_j}^* | \boldsymbol{\phi}^{(t)}, \mathbf{y}_o, \mathbf{y}_{u,i-1}^{(-j)})$ , where  $\mathbf{y}_{u,i-1}^{(-j)} = (\mathbf{y}_{u_1,i}^\top, \mathbf{y}_{u_2,i}^\top, \dots, \mathbf{y}_{u_{j-1},i}^\top, \mathbf{y}_{u_{j+1},i-1}^\top, \dots, \mathbf{y}_{u_k,i-1}^\top)^\top$ .
- 5:     Sample  $u$  from uniform distribution,  $u \sim \mathcal{U}(0, 1)$
- 6:     Calculate  $a = \min\left(1, \frac{p(\mathbf{m}|\mathbf{y}^*, \boldsymbol{\psi}^{(t)})}{p(\mathbf{m}|\mathbf{y}_{i-1}, \boldsymbol{\psi}^{(t)})}\right)$ , where  $\mathbf{y}^* = (\mathbf{y}_o^\top, \mathbf{y}_u^{(-j)\top}, \mathbf{y}_{u_j}^{\top})^\top$  and  $\mathbf{y}_{i-1} = (\mathbf{y}_o^\top, \mathbf{y}_u^{(-j)\top}, \mathbf{y}_{u_j, i-1}^\top)^\top$
- 7:     **if**  $a > u$  **then**
- 8:        $\mathbf{y}_{u_j, i} = \mathbf{y}_{u_j}^*$
- 9:     **else**
- 10:        $\mathbf{y}_{u_j, i} = \mathbf{y}_{u_j, i-1}$
- 11:     **end if**
- 12:   **end for**
- 13:    $\mathbf{y}_{u,i} = (\mathbf{y}_{u_1,i}^\top, \dots, \mathbf{y}_{u_k,i}^\top)^\top$
- 14: **end for**
- 15: Output  $\mathbf{y}_u^{(t)} = \mathbf{y}_{u, N_1}$

---

## 4 Simulation result

This section investigates the performance of the VB methods to estimate the SEM under MAR and MNAR mechanisms. We compare the posterior density estimates from the VB methods to those obtained from the Hamiltonian Monte Carlo method (HMC). All examples are implemented using the R programming language. The HMC is implemented using the RStan interface (Stan Development Team, 2023). We use the HMC method from Hoffman et al. (2014), known as the No U-Turn Sampler (NUTS). For details on the generic HMC algorithm, see Section S3 of the online supplement.

In all simulation studies, we simulate  $n$  observations from a standard SEM according to Equation (1) with 10 covariates. Each covariate for every observation is drawn from a standard normal distribution  $N(0, 1)$ . The weight matrices are constructed based on a regular grid of size  $\sqrt{n} \times \sqrt{n}$ , where neighbours are defined using the Rook neighbourhood method (refer to Wijayawardhana et al. (2024) for details on constructing the weight matrix based on the Rook neighbourhood). We generate the true values of the 11 fixed effects ( $\boldsymbol{\beta}$ 's) randomly from discrete uniform random numbers between 1 and 5. We set

$\sigma_{\mathbf{y}}^2 = 1$  and  $\rho = 0.8$ . The subsequent steps in the simulation process vary depending on the missing value mechanisms.

For the MAR mechanism, after simulating  $n$  observations from a standard SEM, we randomly select  $n_o$  units to form the observed data set. In the MNAR mechanism, we generate missing responses using the logistic regression model regressed on a randomly chosen covariate from the 10 covariates and the response variable of SEM ( $\mathbf{y}$ ) as covariates, which is given by

$$p(\mathbf{m} \mid \mathbf{y}, \mathbf{X}^*, \boldsymbol{\psi}) = \prod_{i=1}^n \frac{e^{\mathbf{x}_i^* \boldsymbol{\psi}_{\mathbf{x}} + y_i \psi_{\mathbf{y}}}}{1 + e^{\mathbf{x}_i^* \boldsymbol{\psi}_{\mathbf{x}} + y_i \psi_{\mathbf{y}}}}, \quad (22)$$

where the design matrix  $\mathbf{X}^*$  contains a column of ones and the selected covariate, and  $\mathbf{x}_i^*$  denotes the  $i^{\text{th}}$  row vector of  $\mathbf{X}^*$ . The vector  $\boldsymbol{\psi}_{\mathbf{x}} = (\psi_0, \psi_{\mathbf{x}^*})$  contains the coefficient of the intercept ( $\psi_0$ ), and the coefficient of the selected covariate ( $\psi_{\mathbf{x}^*}$ ). The coefficient corresponding to  $\mathbf{y}$  is  $\psi_{\mathbf{y}}$ .

All VB and HMC algorithms in this work utilise the same prior distributions,  $p(\boldsymbol{\theta})$ , for the parameters (under MAR  $p(\boldsymbol{\theta}) = p(\boldsymbol{\phi})$ , and under MNAR  $p(\boldsymbol{\theta}) = p(\boldsymbol{\phi}, \boldsymbol{\psi}) = p(\boldsymbol{\phi})p(\boldsymbol{\psi})$ ). The priors for the parameters are given in Section S2 of the online supplement. When implementing VB algorithms, the initial values are set as follows: Under MAR, the ordinary least squares (OLS) estimates are used for the initial values for the fixed effect parameters ( $\boldsymbol{\beta}$ 's) and the error variance ( $\sigma_{\mathbf{y}}^2$ ). Additionally, we assign a value of 0.01 to  $\rho$ , reflecting a very weak spatial dependence. Under MNAR, we have additional three parameters  $\psi_0, \psi_{\mathbf{x}^*}$  and  $\psi_{\mathbf{y}}$ . For all these coefficients, we set the starting value to 0.01. The initial values for the missing data under MAR and MNAR are simulated from the conditional distribution  $p(\mathbf{y}_u \mid \boldsymbol{\phi}^{(0)}, \mathbf{y}_o)$ , where  $\boldsymbol{\phi}^{(0)}$  is the vector containing the initial parameter values. We use  $p = 4$  factors for HVB and JVB for the simulation study. The results do not improve when we increase the number of factors. We run the VB and HMC methods for 10,000 iterations for all simulation studies. Section S7 of the online supplement presents convergence plots for the VB algorithms and trace plots of posterior samples from HMC.

In Section 4.1, we examine the accuracy and computational cost of proposed VB methods for estimating SEM under the MAR mechanism. Section 4.2 presents the simulation

results for estimating SEM under the MNAR mechanism.

## 4.1 Simulation study under MAR

This section discusses the simulation results for estimating SEM under the MAR mechanism. We investigate the accuracy of the proposed VB methods using two sample sizes:  $n = 625$  and  $n = 10,000$ . For  $n = 625$ , we consider scenarios with 25% and 75% missing data. For  $n = 10,000$ , we only consider the scenario with 75% missing data. This section discusses the results for the 75% missing data scenario for  $n = 625$  and  $n = 10,000$ . The results for  $n = 625$  with 25% missing data are provided in Section S4.1 of the online supplement.

Figure 1 presents the posterior densities of SEM parameters estimated using the HMC, JVB, and HVB methods for the simulated dataset with  $n = 625$  and 75% missing values ( $n_u = 468$ ). Since  $n_u$  is small ( $< 1,000$ ), we use the standard HVB without the Gibbs steps, the HVB-NoB method, given in Algorithm 2. For the fixed effects parameters ( $\beta$ 's), the posterior densities from the JVB and HVB-NoB are nearly identical to those from HMC, with HVB-NoB being the closest to HMC. However, the posterior densities of  $\sigma_y^2$  and  $\rho$  from the JVB method exhibit significant deviations from those obtained by HMC, whereas the posterior densities from the HVB align well with those of HMC.

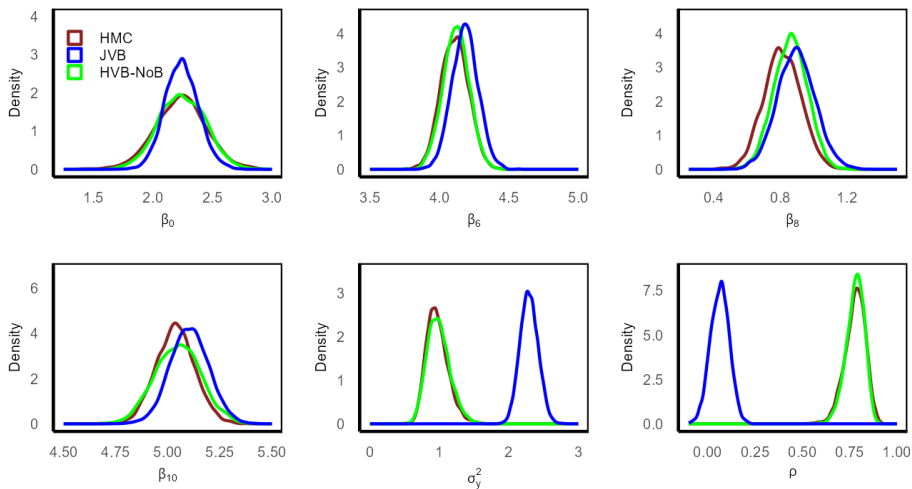


Figure 1: Posterior densities of SEM parameters under MAR for the simulated dataset with  $n = 625$  and  $n_u = 468$  (75% missing values) estimated using the HMC, JVB and HVB-NoB methods

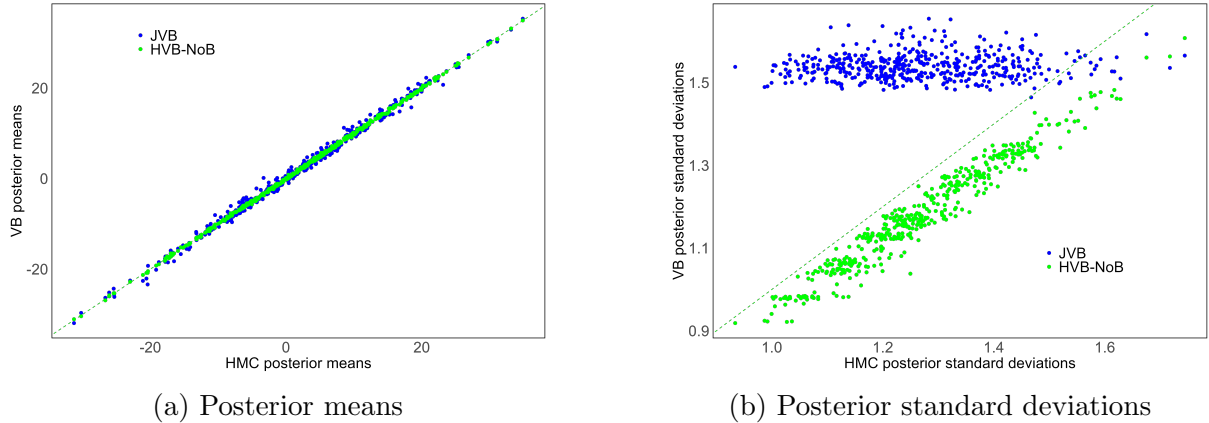


Figure 2: Comparison of the posterior means and standard deviations of the missing values obtained from JVB and HVB-NoB with those of HMC under MAR for the simulated data with  $n = 625$  and  $n_u = 468$  (75% missing values)

Figure 2 shows the comparison between the posterior means and standard deviations of the missing values obtained from the JVB, HVB-NoB, and HMC methods for the simulated dataset with  $n = 625$  and  $n_u = 468$ . The posterior means obtained from the JVB and HVB-NoB methods are very close to those obtained from the HMC method, as shown in Figure 2a. However, the posterior standard deviations estimated from the JVB method are significantly different from those obtained using the HMC method, as shown in Figure 2b. On the other hand, the posterior standard deviations estimated from the HVB-NoB method are very close to those of the HMC method.

To investigate the accuracy of the VB methods with relatively large  $n$  and missing values  $n_u$ , we simulated a dataset with  $n = 10,000$  and  $n_u = 7,500$  (i.e. missing percentage is 75%) under MAR. As indicated in Table S2 in Section S4.1 of the online supplement, the average time taken per HMC iteration is notably high for high values of  $n$  and  $n_u$ , making practical implementation of HMC infeasible. Further, when the number of units ( $n_u$ ) is large (exceeding 1,000), utilising the standard HVB without the Gibbs steps becomes computationally intensive. We employ the HVB-G method with  $N_1 = 5$  and  $k^* = 500$  and the JVB method. Table 3 compares the posterior means of the parameters obtained using the two VB methods with their true parameter values. Similar to the simulation results obtained from the simulated dataset with  $n = 625$ , the HVB-G method accurately estimates the posterior means of SEM parameters, in particular for

	JVB	HVB-G
$\beta_0 = 1$	0.9349 (0.0199)	0.9387 (0.0611)
$\beta_7 = 5$	4.9991 (0.0267)	4.9833 (0.0287)
$\sigma_y^2 = 1$	2.1509 (0.0443)	0.9998 (0.0385)
$\rho = 0.8$	0.0844 (0.0134)	0.7971 (0.0131)

Table 3: Posterior means and standard deviations (inside brackets) of SEM parameters under MAR estimated using the JVB and HVB-G methods for the simulated dataset with  $n = 10,000$  and  $n_u = 7,500$  (75% missing values)

$\sigma_y^2$  and  $\rho$  parameters, overcoming the inaccuracy of the JVB method. See Figures S5 and S6 in Section S5.1 of the online supplement for a comparison of posterior densities of parameters and a comparison of estimated missing values from the two VB methods with the true missing values, respectively.

Table S2 in Section S4.1 of the online supplement displays the average computing cost per iteration (in seconds) for the VB and HMC methods for different  $n$  and  $n_u$  under the MAR mechanism. The HVB-G method is not implemented when  $n_u$  is relatively small ( $n_u < 1,000$ ). The HMC method is computationally expensive when  $n$  is large and is not implemented when  $n > 5,000$ . The HMC method is much more computationally expensive than the VB methods, regardless of the values of  $n$  and  $n_u$ . Although it can not accurately capture the posterior distributions of the parameters  $\sigma_y^2$ ,  $\rho$  and the posterior standard deviations of the missing values (see Figures 1, 2 of the main paper, and Figure S5 in Section S5.1 of the online supplement), the JVB method is generally the fastest among all the methods. For smaller values of  $n$  and  $n_u$ , the HVB-NoB algorithm is faster than the HVB-G method. The computational time of HVB-NoB increases rapidly as  $n$  and  $n_u$  increase, while HVB-G exhibits a lower computational cost than HVB-NoB, especially for higher missing value percentages.

## 4.2 Simulation study under MNAR

This section discusses the simulation results for estimating SEM under the MNAR mechanism. When conducting simulations under MNAR, we set  $\psi_{\mathbf{x}^*} = 0.5$  and  $\psi_{\mathbf{y}} = -0.1$  across all simulation studies. The parameter  $\psi_0$  influences the percentages of missing values. We vary  $\psi_0$  to obtain the desired missing value percentages. As discussed in Section 3, when dealing with the MNAR mechanism, the parameters for the SEM and the missing data model in Equation (22) must be estimated to obtain accurate inference. The set of parameters to be estimated is  $\boldsymbol{\theta} = (\boldsymbol{\phi}^\top, \boldsymbol{\psi}^\top)^\top = (\beta_0, \dots, \beta_{10}, \sigma_{\mathbf{y}}^2, \rho, \psi_0, \psi_{\mathbf{x}^*}, \psi_{\mathbf{y}})^\top$ .

It is worth noting that properly selecting the tuning parameters for MCMC steps within the HVB-NoB, HVB-AllB, and HVB-3B algorithms is important for achieving accurate inference and rapid convergence, in particular for a large number of observations  $n$  and a large number of missing values  $n_u$ . Our simulation studies showed that maintaining an acceptance percentage between 20% and 30% in the MCMC steps is necessary to balance between accurate inferences and computational cost. Adjusting the tuning parameters of the proposed MCMC schemes allows us to attain this desired acceptance percentage. For the MCMC steps used in the HVB-NoB method presented in Algorithm 4, there is one tuning parameter, which is the number of MCMC iterations,  $N_1$ . We set this to  $N_1 = 10$  irrespective of the values  $n$  and  $n_u$ . However, as  $n_u$  increases, the acceptance percentage for this MCMC scheme drops rapidly. Increasing the value of  $N_1$  does not improve the acceptance rate of the MCMC steps. The tuning parameters for the MCMC steps in Algorithm 5 used in HVB-AllB and HVB-3B algorithms, include  $N_1$ , and the block size  $k^*$ . We fixed  $N_1$  to 10 irrespective of the values  $n$  and  $n_u$ . If  $n$  is small (say  $n_u \leq 1,000$ ), we set the block size to  $n_u \times 25\%$ . This leads to the number of blocks being 4 or 5. When  $n_u$  is large (say  $n_u > 1,000$ ), we set the block size to  $n_u \times 10\%$ , resulting in 10 or 11 blocks.

We investigate the accuracy of the proposed VB methods for estimating SEM under MNAR with a small number of observations  $n = 625$  and a large number of observations  $n = 10,000$ . For  $n = 625$ , we consider 25% and 75% missing data percentages. This section discusses the results for the 75% missing data percentage. The results for the

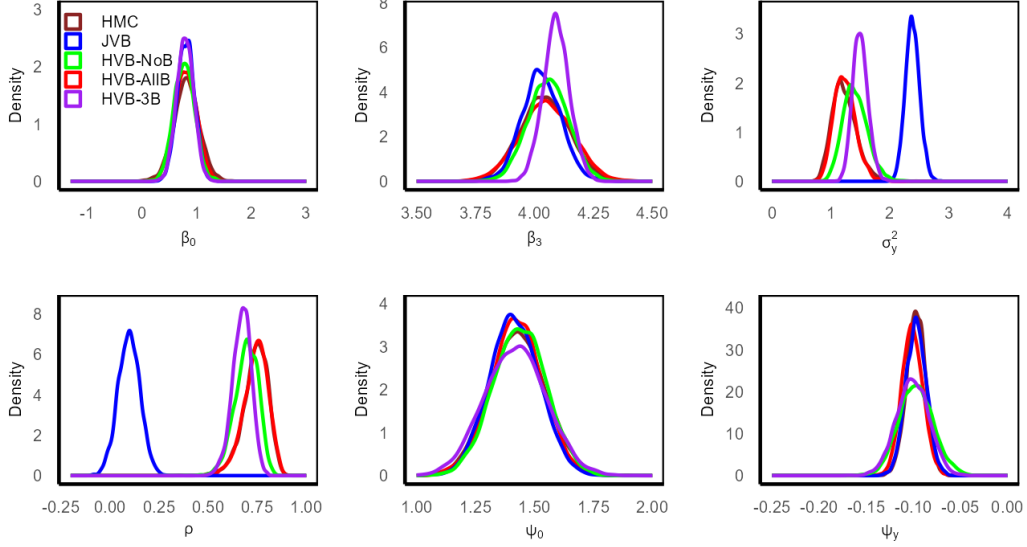


Figure 3: Posterior densities of SEM and missing data model parameters under MNAR for the simulated dataset with  $n = 625$  and  $n_u = 469$  (around 75% missing) estimated using the HMC, JVB, HVB-NoB, HVB-AllB, and HVB-3B methods

25% missing data percentage are given in Section S4.2 of the online supplement. For the large number of observations  $n = 10,000$ , we consider the 75% missing data percentage.

Figure 3 shows the posterior densities of SEM and missing model parameters estimated using different inference methods: HMC, JVB, HVB-NoB, HVB-AllB, and HVB-3B, for the simulated dataset with  $n = 625$  and around 75% missing values ( $n_n = 469$ ). See Sections 3.2, 3.3 to 3.5 for details on each VB method. Similar to the inference under MAR, we observe significant differences in the posterior densities of  $\sigma_y^2$  and  $\rho$  from JVB compared to those from HMC, but the posterior densities from any variant of HVB methods closely resemble those from HMC. Among the three HVB variants, the posterior densities from HVB-AllB closely match those obtained from HMC for all parameters. However, despite its potential for more accurate inferences, HVB-AllB incurs a higher computing cost than HVB-NoB and HVB-3B, as detailed in Table 5.

Figure 4 compares the posterior means and standard deviations of missing values obtained from the JVB method and all three HVB methods with the HMC method for the simulated dataset with  $n = 625$  and  $n_u = 469$ . The JVB posterior means and all the HVB posterior means are very close to those of HMC, as shown in Figure 4a. However, the



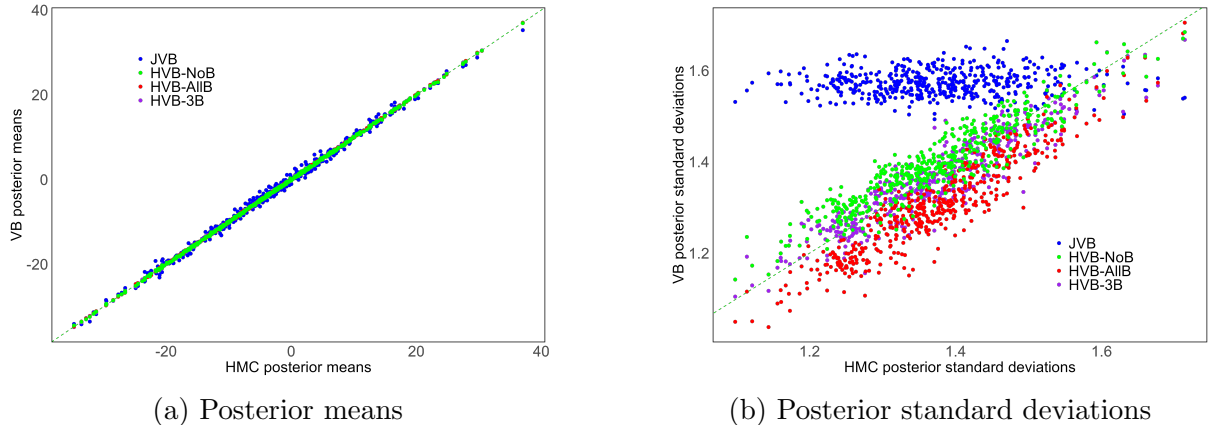


Figure 4: Comparison of the posterior means and standard deviations of missing values from the JVB, HVB-NoB, HVB-AllB, and HVB-3B methods with those obtained using the HMC method under MNAR for the simulated dataset with  $n = 625$ , and  $n_u = 469$  (around 75% missing)

posterior standard deviations estimated from the JVB method are significantly different from those obtained from the HMC method, as shown in Figure 4b, whereas the posterior standard deviations from all the HVB methods closely align with those of HMC.

Similar to SEM under MAR, we also conducted a simulation study with  $n = 10,000$  with approximately 75% of missing values under MNAR. As implementing HMC is infeasible for large  $n$  (refer to Table 5), we implement the JVB, HVB-AllB, and HVB-3B methods on this dataset and compare the estimated posterior means of parameters obtained from VB methods with the true parameter values in Table 4. The HVB-NoB algorithm is not implemented due to its high computational cost (as shown in Table 5). The posterior means obtained by HVB-AllB and HVB-3B algorithms accurately estimate the true parameter values, demonstrating superior accuracy compared to the JVB algorithm. See Figures S7 and S8 in Section S5.2 of the online supplement for a comparison of posterior densities of model parameters and a comparison of estimated missing values from the three VB methods with the true missing values, respectively.

Table 5 presents the average computing time (in seconds) per iteration for the VB and HMC methods across different values of  $n$  and  $n_u$  under MNAR. Regardless of the values of  $n$  and  $n_u$ , the HMC method is much more computationally expensive compared to the VB methods. Despite its limitations in accurately capturing the posterior distributions of  $\sigma_y^2$  and  $\rho$  (see Figure 3 and Figure S7 in Section S5.2 of the online supplement), and the

True value	JVB	HVB-AllB	HVB-3B
$\beta_0 = 2$	2.0190 (0.0358)	1.9849 (0.0494)	1.9973 (0.0547)
$\beta_3 = 5$	5.0077 (0.0247)	5.0118 (0.0214)	4.9898 (0.0081)
$\sigma_y^2 = 1$	2.1769 (0.0441)	0.9682 (0.0286)	0.9209 (0.0152)
$\rho = 0.8$	0.1443 (0.0129)	0.8128 (0.0100)	0.8190 (0.0066)
$\psi_0 = 1.5$	1.5062 (0.0255)	1.5042 (0.0285)	1.5158 (0.0280)
$\psi_k = 0.5$	0.5058 (0.0261)	0.4987 (0.0301)	0.5114 (0.0293)
$\psi_y = -0.1$	-0.1003 (0.0057)	-0.1098 (0.0090)	-0.1002 (0.0083)

Table 4: Posterior means and standard deviations (inside brackets) of SEM and missing data model parameters under MNAR estimated using the JVB and different HVB methods for the simulated dataset with  $n = 10,000$  and  $n_u = 7,542$  (around 75% missing values)

$n$	$n = 625$			$n = 1024$			$n = 2500$		
missing percentage	25%	50%	75%	25%	50%	75%	25%	50%	75%
HMC	28.79	32.31	36.22	42.79	98.59	157.52	1046.23	1100.89	1597.88
JVB	0.03	0.04	0.04	0.06	0.07	0.09	0.30	0.38	0.47
HVB-NoB	0.05	0.07	0.07	0.07	0.12	0.20	0.36	0.88	1.91
HVB-AllB	0.25	0.23	0.29	0.31	0.36	0.43	0.66	1.38	1.60
HVB-3B	0.18	0.19	0.20	0.23	0.26	0.30	0.59	0.60	0.67
$n$	$n = 5,041$			$n = 7,569$			$n = 10,000$		
missing percentage	25%	50%	75%	25%	50%	75%	25%	50%	75%
HMC	-	-	-	-	-	-	-	-	-
JVB	1.34	1.59	2.02	3.52	4.16	5.29	9.23	9.33	13.35
HVB-NoB	1.71	7.29	19.31	4.90	26.62	90.57	11.543	71.82	228.29
HVB-AllB	2.88	3.72	5.43	5.87	8.57	14.54	12.13	17.05	26.29
HVB-3B	1.74	1.98	2.50	4.07	4.95	6.60	9.03	10.53	15.47

Table 5: Average computing time (in seconds) of one iteration of the HMC, JVB, HVB-NoB, HVB-AllB, and HVB-3B methods for estimating SEM under MNAR for different  $n$  and different missing value ( $n_u$ ) percentages. For HVB-AllB and HVB-3B, the tuning parameters, such as the block size and the number of MCMC iterations, are set according to the criteria described at the beginning of Section 4.2

posterior standard deviations of missing values (see Figure 4), the JVB method is faster than the any of HVB methods. For smaller values of  $n$  and  $n_u$ , the HVB-NoB algorithm is significantly faster than its counterparts, HVB-AllB and HVB-3B. However, as  $n$  and  $n_u$  increase, the HVB-AllB and HVB-3B are faster than HVB-NoB, with HVB-3B exhibiting the lowest computing cost, as expected.

## 5 Real example

We utilise the proposed VB methods to analyse a dataset containing votes cast during the 1980 presidential election across 3,107 U.S. counties. This dataset is available in the R package `spData` (Bivand et al., 2023). The dataset includes county-level information on the following: the proportion of votes cast by the eligible population, the proportion of the eligible population with college degrees, the proportion of the eligible population that owns homes, and income per capita. Pace and Barry (1997) applied the SDM to this dataset, choosing the logarithm of the proportion of votes cast as the dependent variable. Furthermore, the dataset contains a pre-defined county-level weight matrix, with an average of 5-6 neighbours per unit (county). The weight matrix from the dataset is denser than those used in our simulation studies, which has an average of only 3-4 neighbours per unit. Therefore, implementing VB algorithms for this dataset requires more computing time than the simulation studies.

In our analysis, we treat the logarithm of the proportion of votes cast as the dependent variable. Additionally, we include the logarithms of the proportions of college degrees and homeownership, as well as income per capita, along with their interaction effects, as the set of covariates. Each covariate is standardized to have a mean of zero and a standard deviation of one.

### 5.1 SEM under MAR

This section investigates the performance of VB methods to estimate SEM under MAR for the 1980 presidential election dataset. Given the full dataset, we randomly select

$n_o$  units to form the observed dataset. The remaining  $n_u$  units are treated as missing responses. We estimate SEM parameters and the missing values using the JVB and HVB-G algorithms. Due to the moderately large number of observations  $n = 3,107$ , employing the HMC algorithm becomes computationally intensive, as detailed in Table S2 in Section S4.1 of the online supplement. We compare the posterior mean estimates of the SEM parameters with those obtained from the marginal maximum likelihood (ML) method of Suesse (2018).

For both VB algorithms, we used the starting values as described in the simulation study in Section 4 and ran the algorithms for 15,000 iterations, at which point both algorithms were well-converged (see Section S7.2.1 of the online supplement for further details). For the HVB-G algorithm, we set the block size to 500 and the number of Gibbs iterations  $N_1$  to 10.

Figure S9 in Section S6.1 of the online supplement presents the posterior densities of the SEM parameters estimated using the JVB and HVB-G methods with 75% missing responses ( $n_u = 2,330$ ). The vertical lines indicate marginal ML estimates. The figure shows that the JVB method yields different posterior density estimates for the parameters  $\sigma_y^2$  and  $\rho$  compared to the HVB-G method. However, the posterior mean estimates of SEM parameters, obtained using the HVB-G method, closely align with the marginal ML estimates compared to those obtained from the JVB method. See Table 6 for a summary of the estimation results.

Figure S10 in Section S6.1 of the online supplement compares the posterior means of missing values obtained from the JVB and HVB-G algorithms with the true missing values. It is evident that the posterior mean estimates of missing values from HVB-G are slightly closer to the true missing values than those from the JVB algorithm; see mean squared errors (MSEs) of estimated missing values in Table 6.

Table 6 presents the marginal ML estimates with their standard errors and the posterior means and standard deviations of the SEM parameters estimated by the two VB methods. The table also includes the computing time of each algorithm and the MSEs of estimated missing values from JVB and HVB. The table shows that the MSE of HVB-G

Table 6: Marginal ML estimates (with standard errors in brackets), and posterior means (with posterior standard deviations in brackets) of SEM parameters estimated by JVB and HVB-G algorithms for the 1980 presidential election dataset with 75% ( $n_u = 2,330$ ) missing values under MAR. The table also includes the MSE of missing values obtained from the JVB and HVB algorithms, along with computing time

	marginal ML	JVB	HVB-G
<i>intercept</i>	-0.5723 (0.01087)	-0.5697 (0.0051)	-0.5696 (0.0091)
$\sigma_y^2$	0.0089 (0.0006)	0.0253 (0.0007)	0.0093 (0.0006)
$\rho$	0.8306 (0.0181)	0.1916 (0.0282)	0.8346 (0.0182)
MSE	-	44.8966	32.9627
Computing time in seconds	277.26	10546.5	36939

is lower than that of JVB. See Table S3 in Section S6.1 of the online supplement for further details on the estimation results, including estimates for all the fixed effects.

## 5.2 SEM under MNAR

This section investigates the performance of VB methods to estimate SEM under MNAR for the 1980 presidential election dataset. The logistic regression in Section 4 is used as the missing data model. We use the logarithms of the proportions of college degrees and the response variable  $y$  of the SEM (logarithm of the proportion of votes cast) as the covariates in the missing data model. The missing data model has three parameters, denoted as  $\boldsymbol{\psi} = (\psi_0, \psi_{\mathbf{x}^*}, \psi_y)$ . We set the values  $\psi_0 = 1.4$ ,  $\psi_{\mathbf{x}^*} = 0.5$ , and  $\psi_y = -0.1$ , resulting in approximately 80% of responses being missing ( $n_u = 2,477$ ).

The JVB, HVB-AllB, and HVB-3B methods are used to estimate the posterior densities of SEM and missing data model parameters. The starting values for all algorithms are chosen similarly to those in the simulation study. The tuning parameters for HVB-AllB and HVB-3B are selected as follows: the number of MCMC iterations is set to  $N_1 = 20$ , and since  $n_u > 1,000$ , the block size  $k^*$  is set to  $n_u \times 10\% \approx 247$ . This led to a total of 11 blocks. All VB algorithms were run for 15,000 iterations, at which point all algorithms had well converged. See Figure S24 in Section S7.2.2 of the online supplement for the

convergence analysis.

Figure S11 in Section S6.2 of the online supplement compares the posterior densities of SEM and missing data model parameters obtained from the three VB methods. The figure shows that the posterior densities of the parameters, except for  $\sigma_y^2$  and  $\rho$ , obtained from different methods, are almost identical. For  $\sigma_y^2$  and  $\rho$ , the posterior densities obtained from HVB-AllB and HVB-3B are closer to each other compared to those from JVB.

Figure S12 in Section S6.2 of the online supplement compares the posterior means of missing values obtained from the JVB, HVB-AllB, and HVB-3B methods with the true missing values. The posterior means of the missing values obtained from the HVB-AllB method are slightly closer to the true missing values than those from the HVB-3B and JVB algorithms, as indicated by their greater concentration along the diagonal line. This is further supported by the lower MSE of estimated missing values from the HVB-AllB method in comparison to both the HVB-3B and JVB methods, as shown in Table 7. The table also includes the posterior means and standard deviations of parameters obtained from the three VB algorithms, the true parameter values for the missing data model parameters, and the computing time for each method. Although the HVB-3B estimates of missing values have a slightly higher MSE than HVB-AllB, its computing time is nearly three times shorter. Therefore, HVB-3B is a computationally less expensive yet reasonably accurate alternative to the HVB-AllB method. Table S4 in Section S6.2 of the online supplement summarises estimates for all the fixed effects.

## 6 Conclusion

Our article proposes VB methods for estimating SEM under missing at random (MAR) and missing not at random (MNAR) missing data mechanisms. The joint VB (JVB) and the class of hybrid VB (HVB) methods are proposed. The posterior densities estimated using the Hamiltonian Monte Carlo (HMC) method are considered as ground truth to assess the accuracy of the VB methods for a small to moderate number of observations  $n$  and missing response values  $n_u$ . The HMC method for this model is infeasible when  $n$

Table 7: Posterior means (with posterior standard deviations inside brackets) of SEM and missing data model parameters, and the true parameter values for the missing data model parameters under MNAR obtained from the JVB, HVB-AllB, and HVB-3B methods for the 1980 presidential election dataset with approximately 80% missing values ( $n_u = 2,477$ ). The table also includes the MSE of missing values by JVB and HVB algorithms, along with computing time

	True value	JVB	HVB-AllB	HVB-3B
$intercept$ ( $\beta_0$ )	NA	-0.5815 (0.0112)	-0.5773 (0.0163)	-0.5689 (0.0078)
$\sigma_y^2$	NA	0.0242 (0.0006)	0.0109 (0.0008)	0.0154 (0.0006)
$\rho$	NA	0.1634 (0.0259)	0.8004 (0.0171)	0.6990 (0.0186)
$\psi_0$	1.4	1.6622 (0.1977)	1.6504 (0.1934)	1.5891 (0.1455)
$\psi_{\mathbf{x}^*}$	0.5	0.5227 (0.0519)	0.5172 (0.0497)	0.5376 (0.0454)
$\psi_{\mathbf{y}}$	-0.1	0.3540 (0.3252)	0.3316 (0.3269)	0.2286 (0.2354)
MSE	NA	46.9063	35.7157	37.6031
Computational time in seconds	NA	11620.5	68035.5	23787

and  $n_u$  are large.

The empirical results show that: (1) All proposed VB methods are computationally less expensive compared to the HMC method; (2) All HVB methods produce posterior density estimates for all model parameters and missing response values that are similar to those obtained using the HMC method for estimating SEM under MAR and MNAR. However, as  $n$  and  $n_u$  increase, HVB-NoB produces inaccurate estimates due to the low acceptance percentage of the underlying MCMC steps; (3) The HVB-3B method generates slightly different posterior estimates compared to other HVB algorithms. This is expected because, for each MCMC step of the HVB-3B algorithm, updates are performed on only randomly selected 3 blocks; (4) HVB-3B is more scalable for large  $n$  and  $n_u$  compared to HVB-AllB while still providing nearly similar posterior density estimates; (5) The JVB method yields quite accurate posterior density estimates for fixed effect parameters and the posterior means of the missing response values. However, it provides inaccurate posterior density estimates for the parameters  $\sigma_y^2$  and  $\rho$ , as well as for the

posterior standard deviations of the missing response values under both MAR and MNAR;

(6) Generally, all HVB algorithms tend to converge in fewer iterations compared to the JVB algorithm.

## Statements and Declarations

The authors declare no potential or apparent conflict of interest in this article.

## References

- Allison, P. D. (2001). *Missing data*. Sage publications.
- Anselin, L. (1988). *Spatial econometrics: methods and models*, volume 4. Springer Science & Business Media.
- Bansal, P., Krueger, R., and Graham, D. J. (2021). Fast Bayesian estimation of spatial count data models. *Computational Statistics & Data Analysis*, 157:107152.
- Benedetti, R., Suesse, T., and Piersimoni, F. (2020). Spatial auto-correlation and auto-regressive models estimation from sample survey data. *Biometrical Journal*, 62(6):1494–1507.
- Bivand, R., Nowosad, J., and Lovelace, R. (2023). *spData: Datasets for spatial analysis*. R package version 2.2.2.
- Blei, D. M. and Jordan, M. I. (2006). Variational inference for Dirichlet process mixtures. *Bayesian Analysis*, 1(1):121 – 143.
- Blei, D. M., Kucukelbir, A., and McAuliffe, J. D. (2017). Variational inference: A review for statisticians. *Journal of the American Statistical Association*, 112(518):859–877.
- Bottou, L. (2010). Large-scale machine learning with stochastic gradient descent. In *Proceedings of COMPSTAT'2010: 19th International Conference on Computational Statistics Paris France, August 22-27, 2010 Keynote, Invited and Contributed Papers*, pages 177–186. Springer.
- Carpenter, B., Gelman, A., Hoffman, M. D., Lee, D., Goodrich, B., Betancourt, M., Brubaker, M. A., Guo, J., Li, P., and Riddell, A. (2017). Stan: A probabilistic programming language. *Journal of statistical software*, 76.
- Casemiro, F. A., Diniz-Filho, J. A. F., Rangel, T., and Bini, L. M. (2007). Spatial autocorrelation, model selection and hypothesis testing in geographical ecology: Implications for testing metabolic theory in new world amphibians. *Neotropical Biology and Conservation*, 2(3):119–126.



- Chappell, M. A., Groves, A. R., Whitcher, B., and Woolrich, M. W. (2008). Variational Bayesian inference for a nonlinear forward model. *IEEE Transactions on Signal Processing*, 57(1):223–236.
- Dao, V. H., Gunawan, D., Tran, M.-N., Kohn, R., Hawkins, G. E., and Brown, S. D. (2024). Efficient selection between hierarchical cognitive models: Cross-validation with variational Bayes. *Psychological Methods*, 29(1):219–241.
- De Oliveira, V. and Song, J. J. (2008). Bayesian analysis of simultaneous autoregressive models. *Sankhyā: The Indian Journal of Statistics, Series B (2008-)*, pages 323–350.
- Di Salvatore, J. and Ruggeri, A. (2021). Spatial analysis for political scientists. *Italian Political Science Review/Rivista Italiana di Scienza Politica*, 51(2):198–214.
- Doğan, O. and Taşpinar, S. (2018). Bayesian inference in spatial sample selection models. *Oxford Bulletin of Economics and Statistics*, 80(1):90–121.
- Duane, S., Kennedy, A. D., Pendleton, B. J., and Roweth, D. (1987). Hybrid Monte Carlo. *Physics letters B*, 195(2):216–222.
- Flores-Lagunes, A. and Schnier, K. E. (2012). Estimation of sample selection models with spatial dependence. *Journal of Applied Econometrics*, 27(2):173–204.
- Gelfand, A. E., Hills, S. E., Racine-Poon, A., and Smith, A. F. (1990). Illustration of Bayesian inference in normal data models using Gibbs sampling. *Journal of the American Statistical Association*, 85(412):972–985.
- Gunawan, D., Kohn, R., and Nott, D. (2021). Variational Bayes approximation of factor stochastic volatility models. *International Journal of Forecasting*, 37(4):1355–1375.
- Gunawan, D., Kohn, R., and Nott, D. (2023). Flexible variational Bayes based on a copula of a mixture. *Journal of Computational and Graphical Statistics*, pages 1–16.
- Han, S., Liao, X., and Carin, L. (2013). Integrated non-factorized variational inference. *Advances in Neural Information Processing Systems*, 26.
- Han, S., Liao, X., Dunson, D., and Carin, L. (2016). Variational Gaussian copula inference. In *Artificial Intelligence and Statistics*, pages 829–838. PMLR.
- Harville, D. A. (1997). *Matrix algebra from a statistician’s perspective*. Springer New York.
- Hoffman, M. D., Gelman, A., et al. (2014). The No-U-Turn sampler: adaptively setting path lengths in Hamiltonian Monte Carlo. *J. Mach. Learn. Res.*, 15(1):1593–1623.
- Kelley pace, R. and Barry, R. P. (1997). Fast cars. *Journal of Statistical Computation and Simulation*, 59(2):123–145.
- Kingma, D. P. and Welling, M. (2013). Auto-encoding variational Bayes. *arXiv preprint arXiv:1312.6114*.
- Leenders, R. T. A. (2002). Modeling social influence through network autocorrelation: constructing the weight matrix. *Social Networks*, 24(1):21–47.

- LeSage, J. and Pace, R. K. (2009). *Introduction to spatial econometrics*. Chapman and Hall/CRC.
- LeSage, J. P. (1997). Bayesian estimation of spatial autoregressive models. *International Regional Science Review*, 20(1-2):113–129.
- LeSage, J. P. and Pace, R. K. (2004). Models for spatially dependent missing data. *The Journal of Real Estate Finance and Economics*, 29(2):233–254.
- Li, H., Calder, C. A., and Cressie, N. (2012). One-step estimation of spatial dependence parameters: Properties and extensions of the aple statistic. *Journal of Multivariate Analysis*, 105(1):68–84.
- Little, R. J. and Rubin, D. B. (2019). *Statistical analysis with missing data*, volume 793. John Wiley & Sons.
- Loaiza-Maya, R., Smith, M. S., Nott, D. J., and Danaher, P. J. (2022). Fast and accurate variational inference for models with many latent variables. *Journal of Econometrics*, 230(2):339–362.
- McElreath, R. (2018). *Statistical rethinking: A Bayesian course with examples in R and Stan*. Chapman and Hall/CRC.
- Mollalo, A., Vahedi, B., and Rivera, K. M. (2020). GIS-based spatial modeling of COVID-19 incidence rate in the continental United States. *Science of the Total Environment*, 728:138884.
- Neal, R. (1995). Bayesian learning for neural networks [phd thesis]. *Toronto, Ontario, Canada: Department of Computer Science, University of Toronto*.
- Neal, R. M. et al. (2011). MCMC using Hamiltonian dynamics. *Handbook of Markov chain Monte Carlo*, 2(11):2.
- Nott, D. J., Tan, S. L., Villani, M., and Kohn, R. (2012). Regression density estimation with variational methods and stochastic approximation. *Journal of Computational and Graphical Statistics*, 21(3):797–820.
- Ong, V. M.-H., Nott, D. J., and Smith, M. S. (2018). Gaussian variational approximation with a factor covariance structure. *Journal of Computational and Graphical Statistics*, 27(3):465–478.
- Ord, K. (1975). Estimation methods for models of spatial interaction. *Journal of the American Statistical Association*, 70(349):120–126.
- Ormerod, J. T. and Wand, M. P. (2010). Explaining variational approximations. *The American Statistician*, 64(2):140–153.
- Pace, R. K. and Barry, R. (1997). Quick computation of spatial autoregressive estimators. *Geographical analysis*, 29(3):232–247.
- Poyiadjis, G., Doucet, A., and Singh, S. S. (2011). Particle approximations of the score and observed information matrix in state space models with application to parameter estimation. *Biometrika*, 98(1):65–80.

- Rabovič, R. and Čížek, P. (2023). Estimation of spatial sample selection models: A partial maximum likelihood approach. *Journal of Econometrics*, 232(1):214–243.
- Rezende, D. J., Mohamed, S., and Wierstra, D. (2014a). Stochastic backpropagation and approximate inference in deep generative models. In *International Conference on Machine Learning*, pages 1278–1286. PMLR.
- Rezende, D. J., Mohamed, S., and Wierstra, D. (2014b). Stochastic backpropagation and approximate inference in deep generative models. In Xing, E. P. and Jebara, T., editors, *Proceedings of the 31st International Conference on Machine Learning*, volume 32 of *Proceedings of Machine Learning Research*, pages 1278–1286, Beijing, China. PMLR.
- Robbins, H. and Monro, S. (1951). A stochastic approximation method. *The Annals of Mathematical Statistics*, pages 400–407.
- Rubin, D. B. (1976). Inference and missing data. *Biometrika*, 63(3):581–592.
- Seya, H., Tomari, M., and Uno, S. (2021). Parameter estimation in spatial econometric models with non-random missing data. *Applied Economics Letters*, 28(6):440–446.
- Stan Development Team (2020). RStan: the R interface to Stan.
- Stan Development Team (2023). RStan: the R interface to Stan. R package version 2.21.8.
- Suesse, T. (2018). Marginal maximum likelihood estimation of SAR models with missing data. *Computational Statistics & Data Analysis*, 120:98–110.
- Suesse, T. and Zammit-Mangion, A. (2017). Computational aspects of the EM algorithm for spatial econometric models with missing data. *Journal of Statistical Computation and Simulation*, 87(9):1767–1786.
- Tan, L. S. and Nott, D. J. (2018). Gaussian variational approximation with sparse precision matrices. *Statistics and Computing*, 28:259–275.
- Titsias, M. and Lázaro-Gredilla, M. (2015). Local expectation gradients for black box variational inference. In Cortes, C., Lawrence, N., Lee, D., Sugiyama, M., and Garnett, R., editors, *Advances in Neural Information Processing Systems*, volume 28. Curran Associates, Inc.
- Titsias, M. and Lázaro-Gredilla, M. (2014). Doubly stochastic variational Bayes for non-conjugate inference. In Xing, E. P. and Jebara, T., editors, *Proceedings of the 31st International Conference on Machine Learning*, volume 32 of *Proceedings of Machine Learning Research*, pages 1971–1979, Beijing, China. PMLR.
- Ver Hoef, J. M., Peterson, E. E., Hooten, M. B., Hanks, E. M., and Fortin, M.-J. (2018). Spatial autoregressive models for statistical inference from ecological data. *Ecological Monographs*, 88(1):36–59.
- Wang, W. and Lee, L.-F. (2013). Estimation of spatial autoregressive models with randomly missing data in the dependent variable. *The Econometrics Journal*, 16(1):73–102.

- Wijayawardhana, A., Suesse, T., and Gunawan, D. (2024). Statistical inference on hierarchical simultaneous autoregressive models with missing data. *arXiv preprint arXiv:2403.17257*.
- Wong, D. W. and Li, Y. (2020). Spreading of COVID-19: Density matters. *Plos One*, 15(12):e0242398.
- Wu, G. (2018). Fast and scalable variational Bayes estimation of spatial econometric models for Gaussian data. *Spatial Statistics*, 24:32–53.
- Xu, M., Quiroz, M., Kohn, R., and Sisson, S. A. (2019). Variance reduction properties of the reparameterization trick. In *The 22nd International Conference on Artificial Intelligence and Statistics*, pages 2711–2720. PMLR.
- Zeiler, M. D. (2012). Adadelta: An adaptive learning rate method. *ArXiv*, abs/1212.5701.
- Zhu, X., Huang, D., Pan, R., and Wang, H. (2020). Multivariate spatial autoregressive model for large scale social networks. *Journal of Econometrics*, 215(2):591–606.

# Online Supplement for Variational Bayes Inference for Spatial Error Models with Missing Data

We use the following notation in the online supplement. Eq. (1), Table 1, Figure 1, and Algorithm 1, etc, refer to the main paper, while Eq. (S1), Table S1, Figure S1, and Algorithm S1, etc, refer to the supplement.

## S1 Derivation of VB algorithms

### S1.1 Derivation of the reparameterisation gradient for JVB algorithm

In the main paper, the reparameterisation gradient of  $\mathcal{L}(\boldsymbol{\lambda})$  for JVB algorithm is given by

$$\nabla_{\boldsymbol{\lambda}}\mathcal{L}(\boldsymbol{\lambda}) = E_{f_{\boldsymbol{\zeta}}}\left[\frac{du(\boldsymbol{\zeta}, \boldsymbol{\lambda})^\top}{d\boldsymbol{\lambda}}\{\nabla_{\boldsymbol{\theta}, \mathbf{y}_u}\log h(\boldsymbol{\theta}, \mathbf{y}_u) - \nabla_{\boldsymbol{\theta}, \mathbf{y}_u}\log q_{\boldsymbol{\lambda}}(\boldsymbol{\theta}, \mathbf{y}_u)\}\right], \quad (\text{S1})$$

where  $\frac{du(\boldsymbol{\zeta}, \boldsymbol{\lambda})}{d\boldsymbol{\lambda}}$  is the derivative of the transformation  $u(\boldsymbol{\zeta}, \boldsymbol{\lambda}) = \boldsymbol{\mu} + \mathbf{B}\boldsymbol{\eta} + \mathbf{d} \circ \boldsymbol{\epsilon}$  with respect to the variational parameters  $\boldsymbol{\lambda} = (\boldsymbol{\mu}^\top, \text{vech}(\mathbf{B})^\top, \mathbf{d}^\top)^\top$ , where "vech" operator is the vectorisation of a matrix by stacking its columns from left to right. We write that  $u(\boldsymbol{\zeta}, \boldsymbol{\lambda}) = \boldsymbol{\mu} + (\boldsymbol{\eta}^\top \otimes \mathbf{I}_{S+n_u})\text{vech}(\mathbf{B}) + \mathbf{d} \circ \boldsymbol{\epsilon}$ , where  $\otimes$  represents the Kronecker product, and  $\mathbf{I}_{S+n_u}$  is the identity matrix of size  $S+n_u$ . It can be shown that  $\nabla_{\boldsymbol{\theta}, \mathbf{y}_u}\log q_{\boldsymbol{\lambda}}(\boldsymbol{\theta}, \mathbf{y}_u) = -(\mathbf{B}\mathbf{B}^\top + \mathbf{D}^2)^{-1}((\boldsymbol{\theta}^\top, \mathbf{y}_u^\top)^\top - \boldsymbol{\mu})$ ,

$$\frac{du(\boldsymbol{\zeta}, \boldsymbol{\lambda})}{d\boldsymbol{\mu}} = \mathbf{I}_{S+n_u} \quad \text{and} \quad \frac{du(\boldsymbol{\zeta}, \boldsymbol{\lambda})}{d\text{vech}(\mathbf{B})} = \boldsymbol{\eta}^\top \otimes \mathbf{I}_{S+n_u}. \quad (\text{S2})$$

The derivatives of the lower bound with respect to variational parameters are:

$$\begin{aligned} \nabla_{\boldsymbol{\mu}}\mathcal{L}(\boldsymbol{\lambda}) &= E_{f_{\boldsymbol{\zeta}}}[\nabla_{\boldsymbol{\theta}, \mathbf{y}_u}\log h(\boldsymbol{\mu} + \mathbf{B}\boldsymbol{\eta} + \mathbf{d} \circ \boldsymbol{\epsilon}) \\ &\quad + (\mathbf{B}\mathbf{B}^\top + \mathbf{D}^2)^{-1}(\mathbf{B}\boldsymbol{\eta} + \mathbf{d} \circ \boldsymbol{\epsilon})], \end{aligned} \quad (\text{S3})$$

$$\begin{aligned}\nabla_{\mathbf{B}}\mathcal{L}(\boldsymbol{\lambda}) &= E_{f_{\zeta}}[\nabla_{\boldsymbol{\theta}, \mathbf{y}_u} \log h(\boldsymbol{\mu} + \mathbf{B}\boldsymbol{\eta} + \mathbf{d} \circ \boldsymbol{\epsilon})\boldsymbol{\eta}^{\top} \\ &\quad + (\mathbf{B}\mathbf{B}^{\top} + \mathbf{D}^2)^{-1}(\mathbf{B}\boldsymbol{\eta} + \mathbf{d} \circ \boldsymbol{\epsilon})\boldsymbol{\eta}^{\top}],\end{aligned}\tag{S4}$$

and

$$\begin{aligned}\nabla_{\mathbf{d}}\mathcal{L}(\boldsymbol{\lambda}) &= E_{f_{\zeta}}[\text{diag}(\nabla_{\boldsymbol{\theta}, \mathbf{y}_u} \log h(\boldsymbol{\mu} + \mathbf{B}\boldsymbol{\eta} + \mathbf{d} \circ \boldsymbol{\epsilon})\boldsymbol{\epsilon}^{\top} \\ &\quad + (\mathbf{B}\mathbf{B}^{\top} + \mathbf{D}^2)^{-1}(\mathbf{B}\boldsymbol{\eta} + \mathbf{d} \circ \boldsymbol{\epsilon})\boldsymbol{\epsilon}^{\top})],\end{aligned}\tag{S5}$$

where  $\text{diag}(\cdot)$  is the vector of diagonal elements extracted from a square matrix. The analytical expressions for  $\nabla_{\boldsymbol{\theta}, \mathbf{y}_u} \log h(\boldsymbol{\mu} + \mathbf{B}\boldsymbol{\eta} + \mathbf{d} \circ \boldsymbol{\epsilon}) = \nabla_{\boldsymbol{\theta}, \mathbf{y}_u} \log h(\boldsymbol{\theta}, \mathbf{y}_u)$  in Equations (S3)-(S5) under MAR and MNAR mechanisms are provided in Section S2. The expectations in these gradients can be estimated using a single sample drawn from  $f_{\zeta}$ , and they provide unbiased estimates  $\widehat{\nabla_{\boldsymbol{\lambda}}\mathcal{L}(\boldsymbol{\lambda})}$  for  $\nabla_{\boldsymbol{\lambda}}\mathcal{L}(\boldsymbol{\lambda})$ . These estimates are utilised in the gradient calculation step (step 4) of Algorithm 1 of the main paper. The adaptive learning rates (step sizes) utilised in Algorithm 1 are determined through the ADADELTA algorithm (Zeiler, 2012), as detailed in Section S1.3.

Computing gradient estimates using Equations (S3), (S4), and (S5) presents computational problems, in particular, when number of covariates and missing values is large. The inversion of  $(S + n_u) \times (S + n_u)$  matrix,  $(\mathbf{B}\mathbf{B}^{\top} + \mathbf{D}^2)$ , is computationally expensive. Using the Woodbury formula (Harville, 1997, p. 427), this inversion can be reformulated as:

$$(\mathbf{B}\mathbf{B}^{\top} + \mathbf{D}^2)^{-1} = \mathbf{D}^{-2} - \mathbf{D}^{-2}\mathbf{B}(\mathbf{I}_p + \mathbf{B}^{\top}\mathbf{D}^{-2}\mathbf{B})^{-1}\mathbf{B}^{\top}\mathbf{D}^{-2},\tag{S6}$$

where  $\mathbf{I}_p$  is the diagonal matrix of dimension  $p \times p$ .

On the right-hand side of Equation (S6), the term  $(\mathbf{I}_p + \mathbf{B}^{\top}\mathbf{D}^{-2}\mathbf{B})$  is a square matrix of size  $p \times p$  (where  $p$  is much smaller than  $S + n_u$ ), and  $\mathbf{D}$  is a diagonal matrix. Directly inverting  $(\mathbf{I} + \mathbf{B}^{\top}\mathbf{D}^{-2}\mathbf{B})$  has a computational complexity of  $O(p^3)$ . Consequently, computing  $(\mathbf{B}\mathbf{B}^{\top} + \mathbf{D}^2)^{-1}$  using this method also involves  $O(p^3)$  complexity. Alternatively, without utilising the Woodbury formula, the complexity increases significantly to  $O((S + n_u)^3)$ .

## S1.2 Derivation of the reparameterisation gradient for HVB algorithm

Since  $\mathcal{L}(\boldsymbol{\lambda}) = E_q(\log p(\mathbf{O} | \boldsymbol{\theta}) + \log p(\boldsymbol{\theta}) - \log q_{\boldsymbol{\lambda}}^0(\boldsymbol{\theta})) = \mathcal{L}^0(\boldsymbol{\lambda})$  as shown in Section 3.3 of the main paper, the reparameterisation gradient of  $\mathcal{L}$  is the same as that of  $\mathcal{L}^0$ ,

$$\nabla_{\boldsymbol{\lambda}} \mathcal{L}(\boldsymbol{\lambda}) = E_{f_{\boldsymbol{\delta}^0}} \left[ \frac{dt^0(\boldsymbol{\delta}^0, \boldsymbol{\lambda}_{\boldsymbol{\theta}})^{\top}}{d\boldsymbol{\lambda}_{\boldsymbol{\theta}}} (\nabla_{\boldsymbol{\theta}} \log p(\boldsymbol{\theta}) + \nabla_{\boldsymbol{\theta}} \log p(\mathbf{O} | \boldsymbol{\theta}) - \nabla_{\boldsymbol{\theta}} \log q_{\boldsymbol{\lambda}}^0(\boldsymbol{\theta})) \right], \quad (\text{S7})$$

where, the random vector  $\boldsymbol{\delta}^0$  has density  $f_{\boldsymbol{\delta}^0}$ , which follows a standard normal, and does not depend on  $\boldsymbol{\lambda}_{\boldsymbol{\theta}}$ , and  $t^0$  is the one-to-one vector-valued transformation from  $\boldsymbol{\delta}^0 = (\boldsymbol{\eta}^{0\top}, \boldsymbol{\epsilon}^{0\top})^{\top}$  to the parameter vector, such that  $\boldsymbol{\theta} = t^0(\boldsymbol{\delta}^0, \boldsymbol{\lambda}_{\boldsymbol{\theta}}) = \boldsymbol{\mu}_{\boldsymbol{\theta}} + \mathbf{B}_{\boldsymbol{\theta}} \boldsymbol{\eta}^0 + \mathbf{d}_{\boldsymbol{\theta}} \circ \boldsymbol{\epsilon}^0$ .

The Fisher's identity is given by

$$\nabla_{\boldsymbol{\theta}} \log p(\mathbf{O} | \boldsymbol{\theta}) = \int \nabla_{\boldsymbol{\theta}} [\log (p(\mathbf{O} | \mathbf{y}_u, \boldsymbol{\theta}) p(\mathbf{y}_u | \boldsymbol{\theta}))] p(\mathbf{y}_u | \mathbf{O}, \boldsymbol{\theta}) d\mathbf{y}_u, \quad (\text{S8})$$

see, for example, Poyiadjis et al. (2011).

Substituting this expression into Equation (S7), and writing  $E_{f_{\boldsymbol{\delta}}}(\cdot)$  for expectation with respect to  $f_{\boldsymbol{\delta}}(\boldsymbol{\delta}) = f_{\boldsymbol{\delta}^0}(\boldsymbol{\delta}^0) p(\mathbf{y}_u | \boldsymbol{\theta}, \mathbf{O})$  and because  $h(\boldsymbol{\theta}, \mathbf{y}_u) = p(\mathbf{O} | \mathbf{y}_u, \boldsymbol{\theta}) p(\mathbf{y}_u | \boldsymbol{\theta}) p(\boldsymbol{\theta})$ , we get

$$\begin{aligned} \nabla_{\boldsymbol{\lambda}} \mathcal{L}(\boldsymbol{\lambda}) &= E_{f_{\boldsymbol{\delta}}} \left[ \frac{dt^0(\boldsymbol{\delta}^0, \boldsymbol{\lambda}_{\boldsymbol{\theta}})^{\top}}{d\boldsymbol{\lambda}_{\boldsymbol{\theta}}} (\nabla_{\boldsymbol{\theta}} \log p(\boldsymbol{\theta}) + \nabla_{\boldsymbol{\theta}} \log p(\mathbf{y}_u | \boldsymbol{\theta}) + \nabla_{\boldsymbol{\theta}} \log p(\mathbf{O} | \mathbf{y}_u, \boldsymbol{\theta}) - \nabla_{\boldsymbol{\theta}} \log q_{\boldsymbol{\lambda}}^0(\boldsymbol{\theta})) \right] \\ &= E_{f_{\boldsymbol{\delta}}} \left[ \frac{dt^0(\boldsymbol{\delta}^0, \boldsymbol{\lambda}_{\boldsymbol{\theta}})^{\top}}{d\boldsymbol{\lambda}_{\boldsymbol{\theta}}} (\nabla_{\boldsymbol{\theta}} \log h(\boldsymbol{\theta}, \mathbf{y}_u) - \nabla_{\boldsymbol{\theta}} \log q_{\boldsymbol{\lambda}}^0(\boldsymbol{\theta})) \right]. \end{aligned} \quad (\text{S9})$$

The term  $\frac{dt^0(\boldsymbol{\delta}^0, \boldsymbol{\lambda}_{\boldsymbol{\theta}})}{d\boldsymbol{\lambda}_{\boldsymbol{\theta}}}$  in Equation (S9) is the derivative of the transformation  $t^0(\boldsymbol{\delta}^0, \boldsymbol{\lambda}_{\boldsymbol{\theta}}) = \boldsymbol{\mu}_{\boldsymbol{\theta}} + \mathbf{B}_{\boldsymbol{\theta}} \boldsymbol{\eta}^0 + \mathbf{d}_{\boldsymbol{\theta}} \circ \boldsymbol{\epsilon}^0$  with respect to the variational parameters  $\boldsymbol{\lambda}_{\boldsymbol{\theta}} = (\boldsymbol{\mu}_{\boldsymbol{\theta}}^{\top}, \text{vech}(\mathbf{B}_{\boldsymbol{\theta}})^{\top}, \mathbf{d}_{\boldsymbol{\theta}}^{\top})^{\top}$ . We can express that  $t^0(\boldsymbol{\delta}^0, \boldsymbol{\lambda}_{\boldsymbol{\theta}}) = \boldsymbol{\mu}_{\boldsymbol{\theta}} + (\boldsymbol{\eta}^0 \otimes \mathbf{I}_S) \text{vech}(\mathbf{B}_{\boldsymbol{\theta}}) + \mathbf{d}_{\boldsymbol{\theta}} \circ \boldsymbol{\epsilon}^0$ , where  $\mathbf{I}_S$  is the identity matrix of size  $S$ , and it can be further shown that  $\nabla_{\boldsymbol{\theta}} \log q_{\boldsymbol{\lambda}}^0(\boldsymbol{\theta}) = -(\mathbf{B}_{\boldsymbol{\theta}} \mathbf{B}_{\boldsymbol{\theta}}^{\top} + \mathbf{D}_{\boldsymbol{\theta}}^2)^{-1} (\boldsymbol{\theta} - \boldsymbol{\mu}_{\boldsymbol{\theta}})$ ,

$$\frac{dt^0(\boldsymbol{\delta}^0, \boldsymbol{\lambda}_\theta)}{d\boldsymbol{\mu}_\theta} = \mathbf{I}_S \quad \text{and} \quad \frac{dt^0(\boldsymbol{\delta}^0, \boldsymbol{\lambda}_\theta)}{d\text{vech}(\mathbf{B}_\theta)} = \boldsymbol{\eta}^{0\top} \otimes \mathbf{I}_S. \quad (\text{S10})$$

The derivatives of the lower bound with respect to variational parameters are:

$$\begin{aligned} \nabla_{\boldsymbol{\mu}_\theta} \mathcal{L}(\boldsymbol{\lambda}) &= E_{f_\delta}(\nabla_{\boldsymbol{\theta}} \log h(\boldsymbol{\mu}_\theta + \mathbf{B}_\theta \boldsymbol{\eta}^0 + \mathbf{d}_\theta \circ \boldsymbol{\epsilon}^0, \mathbf{y}_u)) \\ &\quad + (\mathbf{B}_\theta \mathbf{B}_\theta^\top + \mathbf{D}_\theta^2)^{-1} (\mathbf{B}_\theta \boldsymbol{\eta}^0 + \mathbf{d}_\theta \circ \boldsymbol{\epsilon}^0), \end{aligned} \quad (\text{S11})$$

$$\begin{aligned} \nabla_{\mathbf{B}_\theta} \mathcal{L}(\boldsymbol{\lambda}) &= E_{f_\delta}(\nabla_{\boldsymbol{\theta}} \log h(\boldsymbol{\mu}_\theta + \mathbf{B}_\theta \boldsymbol{\eta}^0 + \mathbf{d}_\theta \circ \boldsymbol{\epsilon}^0, \mathbf{y}_u) \boldsymbol{\eta}^{0\top}) \\ &\quad + (\mathbf{B}_\theta \mathbf{B}_\theta^\top + \mathbf{D}_\theta^2)^{-1} (\mathbf{B}_\theta \boldsymbol{\eta}^0 + \mathbf{d}_\theta \circ \boldsymbol{\epsilon}^0) \boldsymbol{\eta}^{0\top}, \end{aligned} \quad (\text{S12})$$

$$\begin{aligned} \nabla_{\mathbf{d}_\theta} \mathcal{L}(\boldsymbol{\lambda}) &= E_{f_\delta}(\text{diag}(\nabla_{\boldsymbol{\theta}} \log h(\boldsymbol{\mu}_\theta + \mathbf{B}_\theta \boldsymbol{\eta}^0 + \mathbf{d}_\theta \circ \boldsymbol{\epsilon}^0, \mathbf{y}_u) \boldsymbol{\epsilon}^{0\top}) \\ &\quad + (\mathbf{B}_\theta \mathbf{B}_\theta^\top + \mathbf{D}_\theta^2)^{-1} (\mathbf{B}_\theta \boldsymbol{\eta}^0 + \mathbf{d}_\theta \circ \boldsymbol{\epsilon}^0) \boldsymbol{\epsilon}^{0\top}). \end{aligned} \quad (\text{S13})$$

The analytical expressions for  $\nabla_{\boldsymbol{\theta}} \log h(\boldsymbol{\mu}_\theta + \mathbf{B}_\theta \boldsymbol{\eta}^0 + \mathbf{d}_\theta \circ \boldsymbol{\epsilon}^0, \mathbf{y}_u) = \nabla_{\boldsymbol{\theta}} \log h(\boldsymbol{\theta}, \mathbf{y}_u)$  in Equations (S11)-(S13) under both missing data mechanisms are similar to that of for the JVB method, and can be found in Section S2. The expectations in these gradients can be estimated using a single sample  $\boldsymbol{\delta} = (\boldsymbol{\delta}^{0\top}, \mathbf{y}_u^\top)^\top$  drawn from  $f_{\boldsymbol{\delta}^0}$ , and  $p(\mathbf{y}_u | \boldsymbol{\theta}, \mathbf{O}) = p(\mathbf{y}_u | t^0(\boldsymbol{\delta}^0, \boldsymbol{\lambda}_\theta), \mathbf{O})$ .

### S1.3 Calculate adaptive learning rates using ADADELTA

The adaptive learning rates (step sizes) for the VB algorithms of the main paper are calculated using the ADADELTA algorithm (Zeiler, 2012). The ADADELTA algorithm is now briefly described. Different step sizes are used for each element in variational parameters  $\boldsymbol{\lambda}$ .

The update for the  $i^{\text{th}}$  element of  $\boldsymbol{\lambda}$  is

$$\boldsymbol{\lambda}_i^{(t+1)} = \boldsymbol{\lambda}_i^{(t)} + \Delta \boldsymbol{\lambda}_i^{(t)}, \quad (\text{S14})$$

where, the step size  $\Delta \boldsymbol{\lambda}_i^{(t)}$  is  $a_i^{(t)} g_{\boldsymbol{\lambda}_i}^{(t)}$ . The term  $g_{\boldsymbol{\lambda}_i}^{(t)}$  denotes the  $i^{\text{th}}$  component of  $\widehat{\nabla_{\boldsymbol{\lambda}} \mathcal{L}(\boldsymbol{\lambda}^{(t)})}$



and  $a_i^{(t)}$  is defined as:

$$a_i^{(t)} = \sqrt{\frac{E(\Delta_{\lambda_i}^2)^{(t-1)} + \alpha}{E(g_{\lambda_i}^2)^{(t)} + \alpha}}, \quad (\text{S15})$$

where  $\alpha$  is a small positive constant,  $E(\Delta_{\lambda_i}^2)^{(t)}$  and  $E(g_{\lambda_i}^2)^{(t)}$  are decayed moving average estimates of  $\Delta_{\lambda_i}^2$  and  $g_{\lambda_i}^2$ , defined by

$$E(\Delta_{\lambda_i}^2)^{(t)} = vE(\Delta_{\lambda_i}^2)^{(t-1)} + (1-v)\Delta_{\lambda_i}^{(t)2}, \quad (\text{S16})$$

and

$$E(g_{\lambda_i}^2)^{(t)} = vE(g_{\lambda_i}^2)^{(t-1)} + (1-v)g_{\lambda_i}^{(t)2}, \quad (\text{S17})$$

where the variable  $v$  is a decay constant. We use the default tuning parameter choices  $\alpha = 10^{-6}$  and  $v = 0.95$ , and initialize  $E(\Delta_{\lambda_i}^2)^{(0)} = E(g_{\lambda_i}^2)^{(0)} = 0$ .

## S2 Prior distributions of model parameters and gradients $\nabla_{\theta, \mathbf{y}_u} \log h(\boldsymbol{\theta}, \mathbf{y}_u)$

To map the parameters  $\sigma_{\mathbf{y}}^2$  and  $\rho$  into the real line, we use the following transformations.

$$\begin{aligned} \gamma &= \log \sigma_{\mathbf{y}}^2 \\ \sigma_{\mathbf{y}}^2 &= e^\gamma, \end{aligned} \quad (\text{S18})$$

and

$$\begin{aligned} \lambda &= \log(1 + \rho) - \log(1 - \rho) \\ \rho &= \frac{e^\lambda - 1}{e^\lambda + 1}. \end{aligned} \quad (\text{S19})$$

The prior distributions of SEM and missing data model parameters are given in Table S1.

Parameter	Prior distribution	Hyperparameters
$\boldsymbol{\beta}$	$N(\mathbf{0}, \sigma_{\boldsymbol{\beta}}^2 \mathbf{I})$	$\sigma_{\boldsymbol{\beta}}^2 = 10,000$
$\gamma$	$N(0, \sigma_{\gamma}^2)$	$\sigma_{\gamma}^2 = 10,000$
$\lambda$	$N(0, \sigma_{\lambda}^2)$	$\sigma_{\lambda}^2 = 10,000$
$\boldsymbol{\psi}$	$N(\mathbf{0}, \sigma_{\boldsymbol{\psi}}^2 \mathbf{I})$	$\sigma_{\boldsymbol{\psi}}^2 = 10,000$

Table S1: Prior distributions of parameters

## S2.1 Derivation of the gradient $\nabla_{\boldsymbol{\theta}, \mathbf{y}_u} \log h(\boldsymbol{\theta}, \mathbf{y}_u)$ under MAR

Under MAR, the vector of parameters  $\boldsymbol{\theta}$  contains the fixed effects  $\boldsymbol{\beta}$ , the variance  $\sigma_{\mathbf{y}}^2$  and the spatial dependence parameter  $\rho$ . Further, we also know that  $\log h(\boldsymbol{\theta}, \mathbf{y}_u) = \log p(\mathbf{y} | \boldsymbol{\phi}) + \log p(\boldsymbol{\phi})$ ; see Table 2 of the main paper. Note that, for  $\sigma_{\mathbf{y}}^2$  and  $\rho$ , we utilise transformed parameters,  $\gamma = \log \sigma_{\mathbf{y}}^2$  and  $\lambda = \log(1 + \rho) - \log(1 - \rho)$ . This leads to

$$\log h(\boldsymbol{\theta}, \mathbf{y}_u) \propto -\frac{n}{2}\gamma + \frac{1}{2}\log|\mathbf{M}_{\mathbf{y}}| - \frac{e^{-\gamma}}{2}\mathbf{r}^{\top}\mathbf{M}_{\mathbf{y}}\mathbf{r} - \frac{\boldsymbol{\beta}^{\top}\boldsymbol{\beta}}{2\sigma_{\boldsymbol{\beta}}^2} - \frac{\gamma^2}{2\sigma_{\gamma}^2} - \frac{\lambda^2}{2\sigma_{\lambda}^2}, \quad (\text{S20})$$

where  $\sigma_{\boldsymbol{\beta}}^2$ ,  $\sigma_{\gamma}^2$ , and  $\sigma_{\lambda}^2$  are each set to 10,000, as detailed in Table S1.

The derivative of  $\log h(\boldsymbol{\theta}, \mathbf{y}_u)$  in Equation (S20) with respect to  $\boldsymbol{\beta}$  is

$$\frac{\partial \log h(\boldsymbol{\theta}, \mathbf{y}_u)}{\partial \boldsymbol{\beta}} = e^{-\gamma}(\mathbf{y} - \mathbf{X}\boldsymbol{\beta})^{\top}\mathbf{M}_{\mathbf{y}}\mathbf{X} - \frac{\boldsymbol{\beta}^{\top}}{\sigma_{\boldsymbol{\beta}}^2}, \quad (\text{S21})$$

the derivative of  $\log h(\boldsymbol{\theta}, \mathbf{y}_u)$  with respect to  $\gamma$  is

$$\frac{\partial \log h(\boldsymbol{\theta}, \mathbf{y}_u)}{\partial \gamma} = -\frac{n}{2} + \frac{e^{-\gamma}}{2}(\mathbf{y} - \mathbf{X}\boldsymbol{\beta})^{\top}\mathbf{M}_{\mathbf{y}}(\mathbf{y} - \mathbf{X}\boldsymbol{\beta}) - \frac{\gamma}{\sigma_{\gamma}^2}, \quad (\text{S22})$$

the derivative of  $\log h(\boldsymbol{\theta}, \mathbf{y}_u)$  with respect to  $\lambda$  is

$$\frac{\partial \log h(\boldsymbol{\theta}, \mathbf{y}_u)}{\partial \lambda} = \frac{\partial \log |\mathbf{M}_{\mathbf{y}}|}{2\partial \lambda} - \frac{e^{-\gamma}}{2}(\mathbf{y} - \mathbf{X}\boldsymbol{\beta})^{\top} \left( \frac{\partial \mathbf{M}_{\mathbf{y}}}{\partial \lambda} \right) (\mathbf{y} - \mathbf{X}\boldsymbol{\beta}) - \frac{\lambda}{\sigma_{\lambda}^2}, \quad (\text{S23})$$

where

$$\begin{aligned}\frac{\partial \mathbf{M}_y}{\partial \lambda} &= \frac{\partial \mathbf{M}_y}{\partial \rho} \times \frac{\partial \rho}{\partial \lambda}, \\ \frac{\partial \mathbf{M}_y}{\partial \rho} &= -(\mathbf{W}^\top + \mathbf{W}) + 2\rho \mathbf{W}^\top \mathbf{W}, \\ \frac{\partial \rho}{\partial \lambda} &= \frac{2e^\lambda}{(1+e^\lambda)^2}, \\ \frac{\partial \log |\mathbf{M}_y|}{\partial \lambda} &= \text{tr} \left\{ \mathbf{M}_y^{-1} \left( \frac{\partial \mathbf{M}_y}{\partial \lambda} \right) \right\}.\end{aligned}$$

Additionally, for the JVB algorithm, we require the derivative of  $\log h(\boldsymbol{\theta}, \mathbf{y}_u)$  with respect to  $\mathbf{y}_u$ , and it can be calculated by first calculating the derivative with respect to complete vector  $\mathbf{y}$ ,  $\frac{\partial \log h(\boldsymbol{\theta}, \mathbf{y}_u)}{\partial \mathbf{y}}$  using

$$\frac{\partial \log h(\boldsymbol{\theta}, \mathbf{y}_u)}{\partial \mathbf{y}} = -e^{-\gamma} (\mathbf{y} - \mathbf{X}\boldsymbol{\beta})^\top \mathbf{M}_y, \quad (\text{S24})$$

and then we extract the sub-vector, which corresponds to the missing values,  $\mathbf{y}_u$ .

## S2.2 Derivation of the gradient $\nabla_{\boldsymbol{\theta}, \mathbf{y}_u} \log h(\boldsymbol{\theta}, \mathbf{y}_u)$ under MNAR

Under MNAR, the vector of parameters  $\boldsymbol{\theta}$  contains the fixed effects of the SEM  $\boldsymbol{\beta}$ , the variance  $\sigma_y^2$ , the spatial dependence parameter  $\rho$  and the fixed effects of the missing data model  $\boldsymbol{\psi}$ . We also know that  $\log h(\boldsymbol{\theta}, \mathbf{y}_u) = \log p(\mathbf{y} | \boldsymbol{\phi}) + \log p(\mathbf{m} | \mathbf{y}, \boldsymbol{\psi}) + \log p(\boldsymbol{\phi}) + \log p(\boldsymbol{\psi})$ ; see Table 2 of the main paper. Note that, for  $\sigma_y^2$  and  $\rho$ , we utilise transformed parameters  $\gamma$  and  $\lambda$ , where  $\gamma = \log \sigma_y^2$  and  $\lambda = \log(1 + \rho) - \log(1 - \rho)$ . This leads to

$$\begin{aligned}\log h(\boldsymbol{\theta}, \mathbf{y}_u) &\propto -\frac{n}{2}\gamma + \frac{1}{2}\log |\mathbf{M}_y| - \frac{e^{-\gamma}}{2} \mathbf{r}^\top \mathbf{M}_y \mathbf{r} + \sum_{i=1}^n m_i (\mathbf{x}_i^* \boldsymbol{\psi}_x + y_i \boldsymbol{\psi}_y) \\ &\quad - \log(1 + e^{(\mathbf{x}_i^* \boldsymbol{\psi}_x + y_i \boldsymbol{\psi}_y)}) \\ &\quad - \frac{\boldsymbol{\beta}^\top \boldsymbol{\beta}}{2\sigma_\beta^2} - \frac{\gamma^2}{2\sigma_\gamma^2} - \frac{\lambda^2}{2\sigma_\lambda^2} - \frac{\boldsymbol{\psi}^\top \boldsymbol{\psi}}{2\sigma_\psi^2},\end{aligned} \quad (\text{S25})$$

where  $\sigma_\beta^2$ ,  $\sigma_\gamma^2$ ,  $\sigma_\lambda^2$  and  $\sigma_\psi^2$  are each set to 10,000, as detailed in Table S1. The derivatives of  $\log h(\boldsymbol{\theta}, \mathbf{y}_u)$  in Equation (S25) with respect to  $\boldsymbol{\beta}$ ,  $\gamma$  and  $\lambda$  are similar to that of under MAR given in Equations (S21) (S22), and (S23). The derivative of  $\log h(\boldsymbol{\theta}, \mathbf{y}_u)$  with

respect to  $\boldsymbol{\psi}$  is

$$\frac{\partial \log h(\boldsymbol{\theta}, \mathbf{y}_u)}{\partial \boldsymbol{\psi}} = \sum_{i=1}^n \left( m_i - \frac{e^{\mathbf{x}_i^* \boldsymbol{\psi}_x + y_i \boldsymbol{\psi}_y}}{1 + e^{\mathbf{x}_i^* \boldsymbol{\psi}_x + y_i \boldsymbol{\psi}_y}} \right) \mathbf{z}_i - \frac{\boldsymbol{\psi}^\top}{\sigma_\psi^2}, \quad (\text{S26})$$

where  $\mathbf{z}_i = (\mathbf{x}_i^{*\top}, y_i)$  is the vector containing the  $i^{\text{th}}$  row vector of matrix  $\mathbf{X}^*$ , and the  $i^{\text{th}}$  element of the vector  $\mathbf{y}$ , see Section 2.2 of the main paper.

Similar to MAR case, for the JVB algorithm, we require the derivative of  $\log h(\boldsymbol{\theta}, \mathbf{y}_u)$  with respect to  $\mathbf{y}_u$ , and it can be calculated in two steps. First, calculate the derivatives of  $\log p(\mathbf{y} | \boldsymbol{\phi})$  and  $\log p(\mathbf{m} | \mathbf{y}, \boldsymbol{\psi})$  with respect to  $\mathbf{y}_u$  separately and sum them up.

We first focus on the derivative of  $\log p(\mathbf{m} | \mathbf{y}, \boldsymbol{\psi})$  with respect to  $\mathbf{y}_u$ . The derivative with respect to the  $i^{\text{th}}$  missing value  $y_{u_i}$  is

$$\frac{\partial \log p(\mathbf{m} | \mathbf{y}, \boldsymbol{\psi})}{\partial y_{u_i}} = \left( 1 - \frac{e^{\mathbf{z}_i \boldsymbol{\psi}}}{1 + e^{\mathbf{z}_i \boldsymbol{\psi}}} \right) \boldsymbol{\psi}_{\mathbf{y}}. \quad (\text{S27})$$

Now, by stacking partial derivatives with respect to the individual missing values we obtain  $\frac{\partial \log p(\mathbf{m} | \mathbf{y}, \boldsymbol{\psi})}{\partial \mathbf{y}_u}$  as

$$\frac{\partial \log p(\mathbf{m} | \mathbf{y}, \boldsymbol{\psi})}{\partial \mathbf{y}_u} = \begin{bmatrix} \frac{\partial \log p(\mathbf{m} | \mathbf{y}, \boldsymbol{\psi})}{\partial y_{u_1}} \\ \frac{\partial \log p(\mathbf{m} | \mathbf{y}, \boldsymbol{\psi})}{\partial y_{u_2}} \\ \vdots \\ \frac{\partial \log p(\mathbf{m} | \mathbf{y}, \boldsymbol{\psi})}{\partial y_{u_{n_u}}} \end{bmatrix}. \quad (\text{S28})$$

For the derivative of  $\log p(\mathbf{y} | \boldsymbol{\phi})$  with respect to  $\mathbf{y}_u$ , we first calculate the derivative with respect to complete vector  $\mathbf{y}$ ,

$$\frac{\partial \log p(\mathbf{y} | \boldsymbol{\phi})}{\partial \mathbf{y}} = -e^{-\gamma} (\mathbf{y} - \mathbf{X}\boldsymbol{\beta})^\top \mathbf{M}_{\mathbf{y}}, \quad (\text{S29})$$

and then we extract the sub-vector, which corresponds to the missing values  $\mathbf{y}_u$ .

Finally, the gradient of  $\log h(\boldsymbol{\theta}, \mathbf{y}_u)$  with respect to  $\mathbf{y}_u$  is

$$\frac{\partial \log h(\boldsymbol{\theta}, \mathbf{y}_u)}{\partial \mathbf{y}_u} = \frac{\partial \log p(\mathbf{m} | \mathbf{y}, \boldsymbol{\psi})}{\partial \mathbf{y}_u} + \frac{\partial \log p(\mathbf{y} | \boldsymbol{\phi})}{\partial \mathbf{y}_u}. \quad (\text{S30})$$

## S3 Hamiltonian Monte Carlo

We compare the performance of the proposed VB methods with the Hamiltonian Monte Carlo (HMC) method, which was initially introduced by Duane et al. (1987), and was primarily developed for calculations within the field of lattice quantum chromodynamics. Neal (1995) introduced the HMC methods into applied statistics in the field of Bayesian neural networks. With the rise of high-performance software implementations such as Stan (Carpenter et al., 2017), the HMC method has now become a pervasive tool across many scientific, medical, and industrial applications.

HMC is a method for generating random samples from a desired probability distribution. This approach proves especially useful when obtaining samples directly from the target distribution poses difficulties (McElreath, 2018). It achieves this by mimicking the dynamics of a system using Hamiltonian dynamics and a numerical integrator, such as the leapfrog integrator.

The main difference between conventional MCMC sampling methods and HMC lies in their proposal mechanisms and exploration strategies. MCMC methods typically make small changes to the current values, which can be inefficient in high-dimensional spaces with complex distributions, such as posterior distributions with many parameters and a large number of missing values. HMC, on the other hand, uses the gradient of the log posterior to simulate the trajectory of parameters and missing values governed by Hamilton equations. This approach enables more efficient exploration of the parameter space and missing value space, particularly in high dimensions, leading to faster convergence and improved sampling efficiency.

Consider the problem of sampling from the joint posterior distribution of the parameter vector  $\boldsymbol{\theta}$  and the missing values vector  $\mathbf{y}_u$  of SEM with missing data. For simplicity of the illustration, let  $\boldsymbol{\chi} = (\boldsymbol{\theta}^\top, \mathbf{y}_u^\top)^\top$ . Let  $\mathbf{s}$  be an auxiliary parameter vector with the same dimensions as  $\boldsymbol{\chi}$ . The Hamiltonian's equation,  $\mathcal{H}(\boldsymbol{\chi}, \mathbf{s})$  is a function that combines the potential energy;  $\mathcal{U}(\boldsymbol{\chi})$  and the kinetic energy;  $\mathcal{K}(\mathbf{s})$  of a system through

$$\mathcal{H}(\boldsymbol{\chi}, \mathbf{s}) = \mathcal{U}(\boldsymbol{\chi}) + \mathcal{K}(\mathbf{s}), \tag{S31}$$

with

$$u(\boldsymbol{\chi}) = -\log(h(\boldsymbol{\chi})), \quad \mathcal{K}(\mathbf{s}) = \frac{1}{2}\mathbf{s}^\top \mathbf{R}^{-1}\mathbf{s}, \quad (\text{S32})$$

where  $h(\boldsymbol{\chi}) = h(\boldsymbol{\theta}, \mathbf{y}_u)$  is given in Table 2 for MAR and MNAR mechanisms, and  $\mathbf{R}$  is a positive definite mass matrix, usually chosen as the identity matrix.

In the HMC algorithm, the numerical integration of the Hamiltonian equations is performed using the leapfrog integrator. This involves updating the momentum variable  $\mathbf{s}$  and the position of  $\boldsymbol{\chi}$  over a series of  $L$  iterations. The three steps of the leapfrog algorithm are: (1) half-step momentum update:

$$\mathbf{s} = \mathbf{s} + \frac{\epsilon}{2}\nabla_{\boldsymbol{\chi}}u(\boldsymbol{\chi}), \quad (\text{S33})$$

(2) full-step Position Update:

$$\boldsymbol{\chi} = \boldsymbol{\chi} + \epsilon\mathbf{R}^{-1}\mathbf{s}, \quad (\text{S34})$$

and, (3) half-step momentum update:

$$\mathbf{s} = \mathbf{s} + \frac{\epsilon}{2}\nabla_{\boldsymbol{\chi}}u(\boldsymbol{\chi}), \quad (\text{S35})$$

where  $\nabla_{\boldsymbol{\chi}}u(\boldsymbol{\chi})$  is the gradient of the negative log-posterior with respect to  $\boldsymbol{\chi}$ , see Equation (S32). The Leapfrog algorithm is shown in Algorithm S2. The HMC algorithm for sampling from the joint posterior  $\boldsymbol{\theta}$  and  $\mathbf{y}_u$  is described in Algorithm S1.

We employ the widely-used R package RSTAN (Stan Development Team, 2020) to perform HMC sampling as described in Algorithm S1 for sampling from the joint posterior of parameters and missing values of the models under consideration. In particular, we use the No U-Turn Sampler (NUTS) (Hoffman et al., 2014), which adaptively selects the number of leapfrogs  $L$  and the step size  $\epsilon$ . We apply the same prior distributions for the model parameters as in the two VB algorithms.

---

**Algorithm S1** The Hamiltonian Monte Carlo (HMC) Algorithm for sampling from joint posterior of  $\boldsymbol{\theta}$  and  $\mathbf{y}_u$  of SEM with missing values

---

- 1: Set number of samples  $N$ , number of leapfrog steps  $L$ , step size  $\epsilon$
  - 2: Initialize starting position  $\boldsymbol{\chi}^{(1)} = (\boldsymbol{\theta}^{(1)\top}, \mathbf{y}_u^{(1)\top})^\top$
  - 3: **for**  $i = 1$  to  $N$  **do**
  - 4:   Sample momentum  $\mathbf{s}^{(i)} \sim N(\mathbf{0}, \mathbf{R})$
  - 5:   Compute initial Hamiltonian  $H(\boldsymbol{\chi}^{(i)}, \mathbf{s}^{(i)}) = \mathcal{U}(\boldsymbol{\chi}^{(i)}) + \frac{1}{2}\mathbf{s}^{(i)\top}\mathbf{R}^{-1}\mathbf{s}^{(i)}$
  - 6:   Set  $\boldsymbol{\chi}^* \leftarrow \boldsymbol{\chi}^{(i)}$  and  $\mathbf{s}^* \leftarrow \mathbf{s}^{(i)}$
  - 7:   **for**  $j = 1$  to  $L$  **do**
  - 8:     Set  $(\boldsymbol{\chi}^*, \mathbf{s}^*) \leftarrow \text{Leapfrog}(\boldsymbol{\chi}^*, \mathbf{s}^*, \epsilon)$ . The Leapfrog function is given in Algorithm S2.
  - 9:   **end for**
  - 10:   Compute final Hamiltonian  $H^*(\boldsymbol{\chi}^*, \mathbf{s}^*) = \mathcal{U}(\boldsymbol{\chi}^*) + \frac{1}{2}\mathbf{s}^{*\top}\mathbf{R}^{-1}\mathbf{s}^*$
  - 11:   Accept sample with probability  $\min(1, \exp(H^*(\boldsymbol{\chi}^*, \mathbf{s}^*) - H(\boldsymbol{\chi}^{(i)}, \mathbf{s}^{(i)})))$
  - 12:   **if** Accepted **then**
  - 13:     Set  $\boldsymbol{\chi}^{(i+1)} \leftarrow \boldsymbol{\chi}^*$
  - 14:   **else**
  - 15:     Set  $\boldsymbol{\chi}^{(i+1)} \leftarrow \boldsymbol{\chi}^{(i)}$
  - 16:   **end if**
  - 17: **end for**
- 

---

**Algorithm S2** The Leapfrog Algorithm

---

- 1: function Leapfrog( $\boldsymbol{\chi}, \mathbf{s}, \epsilon$ )
  - 2: Set:  $\mathbf{s}^* = \mathbf{s} + \frac{\epsilon}{2}\nabla_{\mathbf{x}}\mathcal{U}(\boldsymbol{\chi})$
  - 3: Set:  $\boldsymbol{\chi}^* = \boldsymbol{\chi} + \epsilon\mathbf{R}^{-1}\mathbf{s}^*$
  - 4: Set:  $\mathbf{s}^* = \mathbf{s}^* + \frac{\epsilon}{2}\nabla_{\mathbf{x}}\mathcal{U}(\boldsymbol{\chi}^*)$
  - 5: return  $\boldsymbol{\chi}^*, \mathbf{s}^*$
-

## **S4 Simulation study with small missing value percentages**

In Section 4 of the main paper, we present the results of simulation studies conducted with a large percentage of missing data (approximately 75%). The results presented here relate to a scenario using a small percentage of missing values, specifically  $n = 625$  with 25% missing data.

### **S4.1 Simulation study under MAR**

Under MAR, with  $n = 625$  and 25% missing values ( $n_u = 156$ ), the posterior distributions of SEM parameters obtained from the HVB-NoB algorithm are closer to the posterior distributions obtained from the HMC method than those from the JVB algorithm, as shown in Figure S1. The posterior means of missing values obtained using the HMC, JVB, and HVB-NoB methods are similar. However, the posterior standard deviations of missing values obtained from the JVB method are different from those obtained using the HMC method; see Figure S2 for further details. These findings are very similar to the simulation results conducted with  $n = 625$  and 75% missing values under MAR, presented in Section 4.1 of the main paper.



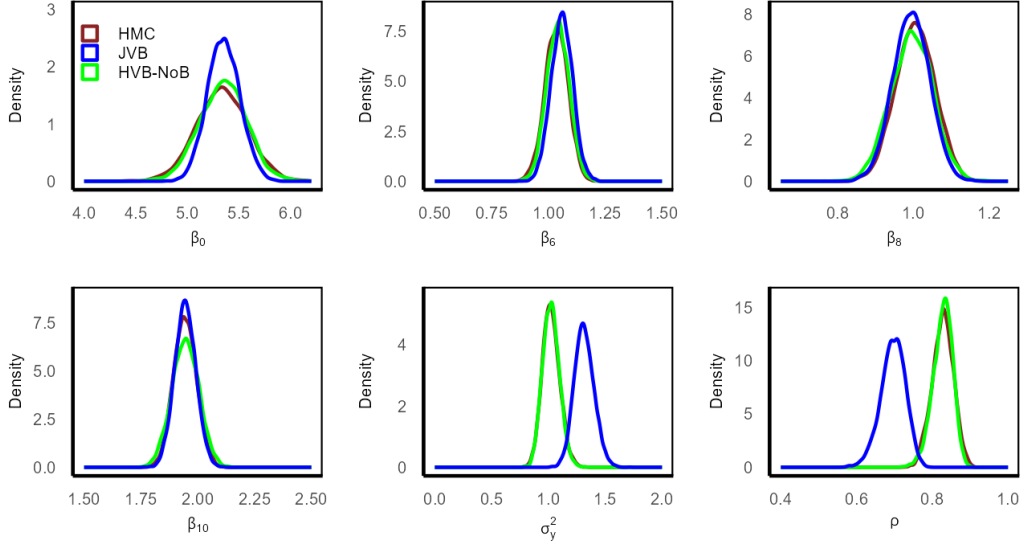


Figure S1: Posterior densities of SEM parameters under MAR for the simulated dataset with  $n = 625$  and 25% missing values ( $n_u = 156$ ) estimated using the HMC, JVB and HVB-NoB methods

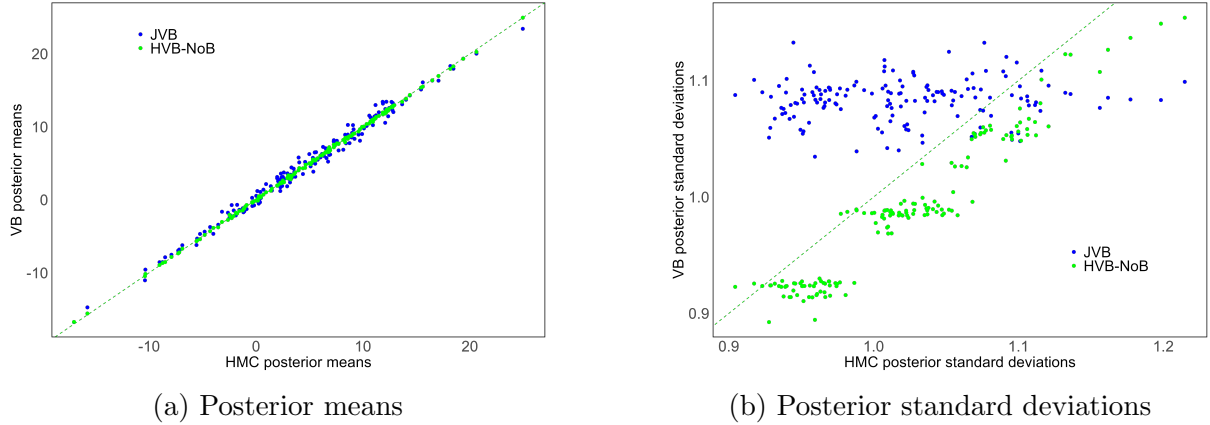


Figure S2: Comparison of the posterior means and standard deviation of missing values obtained using the JVB and HVB-NoB methods to those obtained using the HMC method for SEM under MAR with  $n = 625$  and 25% missing values ( $n_u = 156$ )

Table S2 displays the average computing time per iteration (in seconds) for the VB and HMC methods for different  $n$  and  $n_u$  under the MAR mechanism. The HVB-G method is not implemented when  $n_u$  is relatively small ( $n_u < 1,000$ ). The HMC method is computationally expensive when  $n$  is large and is not implemented when  $n > 5,000$ . The HMC method is much more computationally expensive than the VB methods, regardless of the values of  $n$  and  $n_u$ . Although it cannot accurately capture the posterior

$n$	$n = 625$			$n = 1024$			$n = 2500$		
missing percentage	25%	50%	75%	25%	50%	75%	25%	50%	75%
HMC	9.74	12.19	11.39	39.64	34.03	51.53	533.38	593.77	637.38
JVB	0.04	0.48	0.06	0.07	0.08	0.10	0.38	0.38	0.46
HVB- NoB	0.04	0.05	0.06	0.06	0.10	0.17	0.35	0.79	1.84
HVB- G	-	-	-	-	0.24	0.27	0.47	0.74	1.00

$n$	$n = 5,041$			$n = 7,569$			$n = 10,000$		
missing percentage	25%	50%	75%	25%	50%	75%	25%	50%	75%
HMC	-	-	-	-	-	-	-	-	-
JVB	1.285	1.610	2.066	3.519	4.18	5.09	7.95	7.93	10.46
HVB- NoB	1.63	6.49	16.39	4.49	26.61	72.13	10.44	69.92	201.14
HVB- G	1.69	2.66	3.20	4.04	5.77	6.38	9.06	10.88	12.59

Table S2: Average computing time (in seconds) of one iteration of the HMC, JVB, and HVB methods for estimating the SEM under MAR for different  $n$  and different missing value ( $n_u$ ) percentages. For HVB-G, the tuning parameters, such as the block size ( $k^*$ ) and the number of draws ( $N_1$ ) of the Gibbs iteration scheme, are set to  $N_1 = 5$  and  $k^* = 500$ , respectively. The HVB-G is not implemented for  $n_u < 1000$ . The HMC is not implemented for  $n > 5000$

distributions of the parameters  $\sigma_y^2$ ,  $\rho$  and the posterior standard deviation of the missing values (see Figures 1 and 2 of the main paper, and Figures S1 and S5 of the online supplement), the JVB method is generally the fastest among all the methods. For smaller values of  $n$  and  $n_u$ , the HVB-NoB algorithm is faster than the HVB-G method. The computing time of HVB-NoB increases rapidly as  $n$  and  $n_u$  increase, while HVB-G exhibits lower computing time than HVB-NoB, especially for high missing value percentages.

## S4.2 Simulation study under MNAR

Under MNAR, with  $n = 625$  and 25% missing values percentage, the posterior distributions of the SEM and missing value model parameters obtained from the JVB algorithm and all three HVB algorithms are close to those obtained from the HMC method as shown in Figure S3. While the posterior means of missing values are nearly identical across HMC, JVB, and three HVB methods, the posterior standard deviations of missing values obtained using the JVB method are slightly different from those obtained from HMC, as shown in Figure S4.

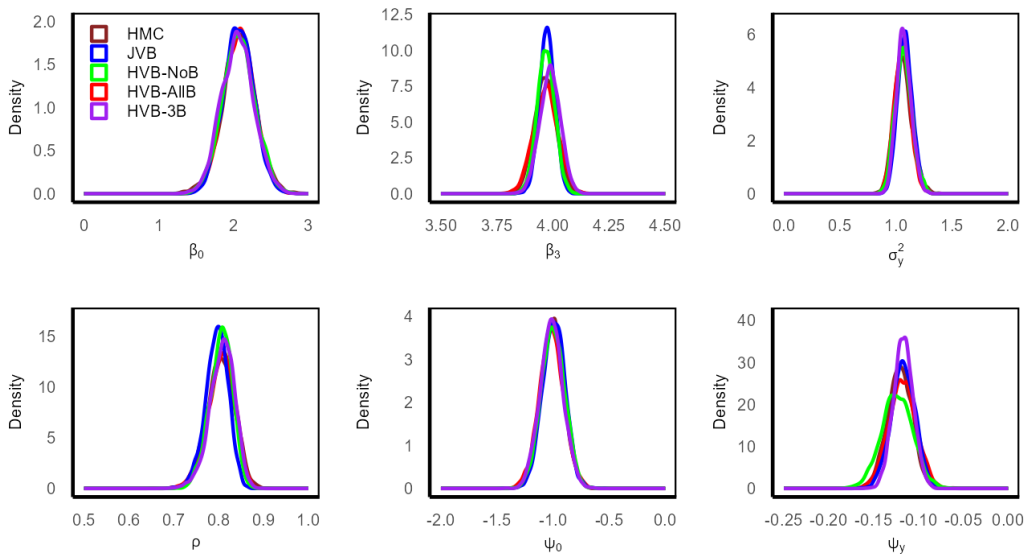
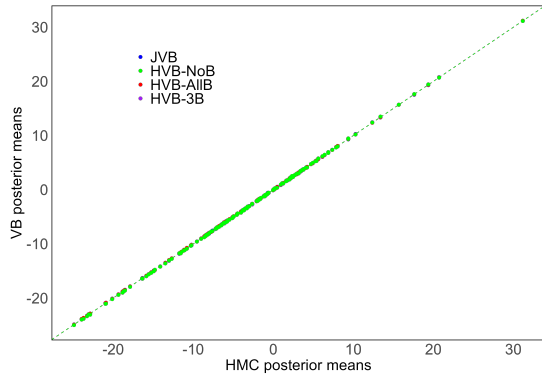
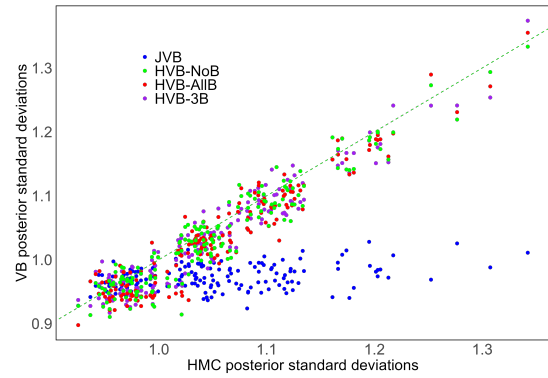


Figure S3: Posterior densities of SEM and missing value model parameters obtained using the HMC, JVB, HVB-NoB, HVB-AllB, and HVB-3B methods, under MNAR with  $n = 625$  and  $n_u = 170$  (around 25% missing)



(a) Posterior means



(b) Posterior standard deviations

Figure S4: Comparison of the posterior means and standard deviations of missing values from JVB and HVBs compared to that of HMC under MNAR with  $n = 625$  and around 75% missing ( $n_u = 170$ )

## S5 Additional figures from simulation study section of the main paper

This section provides additional figures related to the simulation study presented in Section 4 of the main paper.

## S5.1 Simulation study under MAR

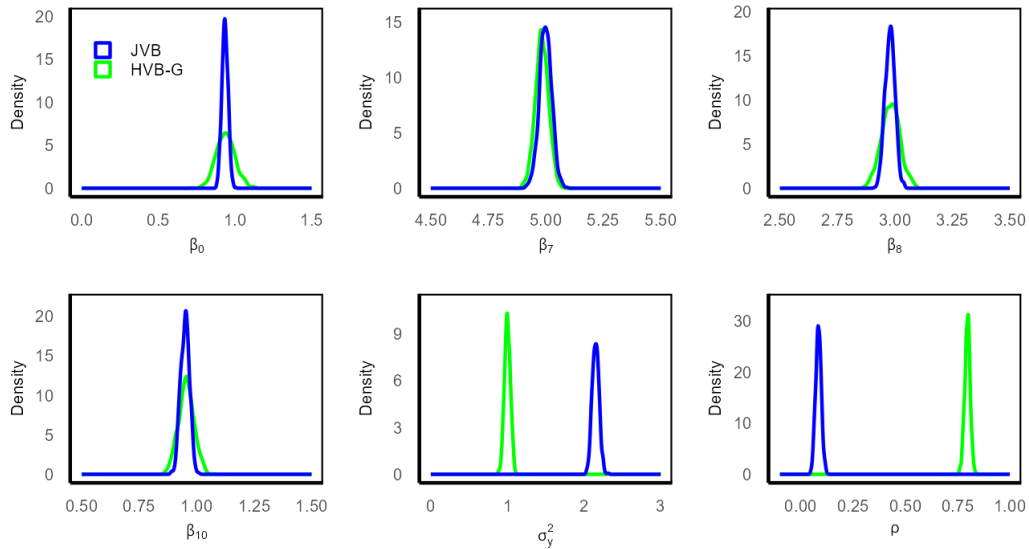


Figure S5: Posterior densities of SEM parameters under MAR for the simulated data with  $n = 10,000$  and 75% missing values ( $n_u = 7,500$ ) estimated using the JVB and HVB-G methods

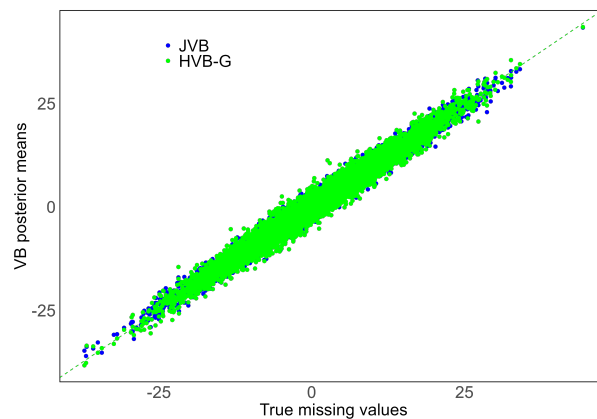


Figure S6: Comparison of the posterior means of missing values estimated using the JVB and HVB-G methods with the true missing values under MAR for the simulated dataset with  $n = 10,000$  and 75% missing values ( $n_u = 7,500$ )

In Figure S5, we compare the posterior densities of SEM parameters obtained using the JVB and HVB-G algorithms for  $n = 10,000$  and  $n_u = 7,500$  under MAR. The posterior distributions of  $\rho$  and  $\sigma_y^2$  obtained from JVB are different from their true values. In contrast, the posterior means from HVB-G align with the true values for all parameters. Figure S6 compares the posterior means of the missing values estimated by the two VB

methods with the true missing values. The posterior means of the missing values obtained from both methods are close to the true values.

## S5.2 Simulation study under MNAR

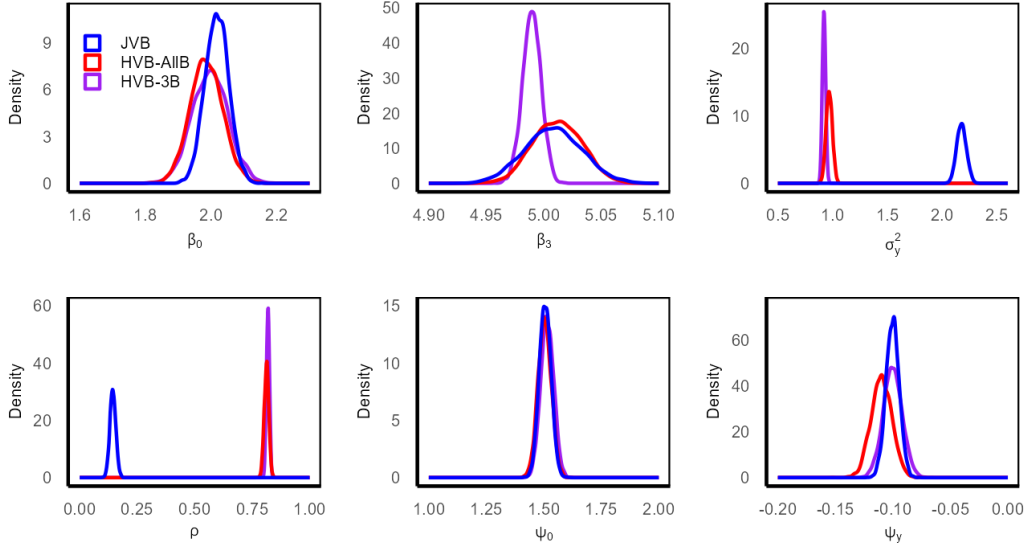


Figure S7: Posterior densities of SEM and missing value model parameters under MNAR with  $n = 10,000$  and  $n_u = 7,542$  (around 75% missing) using the JVB and different HVB methods

In Figure S7, we compare the posterior densities of SEM and missing data model parameters obtained using the JVB, HVB-AllB, and HVB-NoB algorithms for  $n = 10,000$  and  $n_u = 7,542$  under MNAR. The posterior distributions obtained from the HVB-AllB and HVB-3B algorithms are almost identical, except for a slight difference in the posterior distribution of  $\beta_0$ . The posterior distributions of  $\rho$  and  $\sigma_y^2$  obtained from JVB are significantly different from their true values. In contrast, the posterior means of all parameters from HVB-AllB and HVB-3B align with the true values.

Figure S8 compares the posterior means of the missing values estimated by the three VB methods with the true missing values. The posterior means of the missing values obtained from all methods are close to the true values. However, the posterior means of the missing values from the HVB-AllB and HVB-3B methods are closer to the true values, as they are more concentrated along the diagonal line compared to JVB.

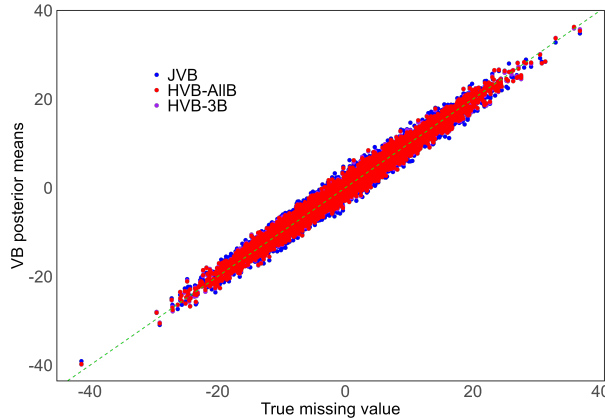


Figure S8: Comparison of the posterior means of the missing values obtained from JVB, HVB-AIIB, and HVB-3B with the true missing values under MNAR with  $n = 7,542$ , and  $n_u = 10,000$  (around 75% missing)

## S6 Additional figures and tables from real data section of the main paper

This section provides additional figures and tables related to the real data application presented in Section 5 of the main paper.

### S6.1 SEM under MAR

Figure S9 presents the posterior densities of SEM parameters estimated using the JVB and HVB-G methods with 75% of missing responses ( $n_u = 2,330$ ). The vertical lines indicate the marginal ML estimates. The figure shows that the JVB method yields different posterior density estimates for the parameters  $\sigma_y^2$  and  $\rho$  compared to the HVB-G method. The posterior mean estimates obtained using the HVB-G algorithm are closer to the marginal ML estimates than those from the JVB method.

Figure S10 compares the posterior means of missing values obtained from the JVB and HVB-G algorithms with the true missing values. The figure shows that the estimates of missing values from HVB-G are slightly closer to the true missing values than those obtained from the JVB algorithm, see also the MSE values in Table 6 of the main paper.

Table S3 presents the ML estimates with their standard errors and the posterior

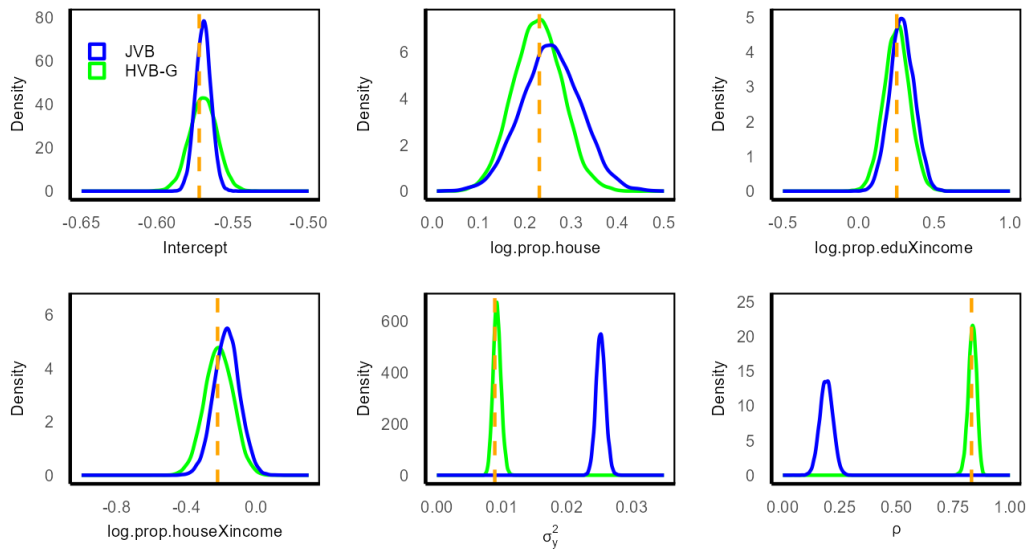


Figure S9: Posterior densities of SEM parameters for 1980 presidential election dataset under MAR using JVB and HVB-G with 75% missing values ( $n_u = 2,330$ ). The vertical lines indicate marginal ML estimates

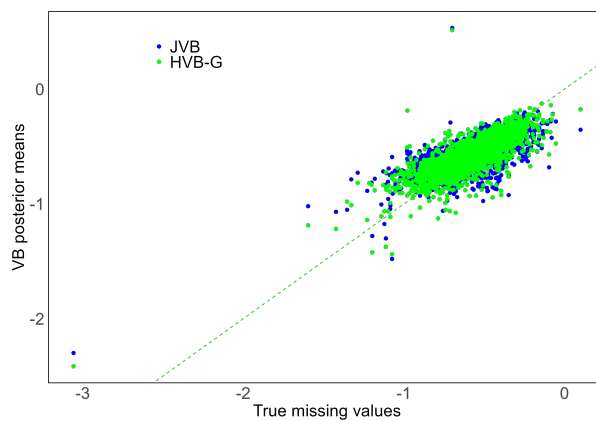


Figure S10: Comparison of the posterior means of missing values obtained from the JVB and HVB-G algorithms with the true missing response values for the 1980 presidential election dataset under MAR with 75% missing values ( $n_u = 2,330$ )



Table S3: Marginal ML estimates (with standard errors in brackets), and posterior means (with posterior standard deviations in brackets) of SEM parameters estimated by the JVB and HVB-G algorithms for the 1980 presidential election dataset with 75% ( $n_u = 2,330$ ) missing values under MAR

	marginal ML	JVB	HVB-G
<i>intercept</i> ( $\beta_0$ )	-0.5723 (0.01087)	-0.5697 (0.0051)	-0.5696 (0.0091)
<i>log.prop.edu</i> ( $\beta_1$ )	-0.1721 (0.1246)	-0.0826 ( 0.0815)	-0.1816 (0.0964)
<i>log.prop.house</i> ( $\beta_2$ )	0.2312 (0.0657)	0.2563 ( 0.0637)	0.2280 ( 0.0527)
<i>income</i> ( $\beta_3$ )	-0.1233 (0.0847)	-0.0946 (0.0525)	-0.1234 (0.0669)
<i>log.prop.edu</i> $\times$ <i>log.prop.house</i> ( $\beta_4$ )	-0.1424 (0.1353)	-0.0780 (0.0804)	-0.1444 (0.1059)
<i>log.prop.edu</i> $\times$ <i>income</i> ( $\beta_5$ )	0.2521 (0.0970)	0.2870 (0.0797)	0.2517 ( 0.0843)
<i>log.prop.house</i> $\times$ <i>income</i> ( $\beta_6$ )	-0.2213 (0.1066)	-0.1690 (0.0733)	-0.2137 (0.0818)
<i>log.prop.edu</i> $\times$ <i>log.prop.house</i> $\times$ <i>income</i> ( $\beta_7$ )	0.2076 (0.1209)	0.2582 (0.0989)	0.2203 (0.1073)
$\sigma_y^2$	0.0089 (0.0006)	0.0253 (0.0007)	0.0093 (0.0006)
$\rho$	0.8306 (0.0181)	0.1916 (0.0282)	0.8346 (0.0182)

means with their standard deviations obtained from the JVB and HVB-G methods for SEM parameters for the 1980 presidential election dataset with 75% missing values under MAR. The posterior means and standard deviations obtained from HVB-G align more closely with the estimates from marginal ML than those from JVB.

## S6.2 SEM under MNAR

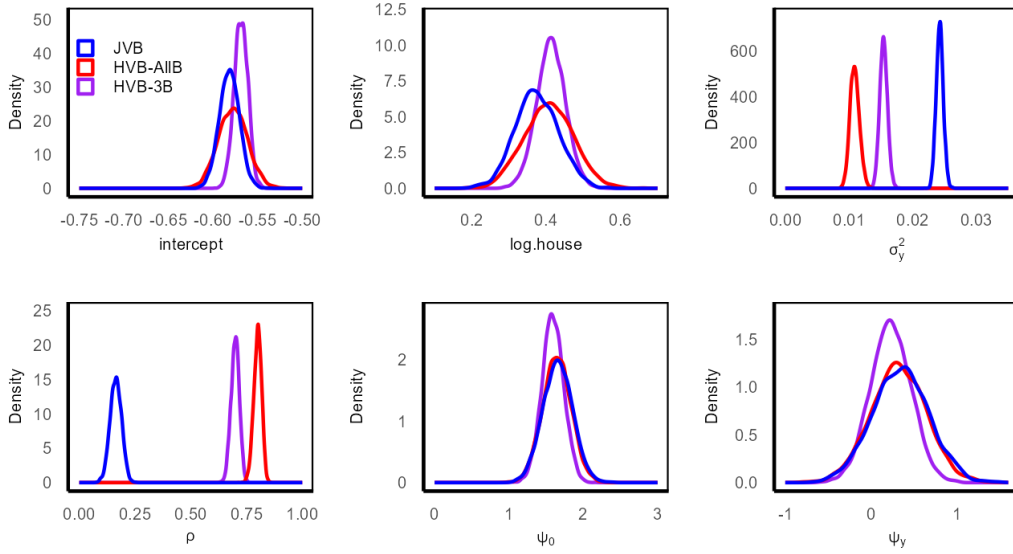


Figure S11: Posterior densities of SEM and missing value model parameters for the 1980 presidential election dataset under MNAR obtained using the JVB, HVB-AllB, and HVB-3B methods with approximately 80% missing values ( $n_u = 2,477$ )

Figure S11 compares the posterior densities of SEM and missing data model parameters obtained from the JVB, HVB-AllB, and HVB-3B methods for the 1980 presidential election dataset with around 80% missing values under MNAR. The figure shows that, except for  $\sigma_y^2$  and  $\rho$ , the posterior densities of SEM and missing data model parameters obtained from different algorithms are almost identical. For  $\sigma_y^2$  and  $\rho$ , the posterior densities obtained from HVB-AllB and HVB-3B differ from those obtained using JVB.

Figure S12 compares the posterior means of missing values obtained from the JVB, HVB-AllB, and HVB-3B methods with the true missing values. The estimates from the HVB-AllB method are slightly closer to the true missing values than those from the HVB-3B and JVB methods.

Table S4 presents the posterior means and standard deviations of SEM and missing data model parameters obtained from the JVB, HVB-AllB, and HVB-3B algorithms, and the true values for missing data model parameters. The posterior means and standard deviations from the HVB-AllB and HVB-3B algorithms are very close. However, the estimates from the JVB algorithm differ, particularly for  $\rho$  and  $\sigma_Y^2$ .

Table S4: Posterior means (with posterior standard deviations inside brackets) of SEM and missing data model parameters, and the true parameter values for the missing data model parameters under MNAR obtained from the JVB, HVB-AllB, and HVB-3B methods for the 1980 presidential election dataset with approximately 80% missing values ( $n_u = 2477$ )

	True value	JVB	HVB-AllB	HVB-3B
<i>intercept</i> ( $\beta_0$ )	NA	-0.5815 (0.0112)	-0.5773 (0.0163)	-0.5689 (0.0078)
<i>log.prop.edu</i> ( $\beta_1$ )	NA	0.1345 (0.0851)	0.1078 (0.0975)	0.0913 (0.0539)
<i>log.prop.house</i> ( $\beta_2$ )	NA	0.3732 (0.0583)	0.4094 (0.0665)	0.4139 (0.0398)
<i>income</i> ( $\beta_3$ )	NA	-0.2617 (0.0629)	-0.2941 (0.0728)	-0.2684 (0.0460)
<i>log.prop.edu</i> $\times$ <i>log.prop.house</i> ( $\beta_4$ )	NA	0.2177 (0.0905)	0.2362 (0.0953)	0.2108 (0.0738)
<i>log.prop.edu</i> $\times$ <i>income</i> ( $\beta_5$ )	NA	0.0582 (0.0499)	0.0312 (0.0487)	0.0736 (0.0395)
<i>log.prop.house</i> $\times$ <i>income</i> ( $\beta_6$ )	NA	-0.4237 (0.0918)	-0.5056 (0.0956)	-0.4701 (0.0556)
<i>log.prop.edu</i> $\times$ <i>log.prop.house</i> $\times$ <i>income</i> ( $\beta_7$ )	NA	-0.0607 (0.0605)	-0.1038 (0.0659)	-0.0848 (0.0457)
$\sigma_{\mathbf{y}}^2$	NA	0.0242 (0.0006)	0.0109 (0.0008)	0.0154 (0.0006)
$\rho$	NA	0.1634 (0.0259)	0.8004 (0.0171)	0.6990 (0.0186)
$\psi_0$	1.4	1.6622 (0.1977)	1.6504 (0.1934)	1.5891 (0.1455)
$\psi_{\mathbf{x}^*}$	0.5	0.5227 (0.0519)	0.5172 (0.0497)	0.5376 (0.0454)
$\psi_{\mathbf{y}}$	-0.1	0.3540 (0.3252)	0.3316 (0.3269)	0.2286 (0.2354)

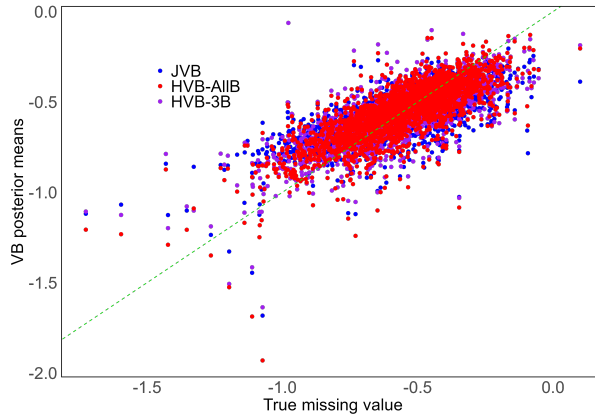


Figure S12: Comparison of the posterior means of the missing values obtained from JVB, HVB-AllB, and HVB-3B with the true missing values for the 1980 presidential election dataset under MNAR with 80% missing values ( $n_u = 2,477$ )

## S7 Convergence analysis of the VB methods

To evaluate the convergence of the proposed JVB method, we plot the lower bound over iterations. For the HVB algorithms, we analyse trajectories of variational means of the parameters across iterations for the simulation study and the real application.

### S7.1 Convergence Analysis for the Simulation Studies

This subsection provides convergence analysis plots for the simulation studies presented in Section 4 of the main paper, as well as in Section S4 of the online supplement. Generally, HVB algorithms converge more rapidly compared to JVB algorithms.

#### S7.1.1 Convergence analysis for the simulation studies for the SEM under MAR

Figures S13, S15, and S17 illustrate lower bounds for the JVB algorithm (the left figure), and the trajectories of variational means of SEM parameters for the HVB algorithm (the right figure) across VB iterations, under MAR, for different values of  $n$  and  $n_u$ . All VB algorithms achieve convergence well before the final iteration. The HVB algorithms consistently reach convergence in fewer iterations than the JVB algorithm.

Figures S14 and S16 display trace plots of posterior samples for SEM parameters under the MAR mechanism, obtained using the HMC method after discarding burn-in

iterations for the simulated datasets with  $n = 625$  and different missing value percentages ( $n_u$ ). The trace plots indicate good mixing for both cases.

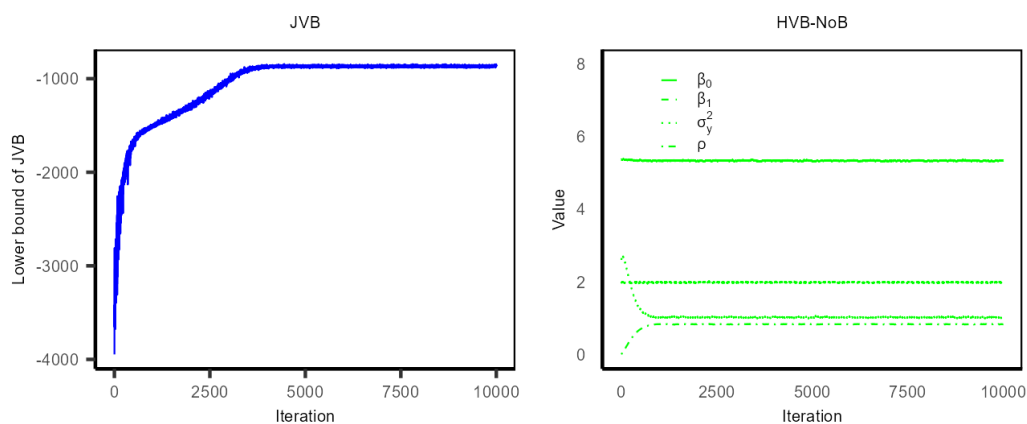


Figure S13: The lower bound for the JVB algorithm (left figure), and the trajectories of variational means of SEM parameters for the HVB-NoB algorithm over iterations (right figure), under MAR for the simulated dataset with  $n = 625$  and  $n_u = 156$  (i.e. missing percentage is 25%)

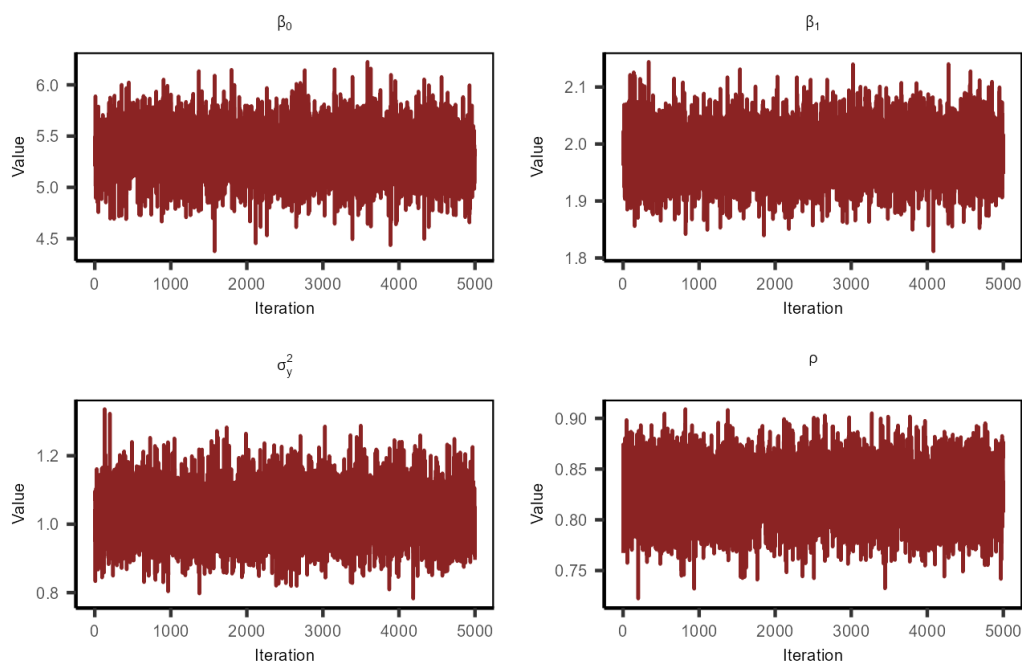


Figure S14: Trace plots of SEM posterior samples of SEM parameters under MAR from the HMC method after excluding burn-in iterations for the simulated dataset with  $n = 625$  and  $n_u = 156$  (i.e., the missing percentage is 25%)

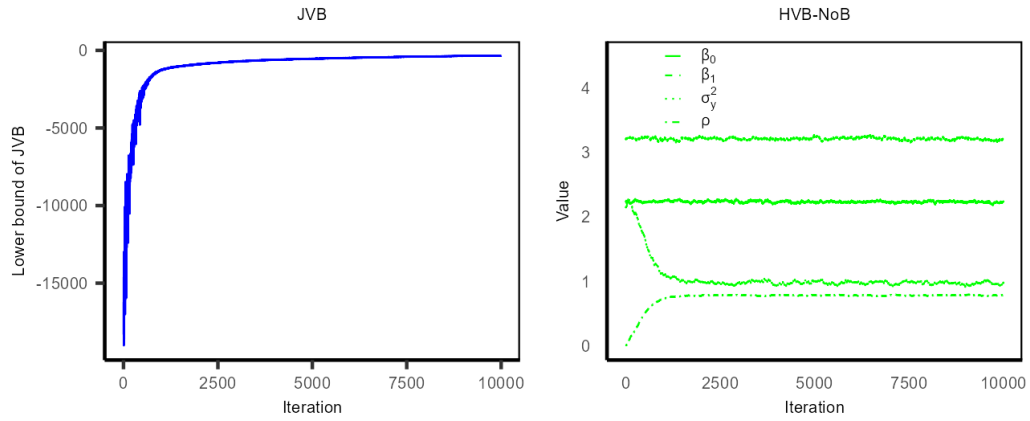


Figure S15: The lower bound for the JVB algorithm (left figure), and the trajectories of variational means of SEM parameters for the HVB-NoB algorithm over iterations (right figure), under MAR for the simulated dataset with  $n = 625$ ,  $n_u = 469$  (i.e. missing percentage is 75%)

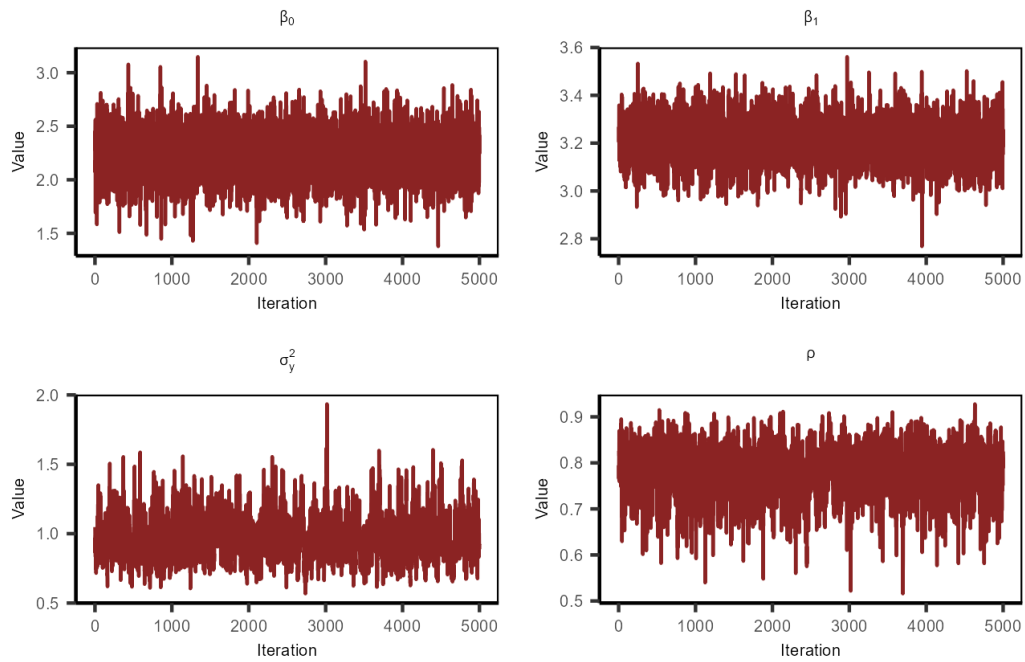


Figure S16: Trace plots of posterior samples of SEM parameters under MAR from the HMC method after excluding burn-in iterations for the simulated dataset with  $n = 625$  and  $n_u = 469$  (i.e., the missing percentage is 75%)

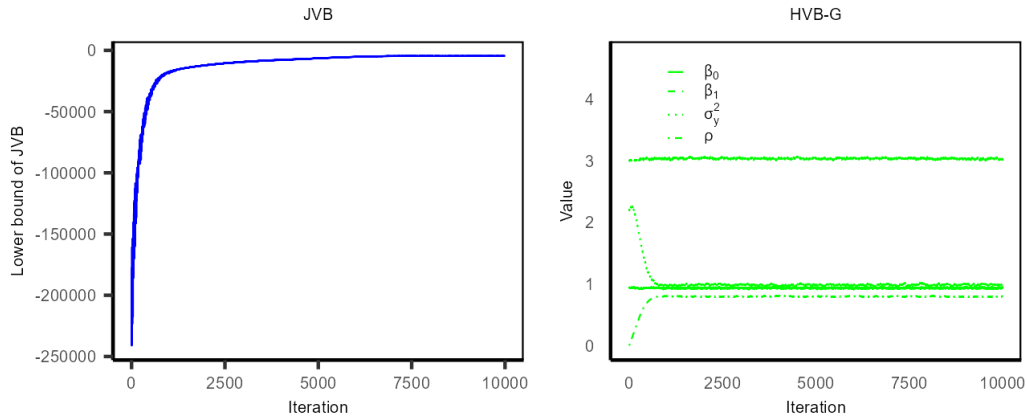


Figure S17: The lower bound for the JVB algorithm (left figure), and the trajectories of variational means of SEM parameters for the HVB-G algorithm over iterations (right figure), under MAR for the simulated dataset with  $n = 10,000$ ,  $n_u = 7,500$  (i.e. missing percentage is 75%)

### S7.1.2 Convergence analysis for the simulation studies for the SEM under MNAR

Figures S18, S20, and S22 show lower bounds for the JVB algorithm (displayed in the top left subplot), and the trajectories of variational means of SEM and missing data model parameters for the HVB algorithms (shown in the remaining subplots) across VB iterations, under MNAR, for the simulated datasets with various combinations of  $n$  and  $n_u$ . As observed in the simulation study under MAR, all VB algorithms achieve convergence well before the final iteration. Additionally, the HVB algorithms consistently achieve convergence in fewer iterations compared to the JVB algorithm.

Figures S19 and S21 present trace plots of posterior samples of SEM parameters under the MNAR mechanism, obtained using the HMC method after discarding burn-in iterations, for the simulated datasets with a sample size of  $n = 625$  and different missing value percentages ( $n_u$ ). These trace plots display stable, random-like patterns, suggesting good mixing for all SEM parameters.

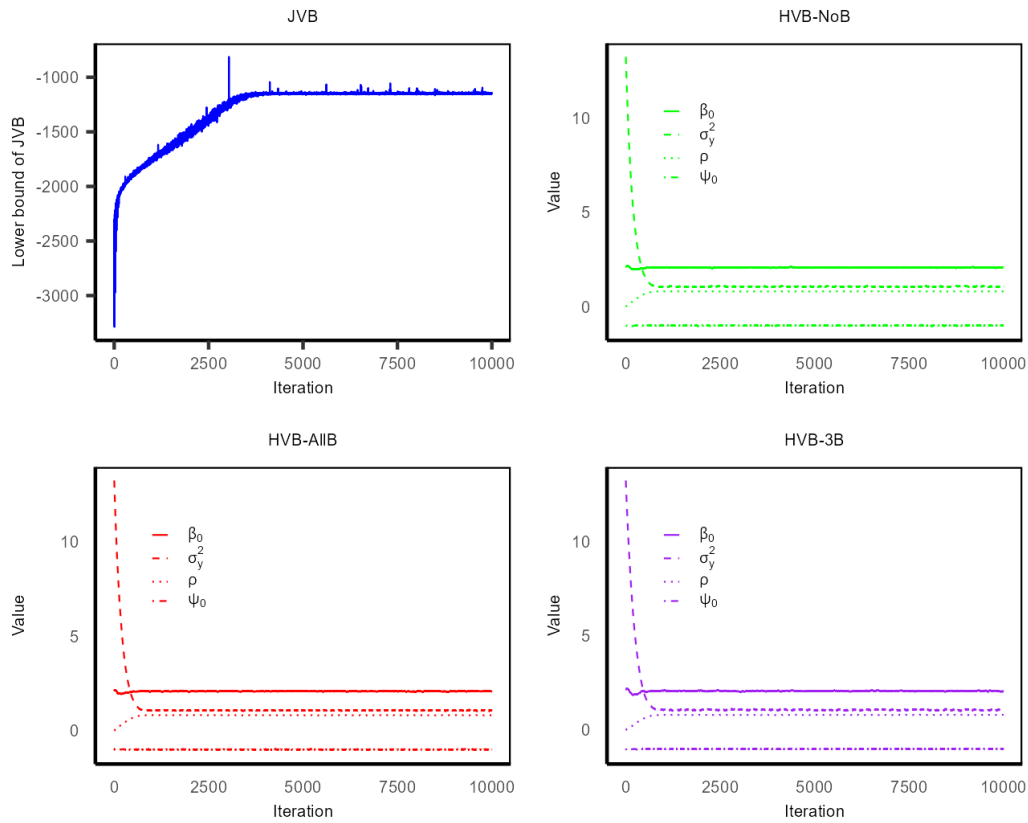


Figure S18: The lower bound for the JVB algorithm (top left figure), and the trajectories of variational means of SEM and missing data model parameters for the HVB algorithms over iterations (top right figure and bottom figures), under MNAR for the simulated dataset with  $n = 625$ ,  $n_u = 170$  (i.e. missing percentage is 25%)



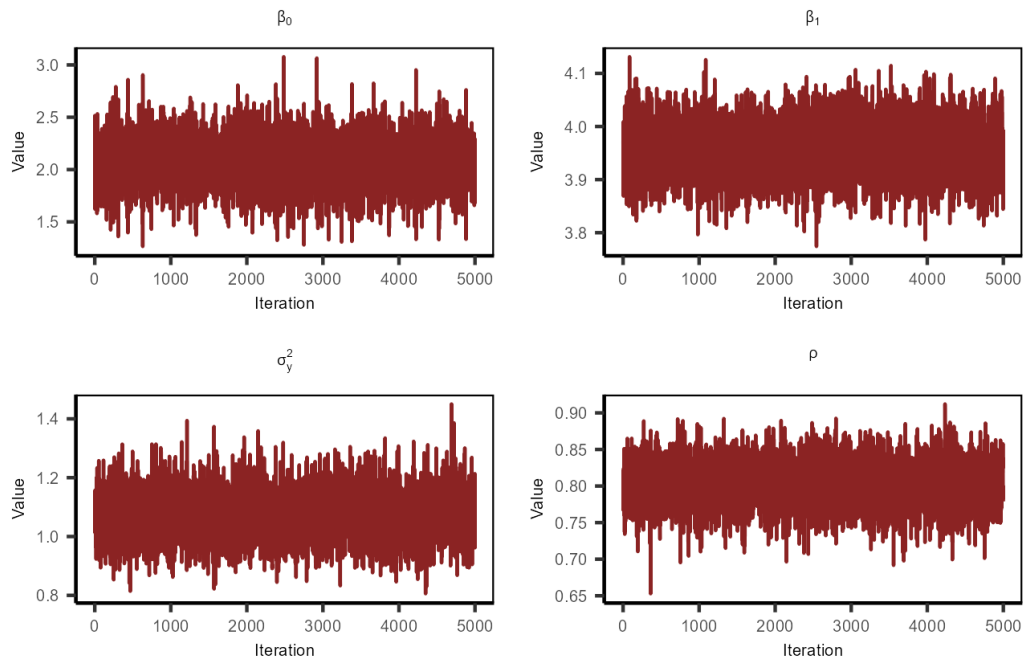


Figure S19: Trace plots of posterior samples of SEM parameters under MNAR from the HMC method after excluding burn-in iterations for the simulated dataset with  $n = 625$  and  $n_u = 170$  (i.e., the missing percentage is 25%)

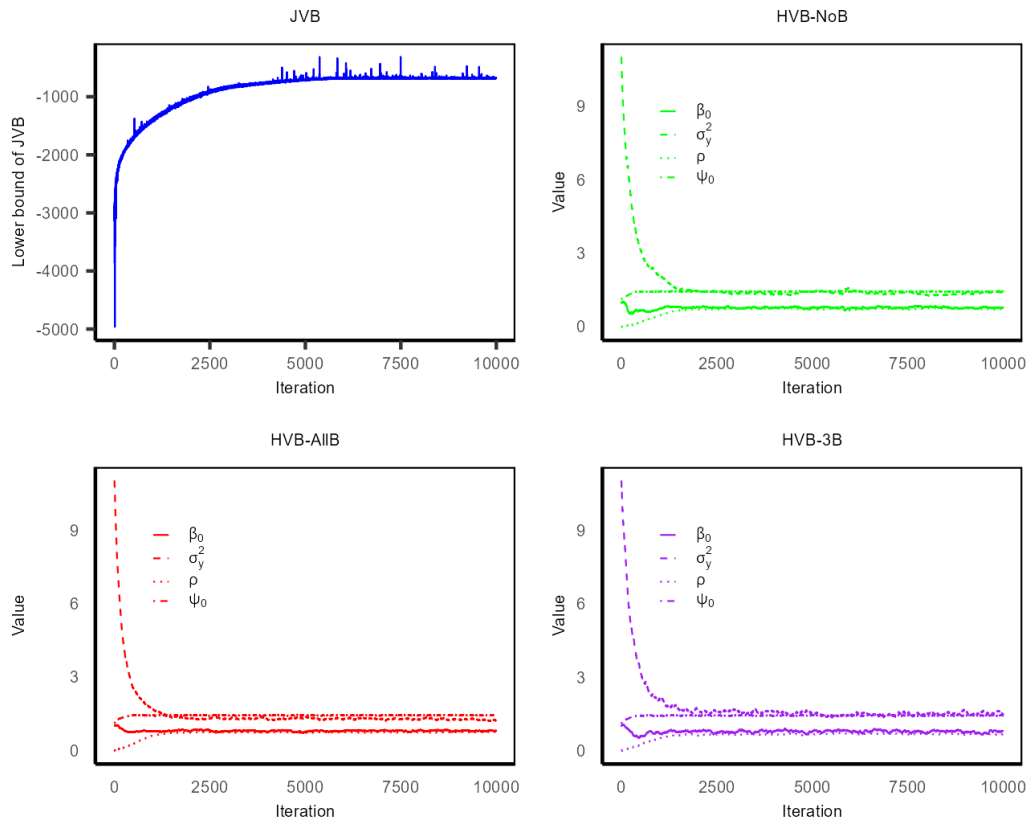


Figure S20: The lower bound for the JVB algorithm (top left figure), and the trajectories of variational means of SEM and missing data model parameters for the HVB algorithms over iterations (top right figure and bottom figures), under MNAR for the simulated dataset with  $n = 625$ ,  $n_u = 469$  (i.e. missing percentage is 75%)

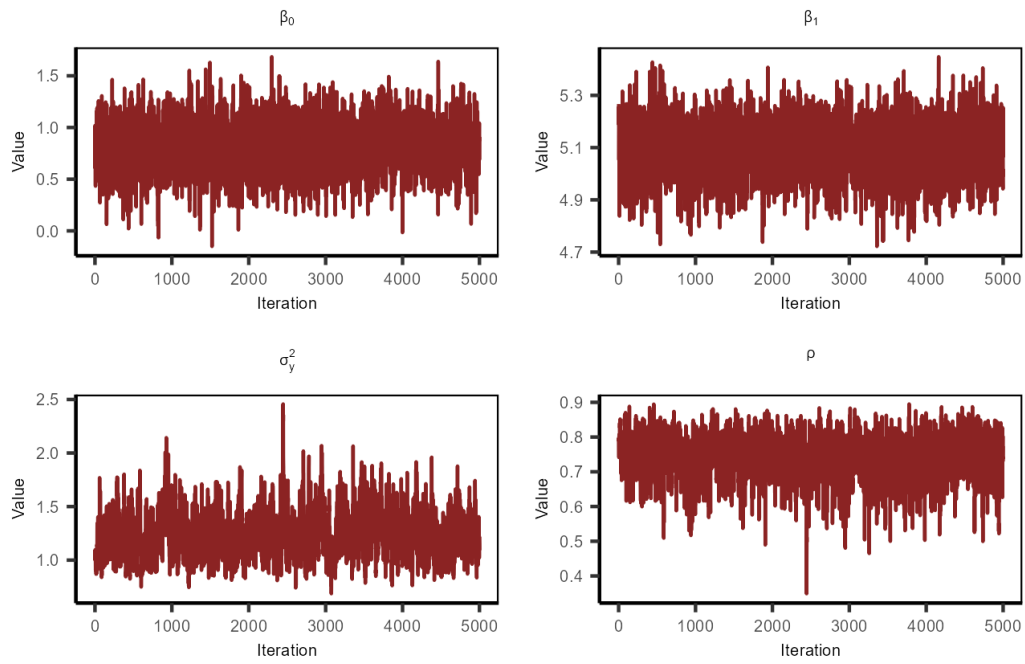


Figure S21: Trace plots of posterior samples of SEM parameters unde MNAR from the HMC method after excluding burn-in iterations for the simulated dataset with  $n = 625$  and  $n_u = 469$  (i.e., the missing percentage is 75%)

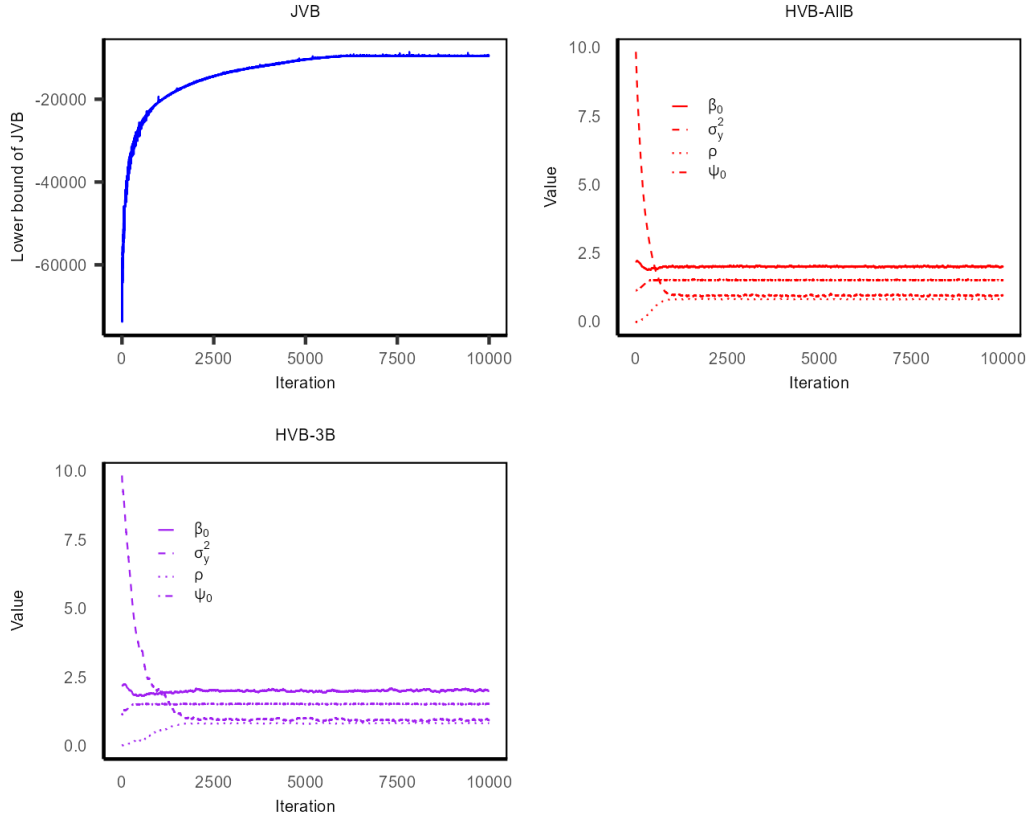


Figure S22: The lower bound for the JVB algorithm (top left figure), and the trajectories of variational means of SEM and missing data model parameters for the HVB algorithms over iterations (top right and bottom left figures), under MNAR for the simulated dataset with  $n = 10,000$ ,  $n_u = 7,542$  (i.e. missing percentage is approximately 75%)

## S7.2 Convergence analysis for the Real data examples

This subsection provides convergence analysis plots for the real world example presented in Section 5 of the main paper.

### S7.2.1 Convergence analysis for Real data examples under MAR

Figure S23 shows the lower bound for the JVB algorithm, and the trajectories of variational means of SEM parameters obtained using the HVB-G algorithm across iterations, for the 1980 presidential election dataset, under MAR with  $n_u = 2,330$ . These plots clearly indicate convergence for both the HVB-G and JVB algorithms.

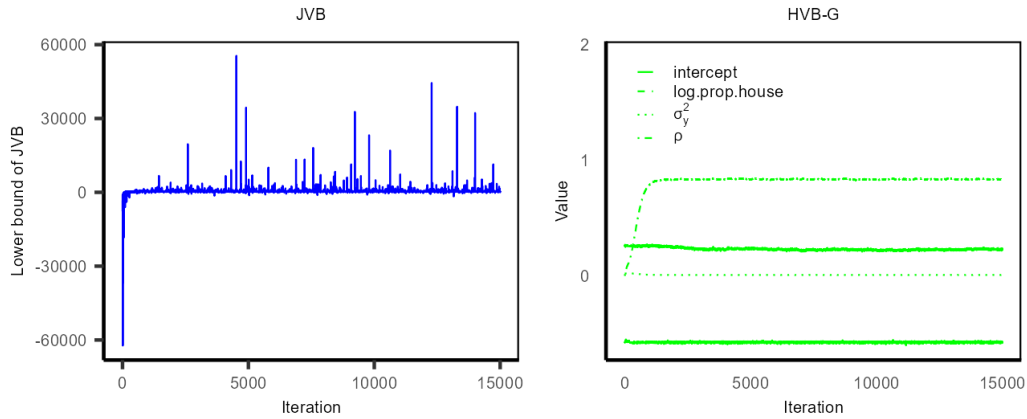


Figure S23: The lower bound for the JVB algorithm (left figure), and the trajectories of variational means of SEM parameters for the HVB-G algorithm over iterations (right figure) for the 1980 presidential election dataset, under MAR with  $n_u = 2,330$  (i.e. missing percentage is 75%)

### S7.2.2 Convergence analysis for the Real data example under MNAR

Figure S24 illustrates the lower bound for the JVB algorithm, and the trajectories of the variational means of SEM and missing data model parameters for the HVB algorithms; HVB-AllB and HVB-3B, across iterations for the 1980 presidential election dataset under MNAR with  $n_u = 2,477$ . Flat lines indicate that all algorithms have converged before the 15,000<sup>th</sup> iteration.

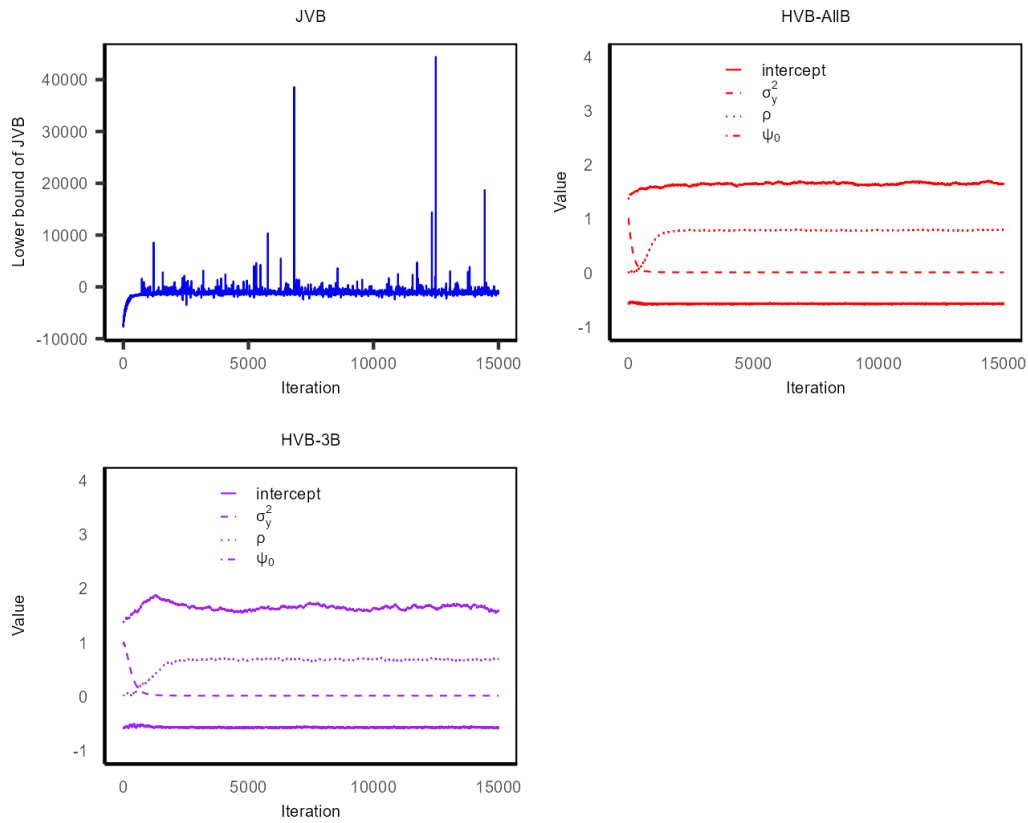


Figure S24: The lower bound for the JVB algorithm (top left figure), and the trajectories of variational means of SEM and missing data model parameters for the HVB-AIIB and HVB-3B algorithms over iterations (top right and bottom left figures) for the 1980 presidential election dataset, under MNAR with  $n_u = 2,477$  (i.e. missing percentage is around 80%)